Russian Original Vol. 34, No. 1, January, 1973

July, 1973

SATEAZ 34(1) 1-100 (1973)

NE
RS

SOVIET ATOMIC ENERGY

АТОМНАЯ ЭНЕРГИЯ
(ATOMNAYA ÉNERGIYA)

TRANSLATED FROM RUSSIAN

c/b CONSULTANTS BUREAU, NEW YORK

SOVIET ATOMIC ENERGY

Soviet Atomic Energy is a cover-to-cover translation of *Atomnaya Énergiya*, a publication of the Academy of Sciences of the USSR.

An arrangement with Mezhdunarodnaya Kniga, the Soviet book export agency, makes available both advance copies of the Russian journal and original glossy photographs and artwork. This serves to decrease the necessary time lag between publication of the original and publication of the translation and helps to improve the quality of the latter. The translation began with the first issue of the Russian journal.

Consultants Bureau journals appear about six months after the publication of the original Russian issue. For bibliographic accuracy, the English issue published by Consultants Bureau carries the same number and date as the original Russian from which it was translated. For example, a Russian issue published in December will appear in a Consultants Bureau English translation about the following June, but the translation issue will carry the December date. When ordering any volume or particular issue of a Consultants Bureau journal, please specify the date and, where applicable, the volume and issue numbers of the original Russian. The material you will receive will be a translation of that Russian volume or issue.

Subscription
$80 per volume (6 issues)
2 volumes per year
(Add $5 for orders outside the United States and Canada.)

Single Issue: $30
Single Article: $15

CONSULTANTS BUREAU, NEW YORK AND LONDON

227 West 17th Street
New York, New York 10011

Davis House
8 Scrubs Lane
Harlesden, NW10 6SE
England

Published monthly. Second-class postage paid at Jamaica, New York 11431.

SOVIET ATOMIC ENERGY

A translation of *Atomnaya Énergiya*

July, 1973

Volume 34, Number 1 January, 1973

CONTENTS

CONTENTS

(continued)

CONTENTS

(continued)

The Russian press date (podpisano k pechati) of this issue was 1/3/1973. Publication therefore did not occur prior to this date, but must be assumed to have taken place reasonably soon thereafter.

ARTICLES

SOME CHARACTERISTICS OF THE RELATIONSHIP BETWEEN URANIUM–MOLYBDENUM MINERALIZATION AND VOLCANOGENIC FORMATIONS

V. M. Konstantinov and D. I. Yakunin

UDC 550.42:553.495

Recent years have seen the publication of a number of papers relating to hydrothermal uranium sites with a considerable amount of molybdenum in the ores; the ores separate out into a uranium–molybdenum formation. A special characteristic of these ore sites is the fact that they are confined to regions characterized by the development of volcanic-intrusive magmatic complexes. Many years' investigations have led to the authors to the conclusion that the relationship between the sites of the uranium–molybdenum formations and the magmatogenic formations is different in regions with a different history of geological development. In this paper we shall present some data as to the relationship between mineralization and magmatogenic formations in two particular regions, and on the basis of these data we shall refine the criteria defining the conditions governing the disposition of the ore sites.

One of the regions belongs to the framework of a median massif and the other to a Caledonian geosynclinal area. The deposits of both regions are characterized by similarity of mineral composition; both are confined to extrusive formations folded with acid rocks, or to their contacts with effusive-sedimentary or metamorphic formations. However, the histories of the geological development of the regions contain certain differences, an analysis of which enables us to gain a better understanding of the relation between hydrothermal uranium–molybdenum mineralization and magmatism, and to estimate their potentialities anew.

The first region is characterized by the following features of development. In the period completing the geosynclinal stage, batholite-like granitoid intrusions were formed, accompanied by finer intrusive regions and dikes represented by rocks of predominantly acid composition. In the orogenic period subvolcanic intrusions and multiple effusions of acid lavas penetrated the system and extrusive regions were formed. At the same time the intrusion of dikes of medium composition occurred. The uranium content of the intrusive and volcanogenic rocks exceeded the Clark values by a factor of several times.

The formation of granitoid intrusive masses was accompanied by quartz–albite metasomatosis, appearing predominantly in gneiss–shales of the proterozoic age. Fine ore manifestations of uranium with uranium pitch were confined to the metasomatites. The uranium mineralization was created after the formation of the metasomatites and was close to them in time.

The principal uranium ore deposits lie in rocks subjected to intensive quartz–sericite metasomatosis associated with the post-volcanic activity of the orogenic period. The time of ore formation is close to the period of formation of the metasomatites.

The ore manifestations of the uranium–molybdenum formation are situated directly in the rocks of the crater facies of paleo-volcanoes (felsites and quartz porphyries), or gravitate toward the contacts of the extrusive beds with surrounding rocks. There is a relationship between the structure of the paleovolcanic masses and the disposition of the uranium ore manifestations. This relationship lies in the fact that, for a low degree of crystallinity of the rocks of the crater facies, in those cases in which they are represented by felsites, the ore beds are situated primarily in the craters. For a higher degree of crystallinity, when the craters are filled with quartz porphyries, the ore beds lie mainly at their contacts with the surrounding rocks. Considerably more rarely the craters are filled with leucocratic granite porphyries;

Translated from Atomnaya Énergiya, Vol. 34, No. 1, pp. 3-5, January, 1973. Original article submitted March 3, 1972.

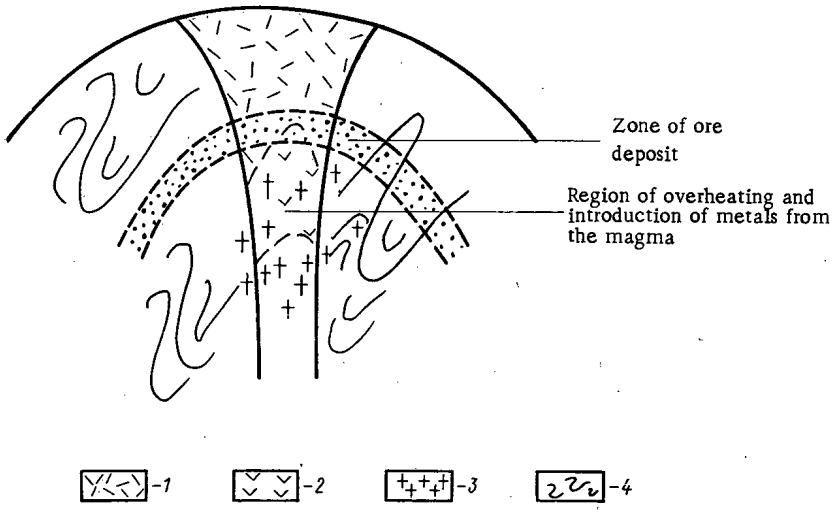

Fig. 1. Scheme for the formation of ore-forming hydrothermal solutions: 1) felsites; 2) quartz porphyries; 3) graphite porphyries; 4) bed rocks.

in these cases the ore manifestations lie in the surrounding rocks at a certain distance from the contacts with the graphite porphyries.

This relationship may be explained [1] by the scheme representing the creation of ore-forming hydrothermal solutions illustrated in Fig. 1. In explaining the scheme we must remember the following: 1) around the cooling magmatic melt there existed a region of superheated rocks through which the gas-hydrothermal distillates passed from the magma, and in which no ores were formed; 2) when the distillates reached a region of comparatively low temperature, unloading and ore-deposition took place.

We see from the scheme that the region of ore deposition lay at a certain distance from the radical part of the paleo-volcanic system. Clearly, depending on the level of the contemporary erosive shear, this region will be established either in the felsites (minimum erosive shear), or close to the contact of the quartz porphyries (medium erosive shear), or in the metamorphic rocks (maximum erosive shear). Thus the relationship between the disposition of the uranium ore manifestations and the degree of crystallinity of the crater facies may be explained by the time proximity between the processes of crystallization and cooling of the magmatic melt in the radical parts of the paleo-volcanoes, on the one hand, and the processes of ore-formation on the other.

Detailed studies of the uranium distribution in volcanogenic rocks [2] show that the uranium content in the beds of felsites is three or four times greater than in the granite prophyries. This aspect of the uranium distribution in rocks formed from a single magmatic melt may be explained by the transfer of uranium from the magmatic melt during the formation of the deepest parts of the paleo-volcanic systems.

It follows from the foregoing data that, in the region under consideration, ore formation takes place in two stages. The slight ore aggregates created after the formation of the batholite-like granitoid massifs are controlled by the regions of development of quartz–albite metasomatites. The second stage of ore formation took place in the period of the completion of magmatic activity. The uranium distribution characteristics in the rocks and the spatial relationship between the ore manifestations and extrusive beds, and also the nearness in time of formation of the mineralizations and volcanogenic rocks, indicate a genetic relationship between the mineralization of the second stage and volcanism. On this basis, regions promising from the point of view of finding sites of uranium–molybdenum formations are determined by the presence of extrusive acid rocks and adjacent areas in which pre-ore quartz–sericite metasomatosis has occurred.

The second region, which lies in a geosynclinical block within a fold region, is characterized by a different history of its development in the concluding stages of formation.

In the geosynclinal period, subvolcanic intrusions of granodioritic and dioritic compositions were formed. After the establishment of these, intensive volcanic activity occurred, revealing itself in multiple volcanic eruptions, which led to the formation of thick beds folded with liparitic lavas and tuffs, and also

necks of rhyolitic porphyries lying among effusive rocks. The volcanic period of magmatic activity was completed by the formation of a subvolcanic mass folded with quartz porphyries and granite porphyries.

Volcanism was accompanied by the formation of low-temperature quartz–sericite metasomatites which exhibited an increase in uranium content and individual points of uranium mineralization. No substantial segregations of uranium were established.

After the creation of the volcanogenic formations, there was an intrusion of large intrusive masses folded with granitoids. The magmatic activity ended with the formation of dike rocks of medium composition.

The final stage in the magmatic activity was accompanied by the formation of quartz–albitic metasomatites in the most crumbling parts. Such parts include necks, folded massifs, severely crumbling rhyolitic porphyries, contacts of dikes with effusive rocks, effusive liparitic porphyries, and ignimbrites.

The ore beds are chiefly confined to necks folded with rhyolitic porphyries. We also encounter ore beds and fields confined to series of effusive rocks and controlled by faults, contacts with dikes, and certain facial varieties of liparitic lavas. In all known fields the ore beds are confined to zones of intensive quartz–albitic metasomatosis. According to absolute age determinations, nasturan was formed in the post-granitic period.

The data relating to the region under consideration leads us to conclude that the ore-bearing thermal springs and volcano-intrusive rocks are related parageneticallly by the common nature of their magmatic center. The fact that the majority of sites are confined to paleo-volcanic structures (necks of rhyolitic porphyries) is due to the fact that these provide favorable structural–lithological conditions for the siting of uranium mineralization. On this basis, we may consider promising regions to be those which contain favorable structures and areas exhibiting intensive post-granite quartz–albite metasomatosis. Regions of ore location favorable as regards lithological–structural conditions may be disposed, not only around necks of rhyolitic porphyries, but also among beds of effusive rocks. It is quite probable that the fact that the majority of fields of this type are found in necks rather than in effusive beds may be attributed to the complexity involved in revealing the latter, since the ore beds of such fields may be controlled by oblique structures, and are not always detected on the surface.

A comparative analysis of the uranium–molybdenum fields shows that in both regions their formation took place after the completion of the magmatic activity, in connection with the quartz–albite and quartz–sericite metasomatosis of the rocks. In the first region the uranium ore beds lie in quartz–sericite metasomatites formed after the completion of the magmatic activity. Only small quantities of uranium are here associated with the quartz–albite metasomatites. In the second region, on the other hand, the uranium ore beds are disposed mainly in the quartz–albite metasomatites, whereas only small segregations of uranium are located in the quartz–sericite metasomatites.

In both regions the sites gravitate toward the extrusive formations. In the first region this is due to the arrival of ore-bearing thermal springs from the volcanic chambers; hence this spatial confinement, in combination with intensive quartz–sericite metasomatosis, is a reliable prospecting criterion. In the second region the confinement of the ore manifestations to extrusive formations is explained by exclusively structural–lithological factors. In this case the control of ore manifestations by necks may this be considered as a particular case of the manifestation of one of the prospecting criteria. In more general form this criterion specifies the confinement of uranium–molybdenum ore manifestations to places in which favorable structures develop (necks, faults, dikes, etc.).

LITERATURE CITED

1. M. M. Konstantinov, Izv. Akad. Nauk SSSR, Ser. Geol., No. 1, 95 (1962).
2. V. M. Konstantinov, At. Énerg., 22, No. 5, 416 (1967).

BIBLIOGRAPHY

NEW BOOKS

A. M. Petros'yants

I. N. Golovin and I. V. Kurchatov. From Scientific Research to Atomic Industry, Modern Problems of Atomic Science and Engineering in the USSR. 2nd Edition. Atomizdat, Moscow, 1972 †

Thousands of Soviet people have worked side by side, during the post-war years, with the late Academician Igor' Vasil'evich Kurchatov, who was mandated by the party and the government to head work on atomic science and engineering in the socialist fatherland.

This book (the first edition of which came out in 1967) tells of the life and deeds of this remarkable scientist, full of the joy of life, a responsive and sympathetic individual, noted for his exacting demands on himself as on others, a leading public activist, communist, fighter for peace and for collaboration between the peoples, three times Hero of Socialist Labor, a recipient of the Lenin Prize and State Prizes, and even while still living a full-fledged national hero of our people.

* * *

F. Ya. Ovchinnikov, L. M. Voronin, L. M. Golubev, et al. Operation of the Reactor Installations at the Novaya Voronezh' Nuclear Electric Power Stations. Atomizdat, Moscow, 1972

Experience in the operation of the reactor installations at the Novaya Voronezh' nuclear-fueled electric power generating station, using water-cooled water-moderated power reactor types, has been reviewed and widely disseminated in the USSR and in the COMECON member-nations. This text offers a concise presentation of the operating principles of water-cooled water-moderated power reactors, basic characteristics and a description of the reactors in service at the Novaya Voronezh' nuclear power station, radiation monitoring and emergency protection systems, and analyzes the performance of the basic equipment and process flowsheets. Close attention is given to the selection of fuel loadings and to examination of the basic characteristics of the reactor cores, to the operating conditions of the reactor units, and to topics involving nuclear and radiation safety, monitoring of the state of the metal in the process equipment and piping, decontamination, and inspection and overhaul of power equipment.

The book will be useful to specialists working in the design, installation, and adjustment of nuclear power stations, and also to students majoring in power engineering, heat transfer, and engineering physics.

* * *

† See review in Atomnaya Énergiya, Vol. 33, No. 6 (1972).

Translated from Atomnaya Énergiya, Vol. 34, No. 1, pp. 6, 16, 38, 69, 70, January, 1973.

I. A. Arshipov, G. A. Vasil'ev, Yu. A. Egorov, et al. Serpentinite Concrete for Shielding of Nuclear Reactors, Yu. A. Egorov (Editor). Atomizdat, Moscow, 1972

Physicomechanical, heat-transfer, thermal, vibrational, shielding, and other relevant properties of serpentinite concrete responsible for the great popularity of that material in reactor design and construction are described. Constants and procedures for design calculations of serpentinite shielding are cited. Topics concerning the fabrication and laying of concrete in the construction of shielding are discussed.

The text can be used as a reference manual by engineers and designers concerned with nuclear reactor shielding problems.

* * *

L. R. Kimel' and V. P. Mashkovich. Protection against Ionizing Radiations, Reference Handbook, 2nd Edition. Atomizdat, Moscow, 1972

This manual contains all necessary data for design calculations of protection and shielding installations needed for work where radioactive materials are handled. Measurement units are presented, with some information pertaining to ionizing radiations, the principal characteristics of radiation sources, limiting permissible radiation levels, and so forth. Information is provided on protection against γ-radiations, neutrons, α- and β-radiations, and x-rays. Passage of radiation through inhomogeneities in shielding is discussed.

The second edition of the handbook has been extensively revised and enlarged. Solutions of specific problems are provided as examples in the treatment of the most difficult sections. The handbook is supplemented with new tabular functions.

The book is written for engineers and physicists, research workers, graduate students, and undergraduates, and also for a wide range of persons concerned with shielding and protection against radiations in work where sources of ionizing radiations and radioactive materials are handled.

* * *

B. V. Nemirovskii, A. P. Serzhantov, and V. V. Shipulin. Operation and Maintenance of Equipment for Measurements of Ionizing Radiations, No. 2, Radiometers. Atomizdat, Moscow, 1972

Radiometric instruments are employed to monitor the radiation environment in different rooms exposed to radiations, to monitor the extent of contamination of surfaces of special clothing and protective overalls worn by personnel, and also to monitor radiation exposure of the skin of personnel, to take readings on the concentration of radioactive gases and aerosols in air and of radioactive substances in liquid, and to monitor the activity of preparations and minerals. Reference data are provided in the text on radiation monitoring instruments, on conditions and rules governing their proper use, typical designs and arrangements, adjustments, care and maintenance.

The book is written for workers and technicians engaged in services responsible for inspection, maintenance, and repair of radiometric instrumentation.

* * *

V. P. Volodin, B. A. Korotin, and E. A. Ryabova. Operation and Maintenance of Equipment for Measurements of Ionizing Radiations, No. 3, Dosimeters. Atomizdat, Moscow, 1972

Reference data are cited on the characteristics of the principal modes of ionizing radiations and their interactions with matter, the basic concepts of the dosimetry of ionizing radiations, terms, formulas, and relationships relating the characteristics of ionizing radiations to dose level, the specific requirements applicable to instruments measuring dose level and dose rate of ionizing radiations. Conditions and rules for handling and operating dosimeters of ionizing radiations, inspection, checkout, and calibration of such dosimeters, and verification of their basic performance parameters at repair and maintenance workshops, are described. Rules governing adjustment and repair, and the requisite inspection and measurement equipment, are covered in detail for each type of dosimeter.

The text is written for technicians in dosimetric service, and also for specialists dealing with radiation measurements.

* * *

V. P. Volodin, B. A. Korotkin, and A. M. Radyvanyuk. Operation and Maintenance of Equipment for Measurements of Ionizing Radiations, No. 4, Detection Units for Ionizing Radiations. Atomizdat, Moscow, 1972

Reference data are cited on the characteristics of the principal modes of ionizing radiations and their interactions with matter, on detectors, photomultipliers, and units for detecting ionizing radiation. Conditions and rules and regulations governing the use of detection units based on different design principles are presented. Standard designs and layouts of detection systems, their functions and operating principles, basic performance parameters, and the functions of subassemblies and subsystems, wiring diagrams for radiation detectors, and the effect of circuit design on the characteristics of the detection units, are among the topics discussed. Rules governing the adjustment and maintenance of detection units and of each individual functional subsystem are covered in detail.

* * *

A. A. Kurashov. Identification of Pulses from Radiation Detectors, Atomizdat, Moscow, 1972

Methods and specific circuitry needed in the identification and separate recording or analysis of pulses from detectors in the case of different species of charged particles are discussed. Attention is centered on techniques used in experimental intermediate-energy physics. A large section of the book is devoted to the methods and arrangements for separating pulses by shape that is now quite popular in neutron spectrometry. Electronic circuitry for gas, scintillation, and semiconductor detectors is discussed. Criteria for evaluating the performance of such circuits and arrangements, and recommendations on the best ways to inspect them and study their characteristics, are cited. Problems encountered in recording rare events against a considerable background of accompanying and masking radiations are discussed.

The book is written for a wide range of scientists, engineers, and technicians specializing in experimental physics. It will also be useful to graduate students and senior undergraduates majoring in electronics and physics.

* * *

R. D. Vasil'ev. Fundamentals of the Metrology of Neutron Radiations. Atomizdat, Moscow, 1972

The scientific fundamentals of the metrology of neutron measurements are laid down. Compatibility between the results of neutron measurements taken with the aid of different techniques and types of equipment is discussed. Methods of direct, indirect, and combined measurements of physical variables characterizing the neutron fields of nuclear reactors, accelerators, and isotope sources are reviewed. Ways of pinpointing, handling, and eliminating systematic errors and bias are analyzed.

Techniques for mutual comparisons of measures and measuring instruments are reviewed systematically. The problem of metrological backup and servicing of neutron measurements is analyzed in detail. Close attention is given to terminology. Pathways of development of the metrology of neutron radiations are outlined, and the principal problems are formulated.

The monograph is written for engineers, scientists, graduate and undergraduate college students specializing in nuclear physics and applied subdivisions, and also for workers in other realms of science whose activities call for ability to deal with neutron measurements.

* * *

N. M. Sinev and P. M. Udovichenko. Packless Water Pumps, 2nd Edition. Atomizdat, Moscow, 1972

The specific features of the design and calculations of packless canned centrifugal water pumps, zero-leakage pumps, used in the nuclear power industry are presented. Special attention is given to bearing supports using "water lubrication," and to calculations of the forces acting on them, as well as to the thin-walled baffle providing a pressuretight enclosure for the stator of the electric drive motor, and the conditions governing reliable pump performance.

Information is provided on the design of circulation type canned pumps on stream at the Novaya Voronezh' nuclear power station and the Belyi Yar nuclear power station, on board the icebreaker Lenin, and at various foreign nuclear power stations.

A large section in the book is devoted to packless pumps with mechanical shaft seals, i.e., to pumps featuring limited or controlled leakage.

The book is written for power engineers and for heat-transfer engineers, for designers and operators of nuclear power plants and nuclear power-generating stations. It would also be useful as a training aid for instructors and students specializing in machinery design, heat transfer, and power engineering.

* * *

F. P. Denisov and V. N. Mekhedov. Nuclear Reactions at High Energies. Atomizdat, Moscow, 1972

Results of theoretical and experimental research findings on high-energy nuclear reactions amassed over the past two decades are discussed in this text. The model of direct interaction is subjected to detailed discussion in its quantum-mechanical and classical variants (impulse approximation with distorted waves), as well as the intranuclear cascade model, and experimental data obtained by techniques involving photographic plates, radiation counters, and radiochemistry are discussed.

The book does not require any special theoretical background of the reader, and may be useful not only to experimental physicists, but also to engineers and radiochemists working on methodological and applied problems in high-energy nuclear physics.

* * *

V. S. Barashenkov and V. D. Toneev. Interaction of High-Energy Particles and Nuclei with Nuclei.

Atomizdat, 1972

The text deals with a domain of high-energy physics that is of major importance and that is undergoing rapid development: strong interactions of particles and nuclei – nuclear processes at high energies with treatment of the most recent achievements and trends in the development of the theory accounting for those processes (the optical model, and Glauber elastic-scattering theory, stochastic treatment of all aspects of intranuclear cascades, etc.).

The book will be of interest to specialists working in the field of nuclear physics and physics of elementary particles, as well as of great benefit to specialists concerned with radiation shielding of spaceships, the study of the biological effects of penetrating radiations, or the design of high-current accelerators.

* * *

L. L. Kunin, E. D. Malikova, and B. A. Chapyzhnikov. Determinations of Oxygen, Carbon, Nitrogen, and Hydrogen in Alkali Metals and Alkali Earths.

Atomizdat, Moscow, 1972

Alkali metals and alkali earths have met with broad applications as coolants in nuclear power practice. The purity of the metal, particularly freedom from gaseous impurities, is of paramount importance in these applications.

The physicochemical fundamentals of the techniques for making oxygen, carbon, nitrogen, and hydrogen determinations in alkali metals and alkali earths are explained. Close attention is given to determination of different forms in which gaseous impurities may be present in metals. Techniques for taking representative samples from a melt, and the equipment employed in analytical inspection of samples, are described. Specific analytical procedures developed in the USSR and elsewhere are covered.

The book is intended for a wide range of analytical chemists engaged in analytical control work in the metallurgical and chemical process industries, and also those engaged in the nuclear power industry, in electronics, in aerospace, etc.

* * *

Yu. P. Belyaev. Applications of Radioactive Tracers to Metallurgical Process Research.

Atomizdat, Moscow, 1972

Applications of radioactive tracers in metallurgical processes are described. The necessary information on the physicochemical fundamentals of the method, and techniques of practical applications of tracers, are cited. Particular examples of the use of radioactive tracers for research on blast-furnace, open-hearth, and converter production processes, as well as research on the crystallization processes of large-size slabs to be rolled into sheet. Special attention is reserved for mass transfer in molten steel in various metallurgical production facilities, when ingots of killed steel and rimmed steel solidify.

The book is written for engineers and technicians employed in scientific-research organizations and metallurgical plants, also for graduate and undergraduate students majoring in radioisotope techniques and in the theory of metallurgical processes.

* * *

I. M. Lipova. Nature of Metamictic Zircons. Atomizdat, Moscow, 1972

This book is devoted to metamixy, one of the urgent problems in mineralogy. Original results from an all-sided investigation of the series of zircons, which constitute a unique series, from crystalline to x-ray-amorphous differences, are reviewed. A detailed study carried out on an extensive and systematically selected collection of samples taken from different types of occurrences in the USSR and in other countries made it possible to present a complete picture of the nature of metamictic zircons. The research findings show that the metamictic state of the mineral is due primarily to the effects of ionizing radiations of uranium and thorium incorporated in the composition of the mineral.

The book is written for mineralogists, crystal chemists, and crystal physicists.

* * *

G. A. Krestov. Thermochemistry of Compounds of Rare-Earth and Actinoid Elements. Atomizdat, Moscow, 1972

The use of thermodynamical characteristics to determine various properties of ions and compounds of all the rare-earth and actinoid elements is discussed in this monograph from the vantage points of currently held concepts. The new standard states for ions in the gaseous state and in solution introduced by the author are used in the text. A systematic analysis of the dependence of interionic distances and crystal–chemical radii of ions on the temperature is carried out. Many unknown properties of the ions and compounds of rare-earth actinoid elements are determined at different temperatures. Modern viewpoints on solvation of ions, the structure of water and ionic solutions are discussed. The thermodynamical characteristics of structural changes in water in response to hydration of ions of rare-earth and actinoid elements are introduced, and also in response to dissolution of the compounds in water.

The text may be a useful aid to research workers, engineers, instructors, graduate students, and senior undergraduates.

* * *

V. L. Barsukov, G. D. Gladyshev, V. N. Kozyrev, et al. Conditions Governing the Formation of Uranium Occurrences in Volcanic Depressions, Edited by Corresponding Member of the USSR Academy of Sciences A. I. Tugarinov. Atomizdat, Moscow, 1972

Conditions governing the formation of uranium occurrences in volcanic depressions typical of many ore provinces in Eurasia and America are discussed in the text. It is demonstrated that the solutions circulating within the confines of the depressions play an important role in ore formation, often showing an acidic reaction, and containing appreciably high concentrations of sulfates, chlorides, and carbonates.

Attention is focused on physicochemical analysis of interactions between ore-bearing solutions with effusive-sedimentary rocks in the depression, and the changes they bring about in the composition of the rocks and solutions. It is established that this interaction is the principal reason for the deposition of uranium and the components accompanying it.

The book is written for a broad readership of geologists, working either in production or at scientific research institutes. It will also be useful to students at graduate or undergraduate level specializing in economic geology.

* * *

Yu. A. Shukolyukov and L. K. Levskii. Geochemistry and Cosmochemistry of Isotopes of the Noble Gases. Atomizdat, Moscow, 1972

This text is the first review literature on the geochemistry and space chemistry of isotopes of the noble gases. Nuclear reactions leading to the formation of isotopes of the noble gases in the lithosphere, isotope anomalies in various media, migration of isotope gases through the lithosphere, hydrosphere, and atmosphere are discussed. Concepts relating to the history of isotopes of the noble gases in the evolution of the lithosphere, hydrosphere, and atmosphere of the earth are put forth. Light is shed on the present status of the problem of the cosmochemistry of isotopes of the noble gases, with attention given to their cosmogenic, radiogenetic, and primary isotopes contained in meteoritic matter and in lunar matter. Possibilities of utilizing isotopes of the noble gases in the solution of various problems in cosmology are explored.

The book is intended for research geochemists, radiochemists, geologists, physicists, and also for instructors, graduate students, and senior undergraduates in the appropriate specialties.

* * *

J. Matthews and R. Walker. Mathematical Methods in Physics (translated from the English). Atomizdat, Moscow, 1972

This book comprises a lecture course given by R. Feynmann at the California Institute of Technology. Most of the standard topics in mathematical physics are discussed in the text in an unusual and novel manner. Normal oscillations of certain symmetric configurations are analyzed by the methods of group theory, there is a diagrammatic decomposition of the Fredholm solution of linear integral equations, dispersion relations and related integral equations are discussed, and, finally, there is a detailed discussion of applications of the theory of probabilities to processing of experimental data.

The book can be used by student majors in physics as a textbook on methods of mathematical physics, and can also be useful to scientists and students studying these topics on their own.

* * *

V. M. Baier, V. M. Katkov, and V. S. Fadin. Radiation of Relativistic Electrons. Atomizdat, Moscow, 1972

This book is devoted to a systematic presentation of the theory of bremsstrahlung and pair production in the passage of a high-energy particle through an externally applied field, or in the collision of high-energy charged particles, with acknowledgement of polarization effects and spin effects. Special features of electromagnetic processes at high energies which aid in simplifying the radiation of relativistic electrons appreciably are given close attention. The book is the first monograph to appear with a detailed discussion of this realm of electromagnetic phenomena.

The book is intended for specialists in the field of high-energy physics and elementary particles, who are concerned with the design and applications of accelerators and storage rings, and may also be found useful by instructors and graduate students in physics.

* * *

E. Kowalski. Nuclear Electronics (translated from the English), Edited by I. V. Shtranikh. Atomizdat, Moscow, 1972

Applications of the widely used nuclear radiation detectors, the particular features of the pulses they generate, pulse shaping, amplification, discrimination of signals from similar detectors, performance

of various arithmetic operations with those signals in analog form, and so on, as well as details of processing those signals, in relation to the statistical nature of their pulse height and time distribution, are discussed. Devices converting the pulse height of signals to analog form, devices recording time intervals, digital pulse counters and digital logic devices for performing arithmetical operations on them on the basis of applications of Boolean algebra, are described.

The design principles of recording single-channel and multichannel systems, including the method of direct application of digital computers for that purpose, are outlined in brief.

The book is written for experimental physicists; it will also be useful to engineers working in electronics, and to instructors and students at engineering colleges.

* * *

A. Lichtenberg. Particle Dynamics in Phase Space (translated from the English). Atomizdat, Moscow, 1972

This book deals with the fundamentals of the theory behind the concept of phase volume, and the problems concerned with utilizing the concept in calculations of beam optics, acceleration and confinement of charged particles. A unified presentation of these topics is made available for the first time.

The author develops the concept of phase space in the theory of the motion of charged particles in electromagnetic fields. Some basic concepts of phase space are introduced, and the discussion proceeds to the adiabatic invariance of systems with one or more degrees of freedom, while the theory of transformation of phase space is presented. Topics in the theory of oscillations, optics of beams of charged particles, particle dynamics in accelerators, and confinement and heating of plasma, are discussed from the vantage points of the general theory. In particular, a detailed treatment is given of such topics as the effect of radiation and space charge on the motion of particles, maximization of particle capture effectiveness in a synchrotron, multiturn injection into storage rings, plasma heating techniques, and particle capture in magnetic traps.

The monograph is written for a broad range of research scientists, graduate students, and senior undergraduates specializing in the areas covered.

* * *

B. Taylor, V. Parker, and D. Langenberg. Fundamental Constants and Quantum Electrodynamics (translated from the English). Atomizdat, Moscow, 1972

This book constitutes a unique survey of precision measurements of the fundamental physical constants, and contains recommendations on their use in several branches of physics, ranging from solid state physics to quantum electrodynamics.

There is a detailed survey of experimental papers on measurements on the fundamental physical constants and their most highly refined values.

The book is written for a broad readership of experimental physicists, and can be used by specialists working in different branches of physics.

* * *

J. Hirt and I. Lote, Theory of Dislocations (translated from the English), Yu. A. Osip'yan and E. M. Nadgornyi (Editors). Atomizdat, Moscow, 1972

This book can be regarded as the first textbook, in the world literature, on the theory of dislocation. The presentation is given on a fairly high and up-to-date scientific level, reflecting achievements scored

in recent years in the field of dislocation theory. The properties, behavior, and interaction of dislocations in crystalline materials is discussed in detailed fashion, with a rather serious mathematical groundwork built up for the physical models considered. The effect of the crystal structure on the properties and behavior of dislocations is demonstrated. Reference material at the back of the book covers elastic constants of materials and values of surface energies.

The book is written for research scientists engaged in various branches of the physics and chemistry of solids, and in metal physics. The text is of especial value for its independent development to specific applied problems which will be of interest to a broad range of specialists.

ARTICLES

DOSIMETRY OF γ AND NEUTRON RADIATION WITH A SCINTILLATION SPECTROMETER

V. P. Kovalev, S. P. Kapchigashev, and L. P. Pavlov

UDC 539.12.08

This paper discusses the possibility of using a scintillation spectrometer having a stilbene crystal as a dosimeter for the dosimetry of mixed γ and neutron radiation. The use of the well-known principle of pulse-shape discrimination makes it possible to determine the dose from neutrons and γ rays separately by means of such a technique.

γ-Ray Dosimetry

If $(dN/dE_e)(E_e)$ is the differential spectrum of the electrons produced in the scintillator, the dose deposited in tissue by γ rays from an arbitrary spectrum can be computed from the expression

$$D = AQ(E_\gamma) K [D'_e + D''_e], \quad (1)$$

where A is a calibration coefficient; K is a coefficient for conversion from absorbed energy to dose, rad; $Q(E_\gamma)$ is a conversion coefficient from dose measured in the scintillator to dose in tissue; $D'_e = \int_{E_{e\,th}}^{E_{e\,max}} (dN/dE_e)(E_e) E_e dE_e$; $D''_e = \int_0^{E_{e\,th}} (dN/dE_e)(E_e) E_e dE_e$. The quantity D''_e defines the dose from electrons with energies below the threshold for separation of the neutron and γ-ray components and is not measured directly. The fraction in this dose depends both on the γ-ray spectrum and on the value of the threshold ($E_{e\,th}$). In general, this quantity also determines the inaccuracy of γ-ray dose measurements in mixed fields.

However, experimental studies have shown that near the threshold for separation of the (γ−n) components, the instrumental spectrum of electrons in a stilbene crystal can be described with satisfactory accuracy by the function $(dN/dE_e)(E_e) = Ce^{-\alpha E_e}$. The studies were carried out over the γ-ray energy range 0.2-4.5 MeV. In this case, only the quantity α in the exponent varies.

Thus the contribution D''_e to the total dose can be determined by extrapolation of the dependence $(dN/dE_e)(E_e)$ from the region of electron energies above the threshold to the unmeasured energy region ($E_e < E_{e\,th}$). A similar method for estimating D''_e was used in [1] in studies of the γ-ray dose from various targets bombarded by α particles with an initial energy of 42 MeV. Calculations showed that the conversion coefficient $Q(E_\gamma)$, which takes into account the lack of tissue equivalence for a stilbene crystal in the γ-ray energy range from 0.1 to 20 MeV, differed from 1 by no more than 1-3%.

TABLE 1. Dose Ratios for Neutrons and γ-Rays

Source	This work	Reference			
		[7]	[6]	[5]	[6]
Pu—Be	1,7±0,2	0,07	2,5	—	—
Po—Be	—	2,5	—	1,84	2,5

TABLE 2. Doses and Dose Ratios of Neutron and γ Components of Radiation Field

Layer thickness, cm	D_n, $\frac{rad}{h \cdot \mu A}$	D_γ, $\frac{rad}{h \cdot \mu A}$	D_n/D_γ
0	11,4	3800	$3 \cdot 10^{-3}$
50	0,38±0,04	0,18±0,01	2,1±0,2

Translated from Atomnaya Énergiya, Vol. 34, No. 1, pp. 7-10, January, 1973. Original article submitted June 7, 1971.

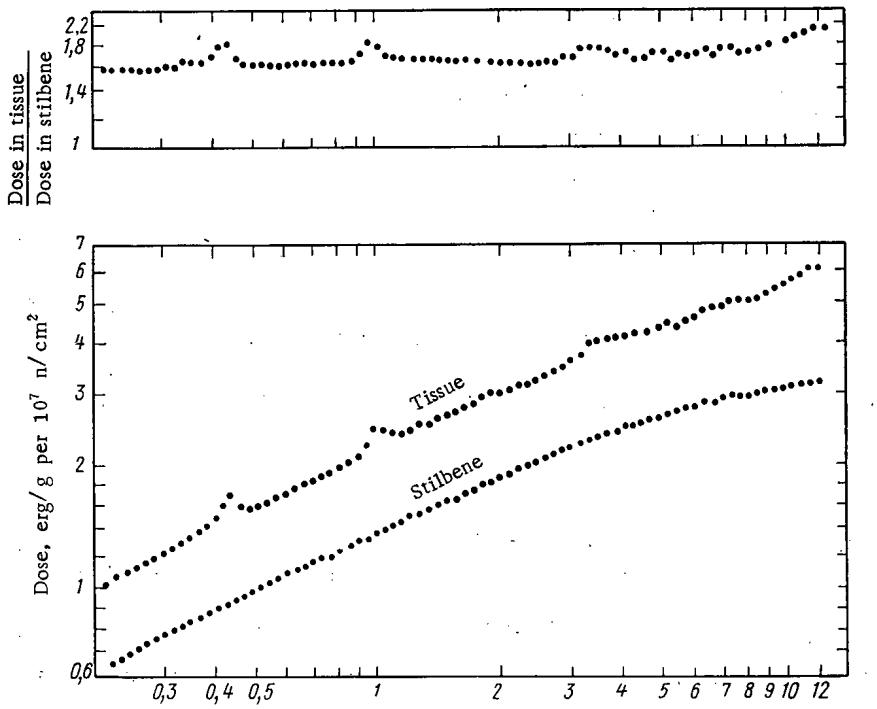

Fig. 1. Dependence of deposited dose on fast-neutron energy for tissue and stilbene.

Neutron Dosimetry

In interactions with organic scintillators, the energy of fast neutrons is transformed into the energy of charged particles mainly through (n–p) scattering by hydrogen and also because of elastic scattering and (n, α) reactions in carbon. However, a carbon nucleus acquires an insignificant amount of energy through elastic scattering and the efficiency for conversion of this energy into light is considerably less than that for recoil protons. The cross section for the C^{12} (n, α)B^9 reaction is several order of magnitude less than the scattering cross section for hydrogen.

Thus only (n–p) scattering in hydrogen makes a contribution to the measured dose in neutron dosimetry with a stilbene crystal.

If $(dN/dE_p)(E_p)$ is the differential spectrum of recoil protons, the dose deposited in tissue by neutrons from an arbitrary spectrum can be calculated (as above) from the expression

$$D = AQ(E_n)\, K\, [D'_p + D''_p]. \tag{2}$$

In the general case, the conversion coefficient $Q(E_n)$ depends on the neutron energy and is determined in the following manner:

$$Q(E_n) = \frac{\sum_i K_i(E_n)\, f_i}{K_H(E_n)\, f_H}, \tag{3}$$

where f_i is the weight percent content of the i-th element in tissue; $K_i(E_n)$ is the energy transferred to the i-th element (kerma) by neutrons with an energy E_n as the result of all possible nuclear reactions; f_H and $K_H(E_n)$ are respectively the percent content of hydrogen in stilbene and the energy transferred to a hydrogen nucleus by neutrons with an energy E_n.

Calculations of the coefficient $Q(E_n)$ were made for the neutron energy range 0.2-14 MeV on the basis of kerma data for hydrogen, carbon, nitrogen, and oxygen given in [2].

The chemical composition of tissue was assumed to be the following (in wt.%): H, 10; C, 12; N, 4; O, 73; and other elements, 1. The chemical formula for a stilbene crystal is $C_{14}H_{12}$ with the following

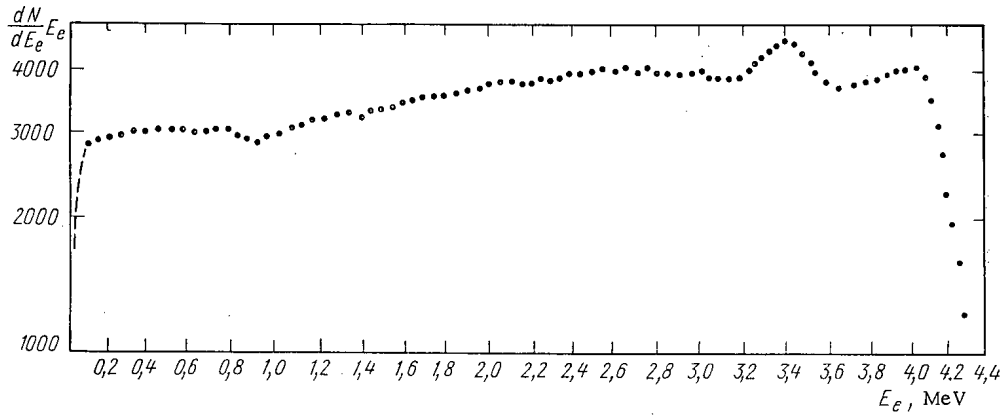

Fig. 2. Dependence of intensity $(dN/dE_e)E_e$ on electron energy.

composition: H, 6.7 wt.%; C, 93.3 wt.%. Results of a calculation of the coefficient $Q(E_n)$ as a function of neutron energy are shown in Fig. 1. The peaks in the region of 0.44 and 1 MeV are the result of resonances in the (n, n'γ) reaction in oxygen. The slow rise at neutron energies above 20 MeV is explained by the decrease in the (n–p) scattering cross section in hydrogen and the simultaneous increase in the cross sections for neutron interactions in carbon, nitrogen, and chiefly oxygen. Despite some fluctuations, the function varies from 1.6 to 1.8 in the energy range up to 10 MeV. The average value of the conversion coefficient for this range is given as $\bar{Q}(E_n) = 1.7 \pm 0.1$, which can lead to an uncertainty of the order of 6% in the conversion from measured to true tissue dose.

Where the light output of a stilbene crystal for electrons above a few tens of keV is independent of electron energy and consequently the measured pulse height distribution is the electron spectrum, for protons the light output depends significantly on energy and the spectrum of recoil protons is determined from the instrumental distribution dN/ds in the following manner:

$$\frac{dN}{dE_p}(E_p) = \frac{dN}{ds}\frac{ds}{dE_p}(E_p).$$

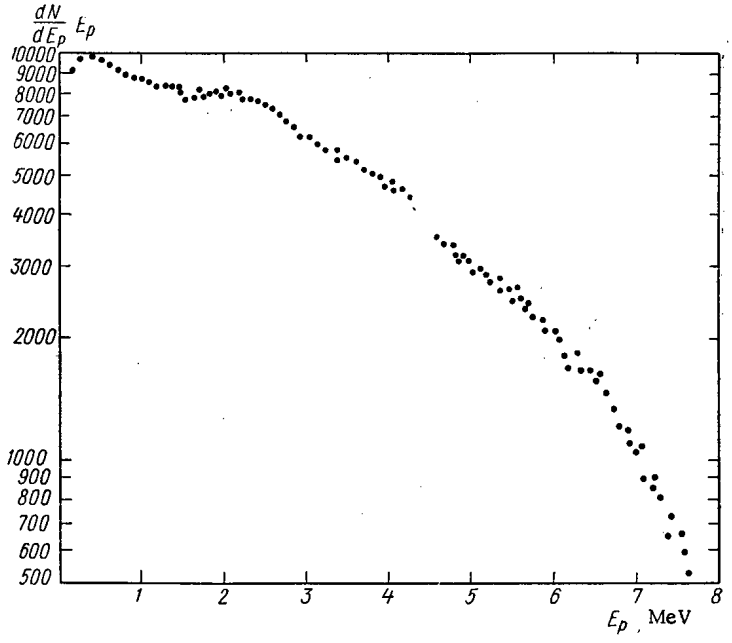

Fig. 3. Dependence of intensity $(dN/dE_p)E_p$ on recoil proton energy.

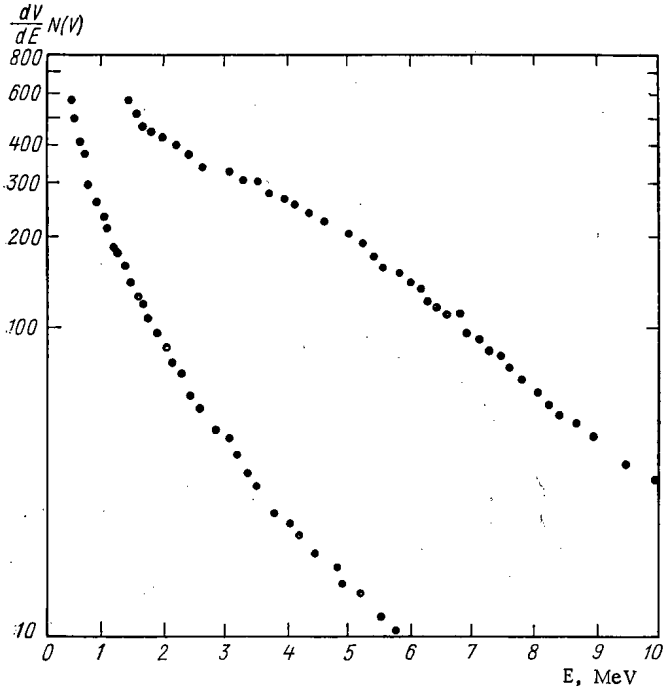

Fig. 4. Spectra of secondary electrons and recoil protons produced by mixed radiation.

In this work, data on the light yields ds/dE_p given in [3] was used in the determination of recoil proton spectra. It should be noted that the measurement accuracy for a neutron dose is somewhat poorer than the accuracy of a γ-ray dose measurement and is mainly determined by the discrimination level for γ-ray pulses.

Dose Characteristics of (Pu–Be) Source

To illustrate the possibilities of the dosimetry method presented above, studies were made of the ratio of the dose from neutrons and γ-rays from a Pu–Be source. Measurements were made with a neutron spectrometer having a stilbene crystal 30 × 30 mm in size and an FÉU-13 photomultiplier. The spectrometric threshold for electrons was 0.1 MeV with a suppression coefficient of $\sim 10^3$ for neutron or γ-radiation.

Figures 2 and 3 show curves for the energy dependence of the intensity (dN/dE)E for electrons and recoil protons in the case of a Pu–Be source having a strength of $4.6 \cdot 10^5$ n/sec. The ratio of neutron dose to γ-ray dose obtained from this data is shown in Table 1. The table also shows calculated results for the dose ratio based on the study of γ-ray yield per neutron for a Pu–Be source [4] and on data from [5, 6].

Satisfactory agreement of the dose ratio D_n/D_γ obtained in the present work with calculated results is observed. At the same time, a considerable disparity is observed between the results obtained for the quantity D_n/D_γ and the data given in [7].

Study of Mixed-Radiation Source (LUÉ-25)

A study was made with an LUÉ-25 linear electron accelerator. A layer of iron 50 cm thick was used as a shield which was located at an angle of 120° to the direction of the electron beam. The distance from the tungsten target (a disk 40 mm in diameter and 8 mm thick) to the front wall of the shield was 700 cm. The scintillation dosimeter was located directly behind the shield. The spectra of secondary electrons and recoil protons produced in the stilbene crystal are shown in Fig. 4. The neutron dose (D_n) and γ-ray dose (D_γ) behind the layer of iron obtained from this data were reduced to the dose values at a distance R = 50 cm and are given in Table 2. The table also gives the value of the mixed-radiation dose in the absence of a shield (x = 0). In this case, the γ-ray dose was measured with a ferrous sulfate dosimeter, and the neutron component of the total dose was determined by calculation based on the known integral yield of

neutrons. The results of the study show that the use of an iron shield 50 cm thick leads to an increase in the D_n/D_γ ratio by approximately a factor of 10^3 in the mixed-radiation field from the target of a linear electron accelerator.

The authors are grateful to N. V. Rodionov for help in the construction of the neutron scintillation spectrometer.

LITERATURE CITED

1. S. S. Omarov et al., At. Énerg., 26, 390 (1969).
2. R. Bach and R. Caswell, Rad. Res., 35, 1 (1968).
3. Yu. A. Kazanskii et al., At. Énerg., 20, 143 (1966).
4. D. Drake et al., Nucl. Instrum. and Methods, 62, 349 (1968).
5. N. A. Bak and N. S. Shimanskaya, Neutron Sources [in Russian], Atomizdat, Moscow (1969).
6. A. T. Bakov et al., Neutron Monitoring, IAEA, Vienna (1967), p. 201.
7. G. M. Fradkin, Isotopic Neutron Sources [in Russian], Gosatomizdat, Moscow (1963).

CHARACTERISTICS OF THE PERSONNEL NEUTRON TRACK DOSIMETER DINA

I. B. Keirim-Markus, T. V. Koroleva, S. N. Kraitor, and L. N. Uspenskii

UDC 539.12.08

The personnel neutron dosimeter DINA based on the use of fission fragment track detectors containing Np^{237} behind a B^{10} filter and U^{235} was proposed in [1]. The composition of the fissile isotopes in the dosimeter and the filter thickness were chosen so that its energy characteristic best reproduced the energy dependence of neutron kerma or of neutron kerma equivalent, i.e., those dosimetric quantities which should be measured by a personnel dosimeter. In accordance with this, the measurement of neutron dose is reduced to the counting of tracks from fission fragments and the multiplication of the resultant number of tracks by the track value. The latter is weakly dependent on the neutron spectra which may be encountered during irradiation. Estimates made in [1] showed that the spread in track value does not exceed 15% for actual neutron spectra in rooms.

A study was made of the characteristics of the DINA personnel dosimeter which are important in its practical use (dosimeter sensitivity, dependence of its readings on distance from surface of the body and angle of irradiation, effect of neutron spectrum on track value).

Experiments were carried out with a dosimeter consisting of two fission fragment detectors, in one of which there was a Np^{237} target with a boron filter and in the other, a U^{235} target (Fig. 1). Fission

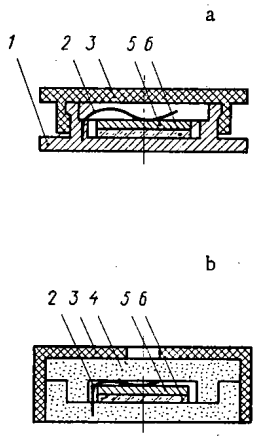

Fig. 1

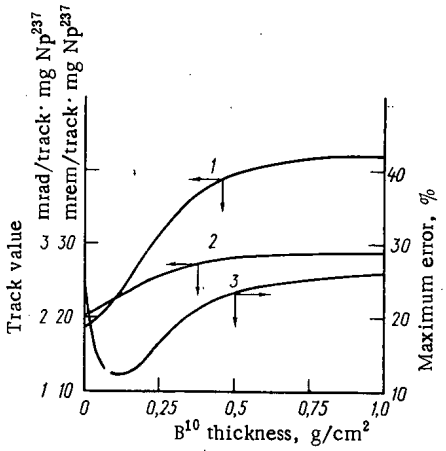

Fig. 2

Fig. 1. Construction of neutron personnel dosimeter. a) Detector containing U^{235}; b) detector containing Np^{237}; 1) case; 2) spring; 3) polyethylene cap; 4) B^{10} filter 0.1 g/cm^2 thick; 5) target; 6) glass track detector.

Fig. 2. Track value of the personnel dosimeter for accident (1) and routine (2) monitoring and maximum measurement error (3) as functions of boron filter thickness.

Translated from Atomnaya Énergiya, Vol. 34, No. 1, pp. 11-15, January, 1973. Original article submitted February 23, 1972; revision submitted May 29, 1972.

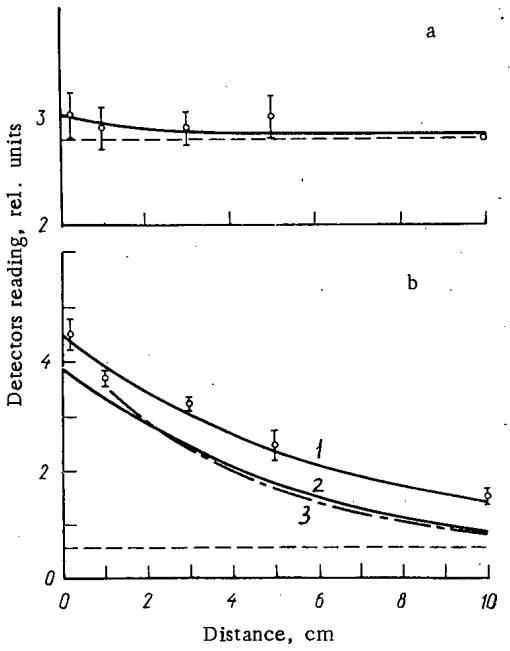

Fig. 3

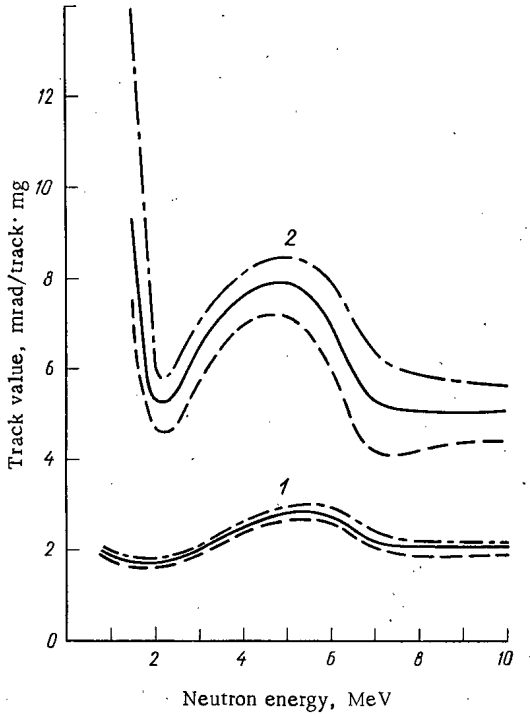

Fig. 4

Fig. 3. Personnel dosimeter readings as a function of distance to phantom surface. a) Detector containing Np^{237} + 0.1 g/cm^2 B^{10}; b) detector containing U^{235}; dashed lines) measurements without phantom; 1) total reading of detector with U^{235}; 2) thermal neutrons from phantom; 3) calculation for disk isotropic source.

Fig. 4. Energy dependence of track value for personnel dosimeter (1), and detector containing U^{238} (2) for irradiation at angles of 0 (dashed line), 45 (straight line), and 90° (dash-dot line).

fragments were recorded by track detectors made of silicate glass which were etched after irradiation for 9 min in 5% hydrofluoric acid and counted under an MBI-9 microscope. Target and detector areas were 1 cm^2 and target thickness was 0.2-0.5 mg/cm^2. Fast-neutron calibration was done with a Pu–Be source and thermal calibration with a Pu–Be source in a paraffin moderator.

The personnel dosimeter track value $\Delta(E)$ is given by the expression

$$\Delta(E) = \frac{\delta(E)}{\sigma_f(E)\,\varepsilon_f n}, \tag{1}$$

where $\delta(E)$ is the specific kerma or kerma equivalent for neutrons of energy E; $\sigma_f(E)$ is the fission cross section; ε_f is the fission fragment detection efficiency; n is the number of nuclei of the fissile isotope in the dosimeter. The track value averaged over a neutron spectrum for optimal isotopic composition in the dosimeter (99.76% Np^{237} and 0.24% U^{235}) was calculated from

$$\bar{\Delta} = \frac{\int \delta(E)\,\varphi(E)\,dE}{\int \sigma_f^{\text{eff}}\,\text{Np}(E)\,\varepsilon_f n\varphi(E)\,dE}, \tag{2}$$

where $\sigma_f^{\text{eff}}\,\text{Np}(E)$ is the effective fission cross section for Np^{237} behind a boron filter, and $\varphi(E)$ is the differential neutron fluence.

Since sensitivity depends on filter thickness, calculations were made for various B^{10} thicknesses. Computed results averaged over the set of spectra [1] for kerma and kerma equivalent are shown in Fig. 2. The same figures gives the dependence of the maximum error of measurement obtained in [1] for a set of actual neutron spectra. Sine the optimal composition of isotopes in the dosimeter is identical for the measurement of kerma and kerma equivalent, the errors are the same. Thus the DINA dosimeter can be used for accident and routine monitoring merely by changing the dose value of a track.

TABLE 1. Track Value for Np^{237} in the DINA Neutron Personnel Dosimeter and for a U^{238} Detector at Various Irradiation Angles

Detector	Track value, mrad/track · mg								
	Pu-Be source			fission spectrum			reactor spectrum		
	0°	45°	90°	0°	45°	90°	0°	45°	90°
DINA personnel dosimeter	2,20	2,35	2,45	2,10	2,21	2,30	2,41	2,52	2,62
U^{238}	8,7	10,0	10,9	10,0	11,4	13,3	14,1	16,4	19,1

Figure 2 indicates that the optimal thickness of the B^{10} filter is 0.1-0.15 g/cm^2. For this thickness, track value for accident monitoring is about 2 mrad/track · mg Np^{237}, and for routine monitoring, about 20 mrem/track · mg Np^{237}. Such a value makes it possible to measure neutron dose in the 5-5000 rad range (this corresponds to the recommendations of the IAEA [2]) with a statistical error no worse than 2% and to measure a dose equivalent of 0.5 rem and above (which corresponds to the maximum permissible quarterly dose in accordance with the requirements of NRB-69 [3]) with a statistical accuracy no worse than 15%.

Since a personnel dosimeter is intended for the measurement of the maximum value of neutron dose at the surface of the body, it is important to evaluate the effect of possible poor approximation of the dosimeter to the body. These evaluations were made by an analysis of the dependence of DINA dosimeter readings on distance to the surface of a tissue-equivalent phantom of the human torso. The measurements were made in a collimated beam from the IBR reactor at JINR [4] at 10 m from the core. The phantom was an elliptical cylinder having semiaxes of 12.7 and 18 cm and a height of 60 cm, which was filled with a tissue-equivalent liquid; the thickness of the vinyl plastic shell of the phantom was 0.3 cm [5]. Dosimeters were set up on the line of the minor semiaxis at various distances from the surface of the phantom with mutual shielding being avoided. The irradiation field was uniform within the limits of a circle 40 cm in diameter.

Figure 3 shows measurement results for detectors containing Np^{237} and U^{235}. Readings of the detector with Np^{237} at the phantom surface were a few percent higher than in air because of fast neutron albedo; furthermore, they depended weakly on distance to the surface since the fast neutrons from the reactor are the predominant factor.

Readings from the detector containing U^{235} depend significantly on distance since the thermal neutron fluence from the phantom is dominant and, at the phantom surface, it is seven times greater than the contribution of thermal neutrons incident on the detector directly from the core. As the distance from the surface increases, the thermal neutron fluence decreases. This dependence is close to that calculated for a disc isotropic source 40 cm in diameter (see Fig. 3). It was obtained on the basis of [6] from

$$\Phi_{\text{therm}}(z) = \frac{A}{4\pi R^2} \ln\left(1+\frac{R^2}{z^2}\right), \tag{3}$$

where A is a constant, z is the distance from the phantom surface, and R = 20 cm is the radius of a disk source equal to the radius of the neutron beam. The calculated dependence was normalized to the experimental values at a distance of 2.5 cm from the phantom.

Measurements were made with an Np^{237} detector for phantom irradiation at angles of 45 and 90° to the surface. These results were similar to those for irradiation along the normal within the limits of experimental error ($\sim$10%).

Thus the readings of the personnel dosimeter for intermediate and fast neutrons within the range of 10 cm from the surface of the body are practically unchanged with distance. Therefore, there is no need to place the dosimeter close to the body (without loss of accuracy, it can be fastened to a pocket on protective clothing and not on a belt). The kerma of thermal and slow neutrons vary by approximately a factor of two at these distances; however, the thermal neutron contribution to total neutron kerma is small as a rule.

When using an accident personnel dosimeter, it is important that its readings do not depend on the direction of irradiation. In track detectors, however, such a dependence appears with fast neutron fission because of the anisotropy of the fission fragment distribution [7]. To evaluate this factor, the track value for Np^{237} in the DINA personnel dosimeter was calculated for various angles of irradiation. The calculation made use of the expression

TABLE 2. Characteristics of the DINA Personnel Neutron Dosimeter

Neutron spectrum	Dosimeter location	Kerma measurement, rad			Track value mrad	Maximum error with respect to set of threshold detectors, %	
		DINA dosimeter	set of threshold detector	Ionization chambers	track · mg Np^{237}	experiment	calculation
IBR spectrum at JNR outside water filter (4 cm thick)	Air	47,5	45,0	—	2,13	5,2	6,0
	Front surface of phantom	49,5	48,3	—	2,15	4,5	4,1
	Rear surface	1,47	1,46	—	2,36	0,5	—1,5
Fission neutrons outside water shield	Air	9,0	8,5	—	2,13	5,4	6,6
	Front surface of phantom	9,6	9,2	9,7	2,18	4,4	5,3
	Rear surface	1,41	1,46	—	2,30	—3,5	—2,0
Fission neutrons outside iron shield	Front surface of phantom	1,94	2,08	2,0	2,48	—6,7	—2,3
Fission neutrons outside iron–polyethylene shield	Front surface of phantom	2,37	2,65	2,58	2,50	—10	—6,6
IRT-1000, boron–lead filter	Air	28,2	26,6	26,1	2,12	6,0	7,0

$$\Delta(E, \theta) = \frac{\delta(E)}{\sigma_f(E)\,\varepsilon_f(E, \theta)\,n}, \tag{4}$$

where θ is the angle of irradiation with respect to the normal to the detector surface, and $\varepsilon_f(E, \theta)$ is the detection efficiency, taken from [8], for fission fragment detection by a silicate glass track detector.

Computed results are shown in Fig. 4 for irradiation angles of 0, 45, and 90°. Shown there also for comparison are the results of similar calculations for a detector containing U^{238}, which is also used in personnel dosimeters in certain cases [9]. As should be expected, the track dose value depends on angle of irradiation. Its variation for irradiation at angles of 0 and 90° is 5-10% for Np^{237} and 15-25% for U^{238}.

In dosimetric measurements, one must deal not with monoenergetic neutrons but with some spectrum $\varphi(E)$; therefore a track value averaged over several spectra was calculated. We chose the spectrum from a Pu–Be source, which is often used in dosimeter calibration, the fission spectrum, and the spectrum from a water-cooled, water-moderated reactor [10], which is close to that met in practice. Averaging was performed in accordance with

$$\overline{\Delta(\theta)} = \frac{\int \Delta(E, \theta)\,\varphi(E)\,dE}{\int \varphi(E)\,dE}. \tag{5}$$

The results are given in Table 1. It is clear that the greatest variation in averaged track value is observed for U^{238}, in which fission anisotropy is greater than in Np^{237}. Such a variation along with the uncertainty in irradiation direction leads to additional error in the evaluation of neutron dose. It is small, amounting to 3-5%, for a Np^{237} dosimeter, but is considerably higher (15-22%) for U^{238} and significantly limits the accuracy of dosimetric measurements.

The angular dependence of the readings from the DINA personnel neutron dosimeter and from a detector containing U^{238} were determined experimentally at the IBR reactor at JINR by irradiation of the dosimeters with a collimated beam of neutrons at angles of 0, 45, and 90° to the target surface. With respect to the 45° angle, the variation of track value for U^{238} was 18% (0° angle); the corresponding values for Np^{237} were 3% and −2.7%. These quantities correspond to the values calculated from Eq. (5) for the neutron spectrum from the IBR reactor at JINR measured in [11].

The data presented above was obtained for dosimeters in air and give an upper estimate of the angular dependence. At the surface of a phantom, the effect of anisotropy on the value of the dose will be somewhat less because of the increase in the contribution to the dose from intermediate neutrons having an

isotropic angular distribution. For U^{235}, the fission of which is produced almost entirely by thermal neutrons, angular dependence is absent both in air and at the surface of a phantom because the distribution of thermal neutron fission fragments is isotropic.

To determine the effect of the response to hardness on the readings of the DINA personnel neutron dosimeter, it was irradiated by fission neutrons outside shields of water, iron, and iron–polyethylene. At the IBR reactor at JINR, dosimeter irradiation was outside a layer of water 4 cm thick and at the IRT-1000 reactor, outside a boron–lead filter [12] with the dosimeters being located both in air and on the surface of a phantom. The results are given in Table 2; shown there also are values of neutron kerma obtained at the same points with a spectrometric set of threshold detectors [11, 13] and kerma values obtained by V. I. Tsvetkov and E. N. Chernov with tissue-equivalent and graphite ionization chambers [14]. Table 2 indicates that the results of kerma measurements by the various methods agree with the limits +10%. In evaluating the response to hardness, the maximum error η of the kerma measurements was calculated with respect to the spectrum obtained from the set of threshold detectors. It agrees with the error in measurement of kerma equivalent and is given by

$$\eta = 1 - \frac{\int \delta(E)\,\varphi(E)\,dE}{\int \Delta(E)\,\varphi(E)\,dE}. \qquad (6)$$

The errors shown in Table 2 are in agreement with experimental errors. The same table gives track values of the DINA personnel dosimeter for various neutron spectra. Its average value, 2.3 mrad/track · mg Np^{237}, has a variance of ±8% and agrees with the calculated value of 2.2 mrad/track · mg Np^{237} (see Fig. 2).

The authors thank L. B. Pikel'ner, N. N. Khot'ko, V. I. Tsvetkov, and E. N. Chernov for valuable discussions and for help with the measurements.

LITERATURE CITED

1. I. A. Bochvar et al., Handling of Radiation Accidents, Proc. Symp, IAEA, Vienna (1969), p. 235.
2. Nuclear Accident Dosimetry Systems, Proc. IAEA Panel, Vienna (1970).
3. Radiation Safety Standards (NRB-69), Atomizdat, Moscow (1970).
4. G. E. Blokhin et al., At. Énerg., 10, 437 (1961).
5. V. G. Zolotukhin et al., Neutron Tissue Doses [in Russian], Atomizdat, Moscow (1972).
6. B. Price, C. Horton, and K. Spinney, Radiation Shielding [Russian translation], Izd-vo Inostr. Lit., Moscow (1959).
7. T. V. Koroleva and S. N. Kraitor, At. Énerg., 31, 52 (1971).
8. T. V. Koroleva and S. N. Kraitor, in: Metrology of Neutron Radiation at Reactors and Accelerators, VNIIFTRI, Moscow (1971), p. 74.
9. G. M. Obaturov and Yu. K. Chumbarov, in: Problems of Dosimetry and Radiation Shielding [in Russian], No. 10, Atomizdat, Moscow (1969), p. 155.
10. Yu. A. Egorov, V. I. Zharkov, and V. V. Postnikov, At. Énerg., 28, 170 (1970).
11. K. K. Koshaeva, S. N. Kraitor, and L. B. Pikel'ner, At. Énerg., 32, 68 (1972).
12. Yu. I. Bregadze et al., At. Énerg., 12, 537 (1962).
13. T. V. Koroleva, K. K. Koshaeva, and S. N. Kraitor, At. Énerg., 32, 157 (1972).
14. V. N. Khrapachevskii, in: Biological Effects of Fast Neutrons [in Russian], No. 1, Naukova Dumka, Kiev (1969), p. 11.

ACTIVATION OF THE WATER COOLING SYNCHROCYCLOTRON COMPONENTS

M. M. Komochkov and Yu. G. Teterev

UDC 539.16.04:621.348.67

Recent improvements to the 680 MeV proton synchrocyclotron in the Laboratory of Nuclear Problems of the Joint Institute for Nuclear Research, aimed at increasing the intensity of the proton and secondary-particle beam by several tens of times, have necessitated a more precise study of the degree of radiation hazard due to the activation of the water cooling various parts of the accelerator. It is important to know tha laws governing the accumulation of radioactivity in the water and the changes taking place in this radioactivity. In order to obtain this information we studied the amount of γ-radioactive isotopes with a life of more than 20 min in the water cooling those synchrocyclotron components subjected to the most intensive irradiation, and also measured the field of γ-radiation close to the tubes of the cooling system. Similar investigations were carried out on a linear electron accelerator by Warren [1].

Cooling System

The cooling system of the synchrocyclotron constitutes a closed circuit communicating with the atmosphere. The volume of the circuit is ~ 36 m^3. The accelerator and the water-supply system of the cooling circuit are sited in different buildings. The heated water from the accelerator building passes into the building containing the heat exchanger and recirculation pump through six tubes 130 mm in diameter, which at the same time act as a reserve volume.

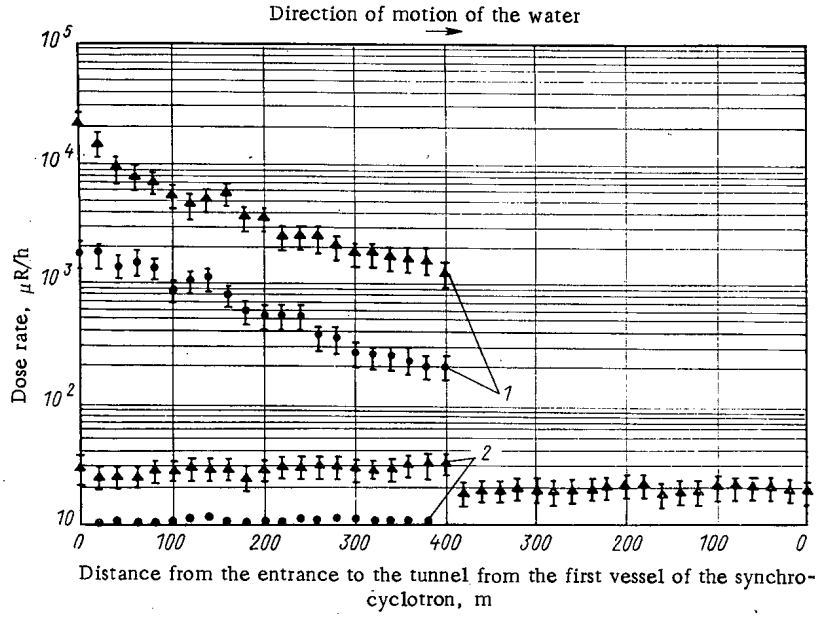

Fig. 1. Distribution of dose rate along the tubes of the cooling circuit: Δ) close to the tube; •) at a distance of 90 cm from the first tube; 1) with the accelerator working; 2) after stopping the accelerator (after 3.5 h).

Translated from Atomnaya Énergiya, Vol. 34, No. 1, pp. 17-22, January, 1973. Original article submitted March 21, 1972.

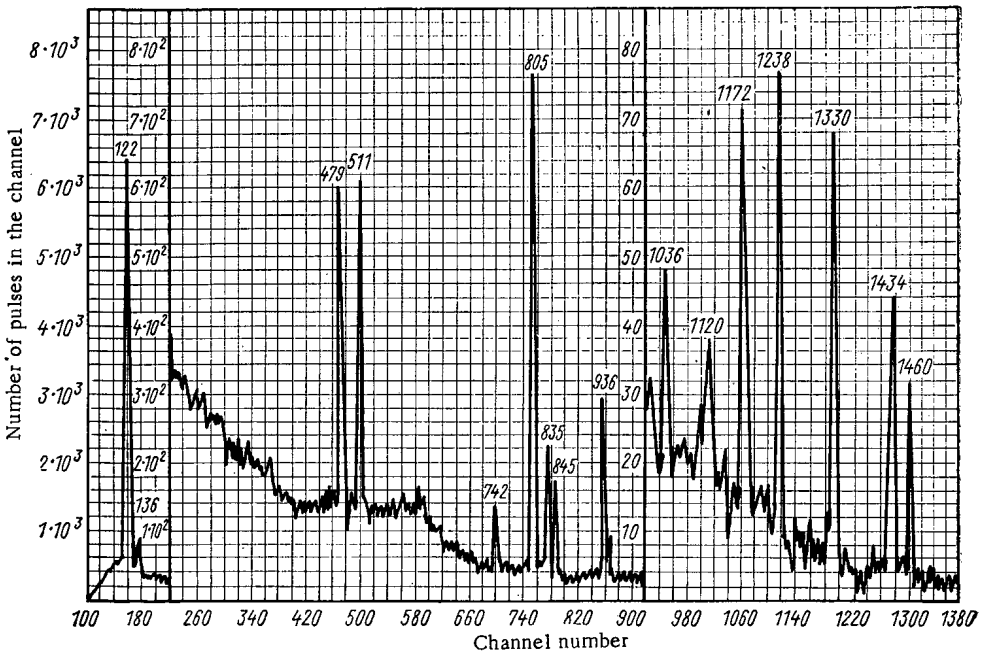

Fig. 2. γ-Spectrum of the dry residue of the water from the synchrocyclotron cooling circuit measured with a Ge(Li) detector (the figures on the peaks represent the energies of the γ-quanta in keV).

TABLE 1. Isotopes Detected in the Cooling Circuit and Their Activity (Measured and calculated)

Sample	Activity of the circuit water, decays/sec · liter		Activity of the deposit, decays/sec · sample
	measured	calculated	
Co^{60}	17 (7) *	73	≤ 2
Co^{58}	150 (60)	218	≤ 2
Co^{57}	100 (40)	133	≤ 2
Co^{56}	35 (14)	50	≤ 1
Mn^{56}	<4	1	≤ 2
Mn^{54}	32 (12)	42	≤ 3
Mn^{52}	31 (12)	33	≤ 1
Cr^{51}	<30	—	50
V^{48}	<4	—	9
Be^{7}	300 (120)	—	1454
C^{11} †	$(3,5\pm0,3)\cdot10^{5}$	—	—

* The brackets indicate the deviation from the mean of the activity in the circuit water (taken over all the samples).

† Activity of carbon at the outlet from the irradiation zone.

The tubes of the cooling system are made of copper, while the recirculation pump, the tube length compensators, and certain valves are made of stainless steel. The inner surface area of the copper tubes is ~ 700 m^2 and that of the steel parts ~ 3 m^2.

The system is filled with distilled water. In order to compensate the evaporating water and slight leaks in the system, 12 m^3 of distilled water and added once a month. The distilled water is obtained by condensation of vapor. The minimum specific electrical resistance of the cooling water is 25 k Ω/cm^3.

Spectral Composition and Dose Rate of γ-Radiation near the Cooling System

Using a spectrometer with an NaI(Tl) crystal we measured the energy spectrum of the γ-quanta arising in the tubes of the cooling circuit during the operation of the accelerator and after its disconnection. The spectrum was measured at a distance of 200 m from the accelerator building, thus avoiding the effect of the background of prompt γ-quanta from the synchrocyclotron building and reducing the load on the spectrometer. The water took 30 min to travel from the point of irradiation to the point of measurement. With the accelerator working, only a peak at 511 keV was observed in the measured spectrum. Some 3.5 h after disconnecting the accelerator only the 480 keV peak, corresponding to Be^7, could be detected.

Using standard dose meters, we measured the distribution of the γ-radiation dose rate along the tubes of the cooling circuit (Fig. 1). The measuring error of the instruments was 20%. In order to eliminate the influence of background prompt γ-quanta, the dose rate corresponding to the working accelerator was measured immediately after its disconnection. The field of present interest may be measured by

TABLE 2. Concentration of Chemical Elements in the Samples from the Cooling Circuit

Sample	Composition, g/liter*			
	copper	zinc	iron	sodium
Water from the circuit	$2{,}4 \cdot 10^{-3}$	$2{,}4 \cdot 10^{-3}$	$< 5 \cdot 10^{-5}$	$3{,}8 \cdot 10^{-3}$
Deposit from circuit walls	$7{,}6 \cdot 10^{-3}$	$1{,}9 \cdot 10^{-3}$	$14{,}8 \cdot 10^{-3}$	$< 1 \cdot 10^{-5}$
Distilled water poured into the circuit	$< 1 \cdot 10^{-5}$	$3{,}1 \cdot 10^{-4}$	$< 5 \cdot 10^{-5}$	$1{,}4 \cdot 10^{-3}$

*For the deposit from the walls of the circuit in g/sample.

moving the sensor from the point at which the water leaves the zone of irradiation at a velocity exceeding that at which the water is pumped out (8 m/min).

Determination of the γ-Active Isotopes in the Water of the Cooling Circuit

In order to determine the isotopic composition of the activation products we took several samples of water from the cooling circuit and deposits from the wall of the tubes. The water samples were evaporated in a glass container with the addition of several drops of hydrochloric acid; the dry residue was placed on a substrate. It was found in a special experiment that the isotopic composition of the sample remained constant for this method of preparation, and the loss of activity was no greater than 20%.

In order to identify the γ-radioactive isotopes and determine their activity the γ-radiation of the water and deposit samples was recorded in spectrometers with an NaI(Tl) detector in one case and a Ge(Li) detector in the other. The resolution of the spectrometer with the NaI(Tl) crystal was 16% and that of the spectrometer with the Ge(Li) crystal 0.5% for a γ-quantum energy of 511 keV.

Using the data obtained with the Ge(Li) detector, all those isotopes with a γ-ray flux or not less than 1/50 of the most active isotope in the sample were identified [2]. This characteristic of the detector was governed by the Compton effect, the speed of the analyzer, and the duration of the measuring period. In this way we detected all the γ-active isotopes in the water and the deposit making an appreciable contribution to the radiation dose. The results of the spectral measurements obtained with the Ge(Li) detector are presented in Fig. 2.

The composition and activity of the isotopes in the water and in the deposit of the synchrocyclotron cooling circuit are presented in Table 1. The measured isotope activities shown constitute arithmetic means of the results of the measurements.

The presence of radioactive isotopes of cobalt, manganese, chromium, and others (apart from Be^7 and C^{11}, formed from the oxygen of the water) in the water samples inspired us to look for possible ways in which these might contaminate the water. We established the composition of the elements in the samples by an activation method (Table 2).

Discussion of the Results of the Measurements

The presence of isotopes of cobalt, manganese, chromium, and vanadium in the cooling circuit and also the relation between the activities of the cobalt isotopes strongly suggest that these isotopes were principally formed as a result of the proton activation of the copper.

The possibility that these isotopes might have been formed in the quantities observed from zinc may be excluded, since hardly any Zn^{65}, with a half life of 245 days, appears in the samples. The upper limit to the activity of Zn^{65} established in the measurements is 30 decays/sec·liter, whereas according to the ratio of the cross sections of formation of the various isotopes in zinc [3] the activity of the Zn^{65} should have been 300 decays/sec·liter. Allowing for the fact that there is as much copper as zinc in the water of the circuit (Table 2) while the cross sections of formation of the isotopes in question from copper and zinc are commensurable, this indicates that the radioactive isotopes may be formed from the irradiated copper in the metal construction itself and not simply from copper dissolved in the water. The observed isotopes of cobalt, manganese, chromium, vanadium, and other radioactive and stable isotopes pass into the water as a result of the corrosion of the inner surface of the activated copper tubes. The corrosion of copper takes place more intensively under the action of radiation and is described in detail in [4].

The measured time dependence of the ratio of the activities of the manganese and cobalt isotopes shows that the accumulation of activity practically ceases several days after changing the water in the

circuit and is independent of the half life for any particular element. This indicates that, in addition to the passage of radioactive isotopes into the water, we also have a reciprocal process – the sorption of radioactive isotopes on the walls of the tubes and vessels of the cooling system. Thus on changing the water in the system the water may be contaminated by radioactive isotopes both on account of radioactivity induced in parts of the tubes and also on account of the desorption process.

An important argument confirming the foregoing mode of contamination of the water with radioactive isotopes formed from copper is the fact that the activity of the water 47 days after making a complete change of water with the accelerator disconnected was commensurable with the activity of the samples taken after prolonged operation of the accelerator. On the basis of the results of these measurements we may describe the accumulation of the radioactive isotopes in the cooling circuit water in analytical form.

Formation of Radioactive Isotopes from the Oxygen in the Water. It may be shown that the specific activity of the i-th isotope of the j-th element $A_{i,j}$ in the water of the cooling circuit at the outlet from the zone of the irradiation after ν periods of water circulation in the circuit equals

$$A_{i,j} = I\sigma_i N \frac{\lambda_i}{\lambda_i + \alpha_j} \frac{[1-e^{-(\lambda_i+\alpha_j)t_0}][1-e^{-(\lambda_i+\alpha_j)T\nu}]}{[1-e^{-(\lambda_i+\alpha_j)T}]}, \quad (1)$$

where I is the mean density of the proton flux in the activation zone; σ_i is the cross section of formation of the i-th isotope; N is the number of nuclei of the element entering into the nuclear reaction in 1 liter (we take only one oxygen isotope O^{16} into account); t_0 is the time for the water to pass through the irradiation zone; λ_i is the decay constant of the i-th isotope; α_j is the constant representing the extraction of the j-th element formed as a result of sorption, precipitation, evaporation, etc., from the water; T is the period of water circulation (in our own case T = 90 min). Equation (1) is valid subject to the condition $(\lambda_i + \alpha_j)t_0 < 1$. For long-living isotopes in which $\lambda_i < \alpha_j$ and $(\lambda_i + \alpha_j)T \ll 1$, Eq. (1) takes the following form

$$A_{i,j} = It_0\sigma_i N \frac{\lambda_i}{(\lambda_i+\alpha_j)T}. \quad (2)$$

We may determine the quantities It_0 if we know the activity of C^{11}. Treating the coefficient α as small compared with the decay constant and remembering that the irradiation time t_0 is small compared with the half life, we obtain an expression for the equilibrium activity of the C^{11}:

$$A_c = \frac{It_0\lambda_c\sigma_c N}{0.95}, \quad (3)$$

where $0.95 = [1-e^{-(\lambda_c + \alpha_c)T}]$.

In our case, measurement of the C^{11} activity gave $3.48 \cdot 10^5$ decays/sec·liter, whence $It_0 = 1.8 \cdot 10^9$ protons/cm^2. Knowing the activity of the Be^7 in the circuit water, from Eq. (2) we may easily find the extraction coefficient of beryllium α, equal to $3.4 \cdot 10^{-5}$ sec^{-1}, and the half-extraction period $T_{1/2} = 6$ h. Thus the equilibrium concentration of Be^7 in the circuit water is established in less than a day.

Using Eq. (2) we may determine the activity of tritium in the circuit water. The extraction coefficient of tritium was calculated on the basis of the fact that every month 12 m^3 of water evaporated from a system with a volume of 36 m^3, and tritium in the form of H_2O or H_2 evaporated with the water. From the calculation we obtain $\alpha = 0.9 \cdot 10^{-7}$ sec^{-1}, giving a half-extraction period of $T_{1/2} = 63$ days. The equilibrium activity of the tritium was $1.8 \cdot 10^{-7}$ Ci/liter.

Using Eq. (2) we may calculate the induced activity due to substances contained in the water. Estimates show that, even if we neglect the sorption of the isotopes so formed, the calculated activity will be 500 times smaller than the observed.

Contamination of the Water with Radioactive Isotopes as a Result of Corrosion. During corrosion isotopes formed in nuclear reactions pass into the water with the copper, these being principally formed in proton reactions. The differential equation describing the accumulation of radioactive nuclei in the water in this case be written in the following form:

$$\frac{dn_{i,j}}{dt} = c_i\beta + c_i'\beta_j' - (\lambda_i + \alpha_j)n_{i,j}, \quad (4)$$

where $n_{i,j}$ is the number of nuclei of the i-th isotope of the j-th element in the circuit water; t is the time passing since the system was filled with water; c_i is the concentration of the i-th isotope in the main volume of the tube material subject to corrosion; β is the rate at which the material of the tube walls subject to irradiation passes into the water; c'_c is the concentration of the i-th isotope in the material sorbed on the surface of the tubes, β'_j is the rate at which material of the j-th element leaves the tubes of the system as a result of desorption.

The solution to Eq. (4) is written in the form

$$n_{i,j} = e^{-(\lambda_i+\alpha_j)t}\left[\int (c_i\beta + c'_i\beta'_j)\, e^{(\lambda_i+\alpha_j)t'}\, dt' + B\right]. \tag{5}$$

With the accelerator working

$$c_i = c_{0i}e^{-\lambda_i t_1} + \frac{I\sigma_i}{\lambda_i}(1 - e^{-\lambda_i t_1}),$$

with the accelerator not working

$$c_i = c_{0i}e^{-\lambda_i t_2},$$

where I is the average density of the proton flux; σ_i is the microscopic cross section for the formation of the i-th isotope from copper; c_{0i} is the initial concentration of the i-th isotope in copper; t_1 is the time elapsed after connecting the accelerator; t_2 is the time elapsed after disconnecting the accelerator. The value of the coefficient β may be obtained from the data of [4] in which the changes taking place in the copper concentration in a mock-up of the circuit were determined experimentally under irradiation with protons. The time dependence of the concentration of copper ions in the water arises from two processes: corrosion and sorption. The increase in the concentration of copper ions q at the initial instant after pouring the water into the model is due to corrosion only, so that $dq/dt|_{t\to 0} = \beta_1$ for the model described in [4]. It is reasonable to assume that for accelerator cooling circuits made of one material the following relation holds:

$$\beta = \beta_1 \frac{S}{S_1}\frac{V_1}{V}, \tag{6}$$

where S_1 and V_1 are respectively the surface area of the model in the zone of irradiation washed by the water and the volume, both indicated in [4]; S and V are the surface area of actual tubes in the irradiation zone washed by the water and the volume of the whole cooling circuit. It follows from [4] that the value of β may differ by approximately a factor of three, depending on whether the corroding surface lies under the irradiation or not. We must therefore distinguish the rates at which tube wall material passes into the water with the accelerator working (β_2) or not working (β_3).

There are insufficient desorption data to be able to give the product $c'_i\beta'_j$ in analytical form as a function of time. Furthermore, there are no quantitative data regarding the desorption process in the cooling circuit at present under consideration. We shall therefore confine ourselves to considering the corrosion process alone as a source of water contamination.

The change taking place in the activity of the long-living isotopes with time after connecting or disconnecting the accelerator is simply due to the extraction of the radioactive isotopes from the water, as indicated by Eq. (5) (since $\lambda_i \ll \alpha_j$). The extraction coefficients α_j were estimated experimentally from the rate of accumulation of isotope activity in the water after connecting the accelerator. The extraction coefficient for cobalt is $\sim 4\cdot 10^{-6}$ sec^{-1}, for manganese $\sim 1.2\cdot 10^{-5}$ sec^{-1}. The half-extraction period for cobalt is ~ 2 days, for manganese ~ 17 h.

We determine the proton flux at the positions occupied by the tubes and the area washed by the water indirectly from the activity of the C^{11} in the water at the outlet from the zone of irradiation. According to (3) we may write

$$A_c = \frac{It_0\lambda_c N\sigma_c}{0.95} = \frac{I\frac{V_{irr}}{Q}\lambda_c N\sigma_c}{0.95} = \frac{IS}{V}\frac{r\lambda_c\sigma_c NT}{2\cdot 0.95}, \tag{7}$$

where $V_{irr} = Sr/2$ is the volume of the water in all the copper tubes subjected to irradiation; $Q = V/T$ is the ratio of flow of the water in the system; r is the radius of the tubes. From Eq. (7) it is easy to determine IS/V.

Thus the parameters of Eq. (5) have been determined, and we may write down an explicit formula for the equilibrium activity in the water of the circuit with the accelerator connected:

$$A_{i,j} = 1.9 A_c \frac{1}{\lambda_c T} \frac{\sigma_i}{\sigma_c} \frac{\beta_1}{N(\lambda_i + \alpha_j)} \frac{V_1}{rS_1}. \quad (8)$$

The values of the equilibrium activities for the isotopes of cobalt and manganese calculated from Eq. (8) are given in Table 1.

The isotopes of chromium and vanadium, which have a large cross section of formation from copper, cannot be detected in the water, probably owing to the large extraction coefficient.

The activity of the sample taken 47 days after filling the circuit with water (with the accelerator disconnected) should be determined by the coefficient β_3. Although the value of this is three times smaller than β_2, the count at the peak of the first sample differs by no more than a factor of two from the count at the peak for the greatest activity of the water in the circuit. This may be explained by the contribution arising from the desorption of radioactive isotopes from the walls of the cooling circuit. The quantitative correspondence between the calculated and experimental results indicates that the process underlying the accumulation of activity in the water of the cooling system has been described correctly.

As a result of our investigation into the radioactivity of the water cooling the JINR synchrocyclotron, we have found that, at the present time, the specific radioactivity of the water passing into the drainage system without previous settling or purification is no greater than the limiting permissible concentrations. The activity of the γ-radioactive isotopes reaches an equilibrium value in no later than six days. The dose rate of γ-radiation obtained from the water in the tubes of the cooling system is commensurable with the limiting permissible values, or even exceeds them at distances of under 200 m from the synchrocyclotron. On increasing the intensity of the inner accelerator beam by a factor of 25-30 times, a special cooling system will this have to be erected so as to avoid the passage of radioactive water into an open tank, as is provided for in project [5].

The authors take this opportunity of thanking V. P. Dzhelepov for useful advice and R. Arl't, T. I. Kaplinskaya, and E. K. Zhuravleva for help in the work.

LITERATURE CITED

1. G. Warren et al., "Radioactivity produced and released from water at high energies," Second International Conference on Accelerator Dosimetry and Experience, USAEC (1969), p. 99.
2. B. S. Dzhelepov and L. K. Peker, Decay Schemes of Radioactive Nuclei [in Russian], Nauka, Moscow–Leningrad (1966).
3. Nuclear Data Tables, Section A, Vol. 7, Nos. 1-2 (1969), p. 1.
4. F. Hoyer et al., "Radiolytic corrosion and related problems in the cooling water circuits of high-energy particle accelerators," CERN, 68-2, DI-HP/MSC (1968).
5. A. A. Glazov et al., "Phasotron with variation of the magnetic field (Apparatus "F")," Preprint JINR 9-3211, Dubna (1967).

MODELING NUCLEAR REACTIONS IN AN ISOTROPICALLY IRRADIATED THICK TARGET

A. K. Lavrukhina, G. K. Ustinova,
V. V. Malyshev, and L. M. Satarova

UDC 539.125.5

The necessity of modeling isotropic irradiation first arose when attempting to analyze and interpret the distribution of the products of nuclear reactions in meteorite material. Under conditions of isotropic irradiation by cosmic rays, both stable and radioactive isotopes accumulate in meteorites; by measuring the concentration or radioactivity of these in meteorites reaching the Earth's surface we may extract valuable information as to the intensity of cosmic rays in various parts of interplanetary space and over various time intervals, and also information relating to the actual history of the meteorites [1]. However, in order to analyze these measurements we must know the laws governing the depth distribution of the cosmogenic isotopes formed both by the primary cosmic rays and by the complete cascade of secondary nuclear-active particles within the meteorites. In order to build up a picture of the depth distribution of activity in meteorites, experimental data relating to the irradiation of thick targets with proton beams were used in [2-4]. However, the authors of these papers themselves acknowledged that subsequent conversion to the condition of isotropic irradiation, covering the complete range of energies of the cosmic

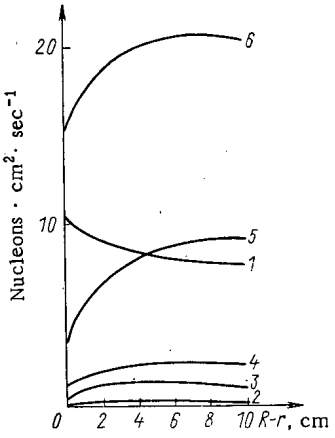

Fig. 1

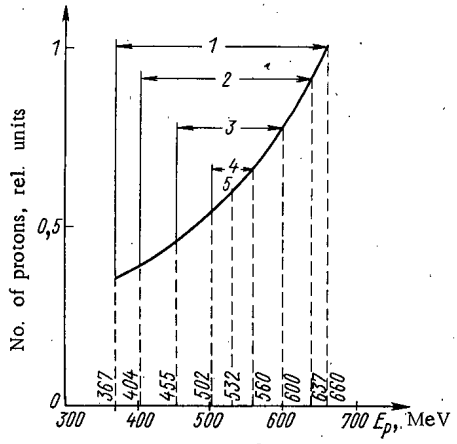

Fig. 2

Fig. 1. Calculated distribution of individual components of nuclear-active particles inside the sphere (in nucleons · cm^{-1} · sec^{-1}): 1) primary protons (I_0 = 1 proton/cm^2 · sec · sr); 2) mesons (E > 150 MeV); 3) protons (E > 200 MeV); 4) neutrons (E > 100 MeV); 5) neutrons (1 < E < 100 MeV); 6) total flux of nuclear-active particles; R = radius of sphere; r = distance from center.

Fig. 2. Energy spectrum of primary protons inside the sphere: 1) at the surface; 2) in the sphere at 2 cm from the surface; 3) in the sphere at 5 cm from the surface; 4) in the sphere at 8 cm from the surface; 5) at the center of the sphere.

Translated from Atomnaya Énergiya, Vol. 34, No. 1, pp. 23-28, January, 1973. Original article submitted June 12, 1972.

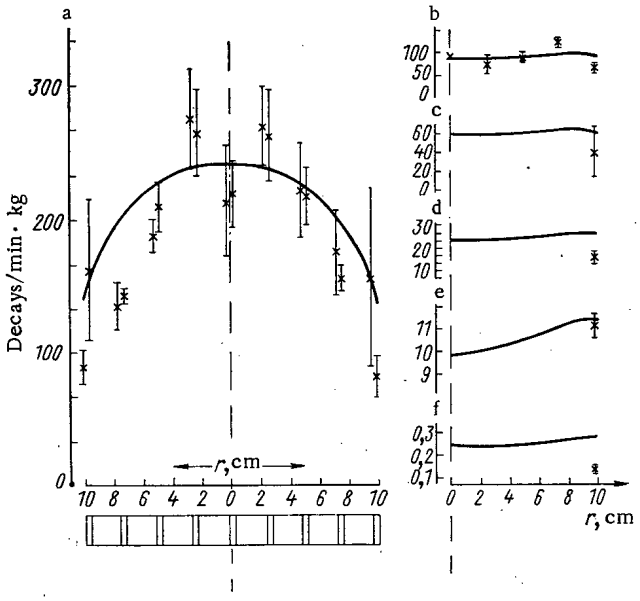

Fig. 3

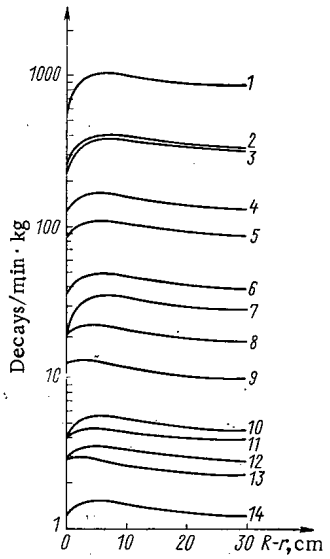

Fig. 4

Fig. 3. Distribution of the activity of radioactive isotopes inside an isotropically-irradiated iron sphere (in decays · $min^{-1} \cdot kg^{-1}$); I_0 = 1 proton · $cm^{-2} \cdot sec^{-2} \cdot sr^{-1}$. Points: measurement; curves: calculation; a) Na^{24} from aluminum plates; under the graph; disposition of the aluminum plates in the can lying along the diameter of the sphere; b), c), d), e), f) Mn^{52}, V^{48}, $Sc^{44}m$, Sc^{47} and Ca^{47} respectively from the iron plates; r = distance from center.

Fig. 4. Distribution of cosmogenic radioactive isotopes in an iron meteorite of radius 30 cm (in decays · $min^{-1} \cdot kg^{-1}$): 1) Fe^{55}; 2) Mn^{54}; 3) Mn^{53}; 4) Cr^{51}; 5) Mn^{52}; 6) V^{48}; 7) Co^{56}; 8) Sc^{46}; 9) P^{32}; 10) Ti^{44}; 11) Al^{26}; 12) Ca^{45}; 13) Na^{22}; 14) Si^{32}.

ray spectrum, involved errors and simplifications greatly affecting the results of any modeling of the depth distributions of cosmogenic isotopes in small targets ($R \leq 20$ cm), whereas meteorites of equivalent dimensions were the most accessible (as regards frequency of falling) and also the best detectors of cosmic rays, since the greatest effects of the nuclear reactions were produced in a distance comparable with the mean free path of the cosmic rays in the material of the meteorites. For these reasons a method based on the use of the cascade-evaporative model for describing the distribution of nuclear-active particles inside meteorites and data relating to the cross sections of formation of radioactive isotopes obtained in experiments involving the irradiation of thin targets would appear more promising [5-8].

Subsequent development of this line of thought led to the creation of an analytical method for calculating the intensity of cosmic radiation and the activity (or content) of cosmogenic isotopes at any point of an isotropically irradiated cosmic body of any size and composition [9-12]. This method found an important application not only when studying meteorites but also when analyzing the activity of lunar samples obtained by the Luna-16, Apollo-11, and Apollo-12 space ships [13-15]. The method is based on the following important assumptions: only the first generation of secondary particles is to be considered, the direction of their motion being in line with that of the primary radiation, i.e., the straight-forward approximation is used. This approximation is also used when calculating cascade processes in the atmosphere [16], calculating radiation doses behind the shielding of space ships [17], and considering the passage of a beam of particles with $E \leq 1$ GeV through shielding [18, 19]. The particle depth and energy distribution functions so achieved agree with those calculated by the Monte Carlo method. Nevertheless, considering the importance of the conclusions which might be drawn by analyzing activity in both meteorites and lunar samples, the authors came to the conclusion that it was essential to effect a direct simulation of nuclear reactions in an isotropically irradiated thick target (a spherical model of a meteorite) so as to compare theoretical and experimental data and estimate the degree of reliability of the computing technique employed. The results of the experiment may also be interesting in connection with calculating the shielding of space ships, while the method of isotropic irradiation will be helpful in biological research.

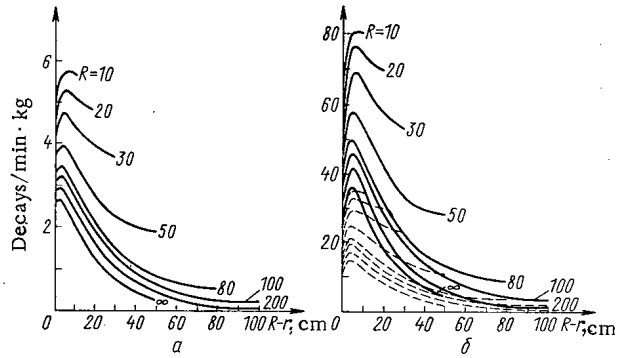

Fig. 5

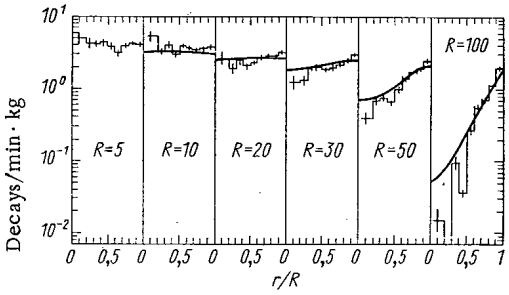

Fig. 6

Fig. 5. Distribution of Al^{26} (a) and V^{48} (b) in iron meteorites of various sizes (in decays · min^{-1} · kg^{-1}): Al^{26} is calculated for a mean intensity over the solar cycle (I_0 = 0.28 particles · cm^{-1} · sec^{-1} · sr^{-1}); V^{48} is calculated for the maximum intensity in 1965 I_0 = 0.39 particles · cm^{-2} · sec^{-1} · sr^{-1} (continuous lines) and for the minimum intensity in 1959 I_0 = 0.18 particles · cm^{-2} · sec^{-1} · sr^{-1} (broken lines).

Fig. 6. Comparison between calculations of the depth distribution of Na^{22} in iron meteorites based on the analytical method (curves) and the Monte Carlo method (histograms).

After calculating the optimum dimensions for the development of a nuclear cascade in iron, an iron sphere 10 cm in radius was chosen. By means of a special transmission system, the sphere was set into rotation in two perpendicular planes (at a velocity of 18 rpm) at a distance of ~6 m from the point at which the protons left the synchrocyclotron chamber. Along the diameter of the sphere an iron can was laid; inside this, lying at equal distances from one another, were nine sets of iron and aluminum targets, separated by iron spacers. The iron targets were discs 18 mm in diameter and < 1 mm thick made of Armco iron (impurity content 0.16%). The aluminum targets were discs of the same size made of spectrally pure (99.9%) foil 0.25 mm thick. Each set of targets consisted of three aluminum targets, two iron, and three more aluminum is succession. The end members of each group of three aluminum discs served to protect the middle aluminum targets from recoil nuclei generated by the iron and to compensate for the loss of recoil nuclei from the central aluminum targets themselves, the activity of Na^{24} being measured in the latter. One of the iron targets served to measure the total activity, the other was used for the radiochemical separation of the isotopes under consideration. The sphere was irradiated with a wide beam of 660 MeV protons in the Joint Institute for Nuclear Research synchrocyclotron. The beam was expanded to the size of the sphere by means of a magnetic lens, sited in the fittings of the electromagnet, at the point at which the proton beam emerged from the synchrocyclotron chamber. The lens was constructed on the principle of magnetic quadrupole lenses as used for beam focusing [20, 21]. On rotating the sphere in two perpendicular planes, isotropic irradiation of its whole surface was achieved, with an intensity of $I_0 = (I/16\pi)\, I_p$ protons · cm^{-2} · sec^{-1} · sr^{-1}, where I_p (protons · cm^{-2} · sec^{-1}) is the mean intensity of the proton beam at the site of the sphere, measured with a monitor. As monitor we used an aluminum foil screen. The intensity of the protons was determined from the yield of the Al^{27} (p, 3pn) Na^{24}. The intensity of the beam was varied from experiment to experiment over the range (5.3-7.6) · 10^8 protons · cm^{-2} · sec^{-1}. The duration of the exposure was 1.5-4 h. The measured distribution of induced activity along the diameter of the sphere exhibited a clear symmetry with respect to the center of the sphere, this being a confirmation of the fact that the irradiation of the surface was isotropic.

In these experiments, particular attention was paid to the measurement of the depth distribution of Na^{24} formed by the bombardment of the aluminum, since the excitation functions of the corresponding reactions initiated by the protons and neutrons were already well known [22, 23], and the contribution from the secondary neutrons was decisive, so that the isotope was very sensitive to the development of an intranuclear cascade. Five experiments were set up to measure the activity of the Na^{24}, the activity being measured in 18 targets placed along the diameter of the sphere. Apart from this, in one experiment the activity of Mn^{52} (in nine targets) V^{48}, Sc^{44m}, Sc^{47} and C^{47} (in two symmetrical targets on the surface of the sphere) was measured in the fractions of manganese, vanadium, scandium, and calcium respectively separated from the iron targets by a radiochemical method. The separation was carried out in the standard

manner [24]. The beta activity of the separated samples and the aluminum targets was measured with an end-window counter having an argon filling of the MST-17 type. The relative error in measuring the activity of the β-emitting isotopes was 20-30%. The isotopes were identified from their half lives.

At the same time we calculated the depth distribution of the primary protons, the secondary nuclear-active particles, and the radioactive isotopes of current interest within the sphere by an analytical method [9-12]. In the calculation we made use of an existing systematization of experimental and computed data relating to the characteristics of an intranuclear cascade under the influence of high-energy protons (spectra of secondary protons, neutrons, and mesons for a primary proton energy of 660 MeV and average multiplicities of the cascade particles $\overline{S}_p$ (200-660 MeV) = 0.57, $\overline{S}_\pi$ (150-660 MeV) = 0.037, $\overline{S}_n$ (100-660 MeV) = 0.61 and the cascade and evaporative neutrons $\overline{S}_n$ (1-100 MeV) = 2.89 [25-27]). The ionization losses in the iron were allowed for in accordance with the data presented in [28]. Figure 1 shows the distribution of various components of nuclear-active particles inside the sphere (I_0 = 1 proton $\cdot$ cm^{-2} $\cdot$ sec^{-1} $\cdot$ sr^{-1}). On the surface the primary protons have the greatest intensity, while in the center of the sphere the cascade and evaporative neutrons with energies under 100 MeV predominate. In the center of the sphere the primary protons have an energy of 532 MeV, while at the remaining depths and on the surface of the sphere the primary protons penetrating the sphere have a certain energy spectrum (Fig. 2).

The excitation functions of the reactions leading to the formation of the isotopes under consideration were plotted in accordance with existing experimental data [23, 29, 30]. The cross sections of formation of Mn^{52}, V^{48}, Sc^{44}, Sc^{47} and Ca^{47} by neutrons were regarded as being equal to the cross sections of the corresponding proton reactions, just as the cross sections of formation by mesons. In order to determine the weighted-mean cross sections of formation of the isotopes by various components of the nuclear-active particles, the excitation functions were averaged over the spectra of the primary protons at different depths in the sphere and over the spectra of the secondary protons, mesons, and neutrons for various energy ranges. In determining the weighted-mean cross section of formation of Sc^{44m} we used the ratio of the statistical weights of the isomeric pair $\sigma(Sc^{44m})$: $\sigma(Sc^{44}) \approx 0.4$ above 100 MeV in the (p, pn) reaction [31].

Figure 3 shows the results of the experiments and the computed curves for the depth distribution of the radioactive isotopes inside the sphere (converted to I_0 = 1 proton $\cdot$ cm^{-2} $\cdot$ sec^{-1} $\cdot$ sr^{-1}). The measuring errors indicated are the mean square errors taken over five experiments for Na^{24} and simple averages over two measurements at symmetrical points relative to the sphere center for the other isotopes. The measured distribution of Na^{24} and Mn^{52} inside the sphere is in good quantitative agreement with the calculated form of the depth distribution of these isotopes. A slight deviation occurs close to the surface (at a depth of < 2 cm from the latter). This is supported by measurement of the activity of the V^{48}, Sc^{44m}, Sc^{47} and Ca^{47} isotopes at the surface of the sphere. The computed data for V^{48} and Sc^{47} agree (within the limits of experimental error) with the measured data, although there is a tendency for the computed data to be too high. In the case of Sc^{44m} and Ca^{47} the overestimate passes outside the limits of the errors in question, and is mainly attributable to the neglect of the angular dependences of the distributions of the nuclear-active particles (the straight-forward approximation), in particular the omission of leakage from the surface of the sphere on the part of nuclear-active particles emitted into the near hemisphere. At a great depth this effect is compensated by the arrival of particles from neighboring points; hence we may also expect that in large-diameter bodies (R > 10 cm) the computing error near the surface will be no greater than that indicated in the present case. Furthermore the surface layers of meteorites are lost in passing through the Earth's atmosphere. The degree of ablation may be 3/4 of the original mass of the meteorite [32], so that the error under consideration is by no means important. Thus the measured activity of cosmogenic isotopes in fallen meteorites should correspond (within the limits of measuring error) to analytical calculations for $R - r > 2$ cm.

Unfortunately, owing to purely technical difficulties, experimental modeling cannot be achieved in large-diameter bodies. However, we may compare our results with Monte Carlo calculations in which the straightforward approximation is not used and allowance is made for all generations of secondary particles. Our recent paper [3] presents a calculation of the accumulation of Na^{22}, V^{49}, Cl^{36} and K^{40} in iron meteorites, based on a statistical simulation of the interaction of high-energy particles with matter, analyzed on an electronic computer.

In contrast to the foregoing experiment, meteorites in cosmic space are irradiated with cosmic rays of a wide spectrum of energies. In the calculation this necessitates averaging the multiplicities of the generation of secondary particles and the cross sections of formation of the isotopes over the primary

spectrum, as a result of which different characteristics of the intranuclear cascade are obtained [$\bar{S}_{shower}$ (> 1 GeV) = 0.6, $\bar{S}_p$ (0.2-1 GeV) = 0.4, $\bar{S}_\pi$ (0.15-1 GeV) = 0.6, $\bar{S}_n$ (0.1-1 GeV) = 1.0, $\bar{S}_n$ (0.001-0.1 GeV) = 6.8 [12]] and also different weighted-mean cross sections of formation of the isotopes as compared with the values corresponding to an energy of 660 MeV. The multiplicities of the secondary particles are increased, in particular the shower and meson components are greatly developed; the weighted-mean cross sections of formation of the isotopes with high threshold are enlarged. Figure 4 shows the depth distributions of fourteen cosmogenic isotopes in an iron meteorite 30 cm in radius. The calculation was carried out analytically for the mean intensity of galactic cosmic rays (with a hardness greater than 0.5 GV) in 1959-1969 (I_0 = 0.28 particles $\cdot$ cm^{-1} $\cdot$ sr^{-1}), and using the spectrum of 1962 corresponding to this mean intensity [34, 35].

The relationship between the rates of formation of the radioactive isotopes is determined by their cross sections of formation by the primary and secondary radiations. The depth distributions of the majority of the isotopes have a maximum at a distance of ~5 cm from the surface due to the contribution of the secondary particles, mainly cascade and evaporative neutrons (Fe^{55}, Mn^{53}, Mn^{54} etc.). Such isotopes as Na^{32}, P^{32}, Sc^{46} are formed by high-energy primary protons; hence the maximum close to the surface is weakly expressed in these and the fall of activity with depth is sharper than in the other isotopes. The observed activities of the isotopes in iron meteorites correspond to the activities of Fig. 4 [1].

With increasing dimensions of the irradiated body the activity of the radioactive isotopes diminishes, the fall in activity with depth becomes sharper, and the maximum in the distribution moves closer to the surface (~2 cm). Figure 5a shows the depth distribution of Al^{26} in iron meteorites of various sizes. Since the eleven-year variations in the intensity of the galactic cosmic rays have no effect on the activity of such a long-living isotope as Al^{26} ($T_{1/2} = 7.4 \cdot 10^5$ years $\gg$ 11 years), the calculation was made for a mean intensity of I_0 = 0.28 particles $\cdot$ cm^{-2} $\cdot$ sr^{-1} $\cdot$ sec^{-1}, using the 1962 spectrum, as in Fig. 4. It should of course be remembered that the Al^{26} activities shown in Fig. 5 are characteristic of meteorites with orbits lying wholly within the region of modulation (the aphelion of the orbits being at a distance of less than 1.9 astronomical units from the Sun, where 1.9 is the upper boundary of the region of effective modulation [36-39]). For more extended orbits, the meteorite travels for a part of the time in the unmodulated region with a maximum intensity of the cosmic rays $\geqslant$ 0.39 particles $\cdot$ cm^{-2} $\cdot$ sec^{-1} $\cdot$ sr^{-1} [34], so that the activity of Al^{26} and other long-living isotopes in them will be higher [40]. The observed values of the Al^{26} activity in fallen iron meteorites, 0.1-7.4 decays $\cdot$ min^{-1} $\cdot$ kg^{-1} [1], correspond to the results obtained. The short-living isotopes ($T_{1/2} \ll 11$ years) such as V^{48} ($T_{1/2}$ = 16 days) accumulate their observed activity entirely on their way from a distance of 1.9 astronomical units to their point of impact on the Earth, and they are sensitive to the phase of the solar cycle during which the meteorite comes to rest, so that the maximum and minimum activities of such isotopes in different meteorites may differ by almost a factor of 2.3, in accordance with the variation in the intensity of the galactic cosmic rays during the cycle [34, 35], and independently of the extent of the orbits (the continuous and broken line gives these two activities of V^{48} in Fig. 5b). The activity of the radioactive isotopes with $T_{1/2} \sim 11$ years is sensitive to both the time and the space variations in the galactic cosmic rays, and also to the instant at which the meteorite strikes the Earth – i.e., before or after passing through perihelion.

Figure 6 represents the depth distribution of the activity of Na^{22} in iron meteorites calculated analytically (curves) and by the Monte Carlo method [33] (histograms) for I_0 = 0.23 particles $\cdot$ cm^{-2} $\cdot$ sec^{-1} $\cdot$ sr^{-1}. The two methods gives results in quantitative agreement. There is a slight tendency to disagree at great depths ($r/R < 0.2$) in large bodies ($R > 50$ cm), which are only rarely observed to fall. However, the sharp falls in activity at depths close to the center of the meteorites obtained on calculating by the Monte Carlo method are never observed in real meteorites. Since as a result of ablation the surface layers of the material are removed, the activity measurement is in actual fact carried out in the central layers of the meteorites, and measurements made at different points generally exhibit no sharp differences [1]. The smoothing of the depth distributions of activities of the cosmogenic isotopes in the central layers of meteorites also follows from a calculation based on the use of experimental data obtained with thick targets [2-4], which on the whole gives a correct description of the true activity distributions in large bodies. In the case of isotopes with low thresholds of formation, on the other hand, there may be a tendency [33] to underestimate the activity at depths of $r/R < 0.2$ ($R > 50$ cm) in the analytical calculation, owing to the fact that only the first generation of the secondary particles is considered. For some isotopes the two effects may compensate one another.

In conclusion, the authors wish to thank V. I. Danilov for indicating the method of expanding the proton beam in the JINR synchrocyclotron and general assistance in setting up the lens and preparing it for use, and A. T. Vasilenko and S. Kh. Biktimirov for useful advice in the construction of the lens, they are also grateful to Academician A. P. Vinogradov for constant interest in the work.

LITERATURE CITED

1. A. K. Lavrukhina, in: Nuclear Chemistry [in Russian], V. I. Gol'danskii and A. K. Lavrukhina (editors), Nauka, Moscow (1965), p. 7.
2. J. Arnold, Ann. Rev. Nucl. Sci., 11, 349 (1961).
3. J. Arnold, M. Honda, and D. Lai, J. Geophys. Res., 66, 3519 (1961).
4. R. Kohman and M. Bender, Trans. Amer. Geophys. Union, 46, 127 (1965); USAEC Report N40-844-72 (1967).
5. K. Ebert and H. Wänke, Z. Naturforsch., 12a, 766 (1957).
6. H. Wänke, Z. Naturforsch., 15a, 953 (1960).
7. A. K. Lavrukhina, L. D. Revina, T. A. Ibraev, and L. V. Yukina, Geokhimiya, No. 1, 20 (1967).
8. A. K. Lavrukhina, L. D. Revina, and L. V. Yukina, Geokhimiya, No. 3, 251 (1968).
9. A. K. Lavrukhina and G. K. Ustinova, Astron, Zh., 44, 1081 (1967).
10. A. K. Lavrukhina and G. K. Ustinova, Dokl. Akad. Nauk SSSR, 179, 1448 (1968).
11. A. K. Lavrukhina, G. K. Ustinova, and T. A. Ibraev, in: Cosmic Rays [in Russian], No. 11, S. N. Vernov and L. I. Lorman (editors), Nauka, Moscow (1969), p. 100.
12. A. K. Lavrukhina et al., in: Meteorite Research, P. Millman (editor), D. Reidel-Publ. Co., Dordretch, Holland (1969), p. 227.
13. A. K. Lavrukhina and G. K. Ustinova, Astron, Vestn., 5, 144 (1971).
14. A. Lavrukhina and G. Ustinova, Nature, 232, 462 (1971).
15. A. P. Vinogradova et al., Dokl. Akad. Nauk SSSR, 202, 293 (1972).
16. I. L. Rozental', Zh. Éksp. Teor. Fiz., 23, 10 (1952).
17. R. Alsmiller, Nucl. Sci. Engng., 27, No. 2 (1967).
18. M. M. Komochkov and B. S. Sychev, At. Énerg., 15, No. 4, 325 (1963).
19. B. M. Karpakov, L. R. Kimel', and V. V. Pichugin, in: Questions of Dosimetry and Protection from Radiations [in Russian], No. 6, Atomizdat, Moscow (1967), p. 84.
20. V. I. Danilov and O. V. Savchenko, Pribory i Tekh. Éksper., No. 3, 17 (1959).
21. M. S. Livingstone, Accelerators [Russian translation], IL, Moscow (1956).
22. J. Cumming, Ann. Rev. Nucl. Sci., 13, 261 (1963).
23. J. Stehn et al., Neutron Cross Sections, BNL-325, Suppl. No. 2, Vol. I, USAEC (1964), p. 13-0-19.
24. A. K. Lavrukhina et al., Radiokhimiya, 5, 721 (1963).
25. V. S. Barashkov et al., Communication of the JINR P2-5118 [in Russian], Dubna (1970).
26. V. S. Barashenkov et al., ibid., R2-5549.
27. A. K. Luvrukhina, Transactions of the All-Union Conference on Cosmic-Ray Physics [in Russian], Part II, No. 1, FIAN, Moscow (1969), p. 54.
28. C. Williamson, J. Boujot, and J. Picard, Rapport CEA-T3042, Centre d'Études Nucléaires de Saclay (1966).
29. E. Bruninx, High-Energy Nuclear Reaction Cross Sections I-II-III, CERN 64-17, Nucl. Phys. Div., Geneva (1961, 1962, 1964).
30. R. Silberberg and C. H. Tsao, Preprint Lab. Cosm. Ray Phys., Naval Res. Lab., Washington (1971).
31. J. Meadows, R. Diamond, and R. Sharp, Phys. Rev., 102, 190 (1956).
32. N. Bhandary, Proc. Second Symp. Cosm. Rays., Astrophys., Geo-Phys., Element. Particle Phys., Vol. 2, Delhi (1969), p. 327.
33. V. S. Barashenkov, N. M. Sobolevskii, and V. D. Toneev, Communications of the JINR, R2-6225 [in Russian], Dubna (1962); Geokhimiya, No. 11 (1972).
34. A. N. Charakhch'yan and T. N. Charakhch'yan, Trans. of the Sixth All-Union Winter School on Cosmic Physics [in Russian], Part 2, Izd. Polyar, Geofiz. Inst. Kol'sk. Fil. Akad. Nauk SSSR (1969), p. 36.
35. G. A. Bazilevskaya et al., Izv. Akad. Nauk SSSR, Ser. Fiz., 35, 2483 (1971).
36. A. K. Lavrukhina, Vestn. Akad. Nauk SSSR, No. 9, 72 (1970).
37. A. K. Lavrukhina, G. K. Ustinova, and A. N. Simonenko, Meteoritika, No. 31 (1972).

38. E. Fireman and G. Spannagel, J. Geophys., Res., 76, 4127 (1971).
39. M. Forman, R. Stoenner, and R. Davis, ibid., 76, 4109 (1971).
40. A. K. Lavrukhina and G. K. Ustinova, Dokl. Akad. Nauk SSSR, 204, 316 (1972).

ABSTRACTS

URANIUM IN CARBONATE HYDROTHERMAL SOLUTIONS

R. P. Rafal'skii

UDC 541.49:546.791.6:550.4

Uranyl carbonate complexes are considered the basic compounds, in the form of which the transfer of uranium by natural hydrothermal solutions from the source to the site of formation of uranium ores occurred. However, the absence of instability constants for these complexes at increased temperatures has hindered the evaluation of their actual role in the hydrothermal process.

The work cites the results of a treatment of the experimental data [1], characterizing the equilibrium in carbonate uranium-containing solutions at 100-200°C. The equilibrium concentrations in a solution of Na^+, H^+, OH^-, CO_3^{2-}, HCO_3^-, H_2CO_3 were calculated; the pressure p_{CO_2} in experiments conducted at 100-170°C in the absence of excess CO_2 in the system, as well as in five series of experiments conducted at 200°C with solutions of various initial compositions, was determined. It was established that at 200°C uranium exists in solution in the form of uranyl tricarbonate $[UO_2(CO_3)_3]^{4-}$. A method of determining the equilibrium concentrations of the components and the composition of the complex is described in the work.

The instability constants of $[UO_2(CO_3)_3]^{4-}$ were calculated by the relation

$$K_{inst} = K^{1/2}\frac{C^3_{CO_3^{2-}}}{C_{[UO_2(CO_3)_3]^{4-}}C_{Na^+}C^3_{OH^-}},$$

where K is the equilibrium constant of the reaction

$$Na_2U_2O_7\ (sol) + 3H_2O\ (liq) = 2UO_2^{2+}\ (soln) + 2Na^+\ (soln) + 6OH^-\ (soln),$$

which proceeds under experimental conditions in which $Na_2U_2O_7$ is formed. The values of K were estimated on the basis of the thermodynamic data. The approximate value of K_{inst} of $[UO_2(CO_3)_3]^{4-}$ obtained at 100, 150 (graphical interpolation), and 200°C pertain to solutions with ionic strengths 0.11-0.30 and are equal to −18.0, −19.0, and −20.1, respectively. Comparing these values with the published values of K_{inst} at 25°C, it was concluded that the curve of the temperature dependence of the constant passes through a maximum close to 100°C.

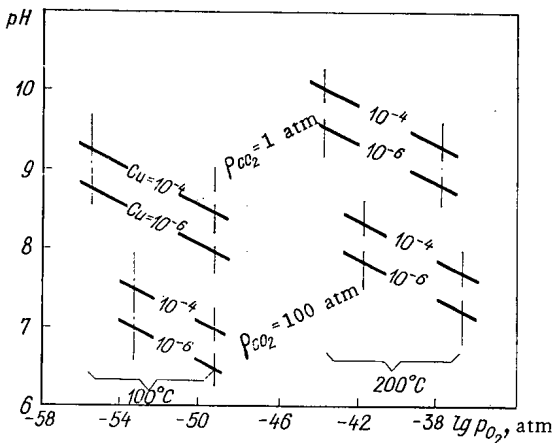

Fig. 1. Isolines of concentrations of $[UO_2(CO_3)_3]^{4-}$ (M).

On the basis of the values obtained for K_{inst}, we calculated the equilibrium constant of the reaction

$$2[UO_2(CO_3)_3]^{4-}\ (soln) + 8H^+\ (soln) = 2UO_2\ (sol) + 6CO_2 + O_2\ (gas) + 4H_2O\ (liq),$$

which permitted an estimation of the concentration of the complex at fixed pH, p_{CO_2}, and p_{O_2}. Figure 1 shows the isolines of two concentrations of $[UO_2(CO_3)_3]^{4-}$, determining the region of most probable concentrations of the heavy metals in natural hydrothermal solutions at $\mu = 0.2$. The vertical lines on the graph delimit the regions of p_{O_2} of coexistence of calcite, sphalerite, galenite, and molybdenite [2]. It is evident that the transport of uranium by hydrothermal solutions in the form of $[UO_2(CO_3)_3]^{4-}$ is

Translated from Atomnaya Énergiya, Vol. 34, No. 1, p. 29, January, 1973. Original article submitted June 14, 1972.

quite probable, although as the temperature is increased, higher partial pressures of CO_2 and pH values are necessary for accomplishing this process.

The instability constant of $[UO_2(CO_3)_2]^{2-}$ at increased temperatures is unknown. The most approximate estimates have shown that the participation of this complex in processes of ore formation at low temperature cannot be excluded. The recently studied [3] uranyl monocarbonate ($UO_2CO_3^0$) could not play an appreciable role in these processes.

LITERATURE CITED

1. R. P. Rafal'skii, Physicochemical Investigation of the Conditions of Formation of Uranium Ores [in Russian], Atomizdat, Moscow (1963).
2. H. D. Holland, in: Thermodynamics of Postmagmatic Processes [Russian translation], Mir, Moscow (1968), p. 9.
3. E. I. Sergeeva, Geokhimiya, No. 11 (1962).

THRESHOLD INSTABILITY OF A REACTOR WITH RESPECT TO THE ONSET OF SPATIAL XENON OSCILLATIONS

V. N. Semenov

UDC 621.039.514

A study of the practical stability of a reactor with respect to the onset of spatial xenon oscillations shows that the amplitude of the steady-state oscillations and the allowance for the loss of stability depend on the sign and magnitude of the nonlinear terms [1, 2], which in ordinary linear analysis are discarded. In the present study it is shown that in reactors with an inhomogeneous core it is possible to have an instability of the threshold type (e.g., a reactor that is stable with respect to small perturbations loses its stability for perturbations of sufficiently large amplitude). Allowance for the loss of stability depends on the magnitude of the inhomogeneity of the core and the magnitude of the damping coefficient, calculated in the linear approximation. We obtain an expression for the "threshold" amplitude (allowance for the loss of stability). In order to describe the space-time distribution of the neutrons $\Phi(x, \tau)$, we use an integral equation in the quasi-stationary approximation:

$$\Phi(x, \tau) = \Phi_0(x) + \int_V T(x', x)\left[\frac{K_\infty(x', \Phi(x', \tau), \rho_{Xe}(x', \tau))}{K_{\text{eff}}\{\Phi\}} - \frac{K_\infty^0(x')}{K_{\text{eff}}^0}\right]\Phi(x', \tau)\,dV', \quad (1)$$

where the kernel $T(x', x)$ is a generalized Green's function, which ensures the conservation of the normalization of the total power; $K_\infty(x, \Phi, \rho_{Xe})$ is the local coefficient of multiplication, which depends on the local power and the local contamination by ρ_{Xe}; the functional $K_\infty\{\Phi\}$ describes the action of the noninertial homogeneous control system, which compensates for every change in reactivity and maintains the total power constant:

$$K_{\text{eff}}\{\Phi\} = K_{\text{eff}}^0 \frac{\int_V K_\infty(x, \Phi, \rho_{Xe})\,\Phi\Phi_0\,dV}{\int_V K_\infty^0(x)\,\Phi\Phi_0\,dV}. \quad (2)$$

The index "zero" in Eqs. (1) and (2) refers to a critical reactor without feedback, for which the coefficient of multiplication of the lattice equals $K_\infty^0(x)$. The feedback equations for xenon and iodine are written in the usual form.

Translated from Atomnaya Énergiya, Vol. 34, No. 1, p. 30, January, 1973. Original article submitted December 3, 1971; abstract submitted July 19, 1972.

By expanding the deviation of the solution from the stationary solution in a series in the eigenfunctions $\psi_n(x)$ of the kernel $T(x', x)$ we can reduce the problem to the investigation of the equations for the coefficients of the expansion that describes the τ dependence of the solution. We assume that the reactor is near the boundary of the stability region. We retain only the first two harmonics and, unlike in [2], we take into account their interaction, using the second method of Lyapunov; we thus can analyze the practical stability of the solution. We obtain explicit expressions for the Lyapunov functions. The expression for the amplitude of the steady-state oscillations $b_{1,\,st}$ (if the coefficient of oscillation $\alpha \gtrsim 0$) and for the threshold amplitude $b_{1,\,thr}$, the allowance for the loss of stability (if the damping coefficient $\alpha \lesssim 0$), has the form

$$b_1^2 = \frac{2\alpha}{A},$$

where A is determined by the nonlinear terms. For reactors with a core that is weakly inhomogeneous with respect to $K_\infty(x)$ in all cases $A > 0$; therefore, b_1 is small when α is small and greater than zero. We also have that the $\psi_1(x)$ distribution is practically stable. For reactors with a core that is strongly inhomogeneous with respect to $K_\infty(x)$ (e.g., for a two-region reactor with $V_2/V_{core} \lesssim 0.4$ and with a balanced field) for sufficiently large power levels it is possible to have a threshold instability with respect to the amplitude of the perturbation $b_{1,\,thr}$ (mathematically, this case corresponds to $A < 0$ and $\alpha \lesssim 0$).

LITERATURE CITED

1. S. Margolis and S. Kaplan, WAPD-1156, WAPD-BT-21 (1960).
2. G. P. Gushchin, I. S. Postnikov, and E. F. Sabaev, At. Énerg., 27, No. 5, 402 (1969).

EXPERIMENTAL INVESTIGATION OF SINGLE-STAGE CONTROL CIRCUIT OF COOLANT OUTLET TEMPERATURE IN THE BOR-60 REACTOR

V. A. Afanas'ev, V. M. Gryazev, and V. N. Efimov

UDC 621.039.56:621.039:526

Automatic control systems of the power of nuclear energy plants with fast reactors do not always prevent the occurrence of dangerous thermal stresses in constructional elements of the reactor and its associated equipment [1]. In the control circuits described in [2, 3], the control parameter is not the reactor neutron power but the coolant temperature at the reactor outlet. Such control systems reduce temperature fluctuations, caused by variation of the input parameters, in the reactor core and in the entire power plant.

The BOR-60 fast reactor [4] has been used in the design and testing of a single-stage coolant outlet-temperature control system employing a commercial RPI regulator. The error signal from the temperature setter and thermocouples at the reactor outlet was balanced by activating the control rods through a relay converter. The system was tested with the neutron power control circuit disconnected. The system provided smooth regulation practically without overshoots in the presence of fluctuations of temperature ($\pm 25 \cdot 10^{-5}\ \Delta C/C$), coolant flow rate ($\pm 100\ m^3/h$), and loading ($\pm 20\%$).

The test proved that better results are obtained in the BOR-60 reactor if the coolant outlet temperature is maintained constant and the neutron power control circuit is disconnected. The experimental results obtained in the BOR-60 reactor are of considerable value in the design of similar control systems for other atomic power plants using fast reactors.

Translated from Atomnaya Énergiya, Vol. 34, No. 1, pp. 30-31, January, 1973. Original article submitted April 30, 1972.

LITERATURE CITED

1. Yu. E. Bagdasarov et al., Fast-Reactor Engineering [in Russian], Atomizdat, Moscow (1969).
2. V. I. Plyutinskii et al., in: Control of Nuclear Power Plants [in Russian], Vol. 2, Atomizdat, Moscow (1967), p. 5.
3. G. A. Karandashov and B. A. Kuvshinnikov, in: Control of Nuclear Power Plants [in Russian], Vol. 2, Atomizdat, Moscow (1969), p. 28.
4. A. I. Leipunskii et al., 4th Geneva Conference (1971), Report No. 750 (USSR).

RELIABILITY OF RADIOCHEMICAL PLANTS WITH γ-RADIATION SOURCES

Yu. D. Kozlov and L. G. Filaretova

UDC 621.039.553

Breakdowns in radiochemical plants are classified as due to structural, technological, or operational failures, and as failures due to aging or sudden damage of components or units [1].

Breakdowns of chemical plants using high-power γ-sources K-60,000 and KSV-500 [2-4], which according to the classification [2] belong to the classes IUP-2 and IP-2, were analyzed for 2000 to 20,000 h of steady-state operation.

Hypotheses concerning the distribution of failures in γ-cell assemblies using Pearson's χ^2 criterion [5] were tested.

An analysis of the failures, and tests of the hypotheses, showed that failures of the control panels and the interlocking system followed an exponential distribution, failures of the lift mechanism a normal distribution, and that of the fuel holders follow a normal logarithmic distribution [6, 7]. The failures of cables with electromagnets follow a compound distribution (exponential and normal logarithmic) so that their basic reliability indicators should be calculated as follows: the integral function of exponential and normal logarithmic distribution is written as

$$F(t)=1-e^{-\lambda t}\left[1-\Phi_0\left(\frac{C-\lg t}{\sigma}\right)\right]; \quad (1)$$

the probability of no-failure operation and the failure rate are respectively

$$P(t)=e^{-\lambda t}\left[1-\Phi_0\left(\frac{C-\lg t}{\sigma}\right)\right]; \quad (2)$$

$$\lambda(t)=\frac{1}{T}+\frac{0.4343}{\sigma t}f_1\left(\frac{C-\lg t}{\sigma}\right), \quad (3)$$

where $\Phi_0(C-\log t/\sigma)$ and $f_1(C-\log t/\sigma)$ are tabulated functions whose values are given in Tables 1.2 and 1.4 in [6]; t is the operating time; T is the mean time between failures, h.

The parameters C and σ are related to mathematical expectation and variance of t by

$$M(t)=C=\hat{U}=\frac{\sum_{i=1}^{\infty}\lg t}{m}; \quad (4)$$

$$D(t)=\sigma^2=\frac{1}{m-1}\sum_{i=1}^{m}(\lg t_i-\hat{U})^2, \quad (5)$$

where m is the number of failures in time t.

Translated from Atomnaya Énergiya, Vol. 34, No. 1, p. 31, January, 1973.

The discussed relations can be used in the calculation of basic reliability parameters of radiochemical plants.

LITERATURE CITED

1. I. B. Gertsbakh and Kh. B. Kordonskii, Models of Failure [in Russian], Sovetskoe Radio, Moscow (1966).
2. A. Kh. Breger et al., Principles of Radiochemical Equipment Design [in Russian], Atomizdat, Moscow (1967).
3. A. Kh. Breger et al., At. Énerg., 8, No. 5, 441 (1960).
4. V. L. Karpov et al., At. Énerg., 15, No. 4, 302 (1963).
5. K. Pearson, "On a new method of determining goodness of fit," Biometrika, 26 (1934).
6. Ya. B. Shor and F. N. Kuz'min, Tables for Reliability Analysis and Control [in Russian], Sovetskoe Radio, Moscow (1968).
7. Ya. B. Shor, Statistical Methods of Quality and Reliability Control, [in Russian], Sovetskoe Radio, Moscow (1968).

EMBRITTLEMENT OF LOW-ALLOYED STEELS CAUSED BY NEUTRON IRRADIATION IN WATER AT TEMPERATURES BELOW 100°C

N. N. Alekseenko and V. A. Nikolaev

UDC 621.039.553

The most accurate data on the efficiency of reactor materials are obtained in experiments which reproduce all the factors affecting the structure under investigation.

If low-alloyed steels are irradiated at temperatures below 100°C (see Table 1), contact between steel and water causes embrittlement, which is fundamentally different from the reduction in plasticity connected with radiation hardening. As a result of irradiation while in contact with water, steel loses much of its capacity to withstand localized strain, which reduces its actual breaking strength. This effect is

TABLE 1. Effect of the Irradiation Medium on the Mechanical Characteristics of 10KhSND and 12KhNM Steels

Steel	Irradiation medium	Irradiation dose neutrons/cm² (E >0.5 MeV)	Irradiation temperature, °C	$\sigma_{0.2}$, kg/mm²	σ_b, kg/mm²	δ_u, %	δ_5, %	δ_e, %	ψ_k, %	s_k, kg/mm²
10KhSND	Initial state	0	—	39	54	14	29	15	80	154
	Water	0	50	37	54	15	29	14	80	146
	Without water	$2,3 \cdot 10^{19}$	100	71	75	2,5	14	11,5	72	149
	Water	$2,3 \cdot 10^{19}$	50	64	66	2,5	6,5	4,0	29	86
12KhNM	Initial state	0	—	52	64	11	24	13	73	—
	Water	0	50	51	62	10	22	12	78	158
	Without water	10^{19}	100	81	82	2,5	14	11	71	164
	Water	10^{19}	50	63	69	3,0	8,0	5,0	38	81

Translated from Atomnaya Énergiya, Vol. 34, No. 1, pp. 32-33, January, 1973. Original article submitted March 3, 1972.

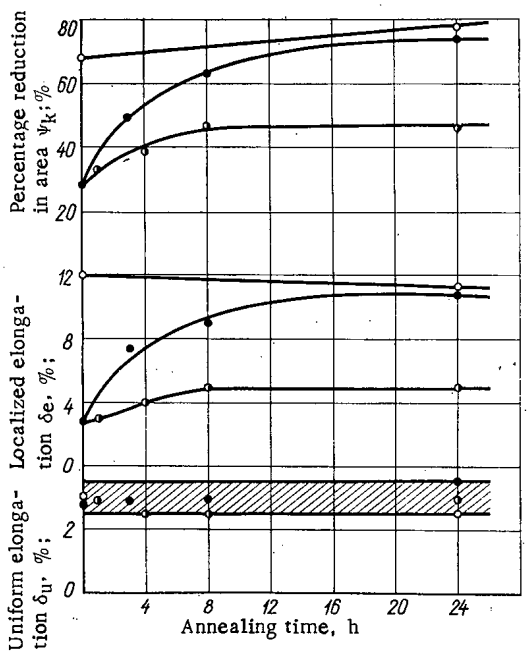

Fig. 1. Effect of annealing on the plasticity of 10KhSND-III steel. ○) Irradiation in hermetically sealed containers; annealing at 150°C; ◑) irradiation while in contact with water; annealing at 100°C; ●) same; annealing at 150°C.

superimposed on the increase in the yield point and the ultimate strength and the reduction in uniform elongation, which are characteristic for radiation hardening.

The necessary conditions for embrittlement are the presence of a medium and the action of a neutron dose exceeding a certain threshold value which is approximately equal to 10^{18} neutrons/cm^2.

The plasticity of 10KhSND-III steel irradiated in water at 100°C over a period of 24 h varies slightly as a result of annealing (see Fig. 1).

The heating of steel to 150-200°C results in almost complete recovery of its capacity for localized strain and its actual breaking strength without affecting its radiation hardening.

The intensive embrittlement of low-alloyed steels irradiated in water is caused by saturation with the hydrogen evolving as a result of steel corrosion and water radiolysis. The absence of embrittlement under corrosion conditions in irradiation with doses smaller than the threshold dose indicates that the dominant factor in this phenomenon is the density of radiation defects in steel and not the hydrogen penetration. It can also be assumed that hydrogen in irradiated steel interacts with the radiation defects and is retained by them.

A γ-RAY AND X-RAY DETECTOR USING INTEGRATION AND COUNTING*

K. M. Kudelin, L. Ya. Zabrodskaya, and V. P. Odintsov

UDC 61.387.46

The article describes a detector whose sensitive element (a single crystal of lithium fluoride) is used in two ways: in an integrating mode (dose measurement), making use of thermoluminescence, and in a counting mode (dose rate measurement), making use of radioluminescence.

The range of dose rate measurements is 0.1-100 R/min, and the range of dose measurements is 0.1-1000 R. In the 25-1300 keV energy range, the variation in sensitivity is no more than ±8%; this is achieved by partial shielding of the crystal. The article gives a design estimate of the filter parameters.

The dose is calculated on the basis of the amplitude of the thermal peak, whose maximum at 140°C occurs 40 sec after the heater voltage has been turned on. At temperatures not exceeding 25°C the drop in the thermal-peak maximum is no more than 10% after 1 day and no more than 30% after 10 days.

γ-RADIATION FIELD OVER AN INFINITE PLANE SOURCE SEPARATED BY AN INACTIVE STRIP†

D. P. Osanov, M. Yu. Tissen, and V. G. Ryadov

UDC 621.039.766: 539.122

In case of extensive radioactive contamination it becomes particularly important to make use of decontaminated strips, areas, etc. As an example of such a deactivated strip can serve a passage cut through a contaminated territory by removing a surface layer of soil or a river whose water becomes gradually less and less active. Such an inactive strip can also be used for radioactive exploration in which the dose rate and activity density over the contaminated territory must be determined from the measured exposure rate over an artificial passage or river.

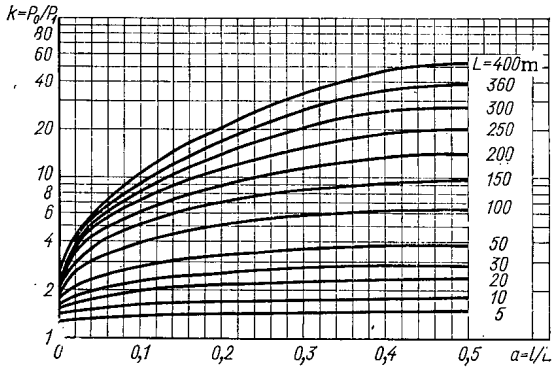

Fig. 1. The function k = f(*a*) for strips of various widths L (where *l* is the distance from the strip edge to the point over which the dose rate is P).

* Translated from Atomnaya Énergiya, Vol. 34, No. 1, p. 33, January, 1973. Original article submitted July 13, 1971.

† Translated from Atomnaya Énergiya, Vol. 34, No. 1, pp. 33-34, January, 1973. Original article submitted October 20, 1971; revision submitted April 10, 1972.

TABLE 1. The Ratio $k = P_0/P_2$ for Points over an Infinite Active Semi-Plane

Distance from strip edge l, m	Width of inactive strip L, m				
	5	10	20	50	⩾ 100
0	1,48	1,4	1,53	1,72	1,9
5	1,07	1,11	1,17	1,26	1,3
10	~1,0	1,06	1,10	1,17	1,2
20	~1,0	~1,0	1,06	1,1	1,1
⩾ 50	~1,0	~1,0	~1,0	~1,0	~1,0

To solve these problems we have determined quantitative relationships between the exposure dose rates over contaminated land and deactivated strip. To compute the quantitative relations we have used expressions derived before [1]. The final results allow for multiple scattering of γ-radiation in air using the method described in [2, 3] as well as the effect of air–soil interface on the basis of data cited in [3, 4]. All calculations were made for a γ-radiation energy of 0.8 MeV corresponding to the average γ-radiation energy of prompt fission products of approximately 10 h age. The results are shown as the ratio of dose rate P_0 over an infinite active plane to the dose rate P_1 at various points over an inactive strip (Fig. 1) and to the dose rate P_2 at various points of a semi-infinite plane adjoining the inactive strip (Table 1). The dose rate was measured in air at a height 1 m over the soil surface.

LITERATURE CITED

1. D. P. Osanov and E. E. Kovalev, At. Énerg., 6, No. 6, 670 (1959).
2. N. G. Gusev et al., Radiation Protection of Extended Sources [in Russian], Gosatomizdat, Moscow (1961).
3. O. I. Leipunskii, B. V. Novozhilov, and V. N. Sakharov, Propagation of γ-Quanta in Matter [in Russian], Fizmatgiz, Moscow (1960).
4. O. I. Leipunskii, γ-Radiation in Atomic Explosions [in Russian], Atomizdat, Moscow (1959).

SEMICONDUCTOR α-SPECTROMETER FOR ANALYSIS

S. M. Solov'ev, A. N. Smirnov, and V. P. Éismont

UDC 535.853:543.52

Isotopic α-analysis based on the spectra of α-particles requires isolation of weak lines on the background of much more intense lines belonging to higher energies. The sensitivity of a spectrometer is characterized by the ratio N_α/N_x, i.e., by the ratio of the number of counts in the channel corresponding to the peak of a monoenergetic α-line to the number of counts in a channel separated from the above line by a given energy interval ΔE. The spectrometer sensitivity can be improved by increasing its resolving power and by reducing the number of pulses having an amplitude reduced by loss of α-particle energy. In [1] the values of N_α/N_x have been found as 2900, 6000, and 8000 for ΔE equal to 200, 400, and 800 keV, respectively.

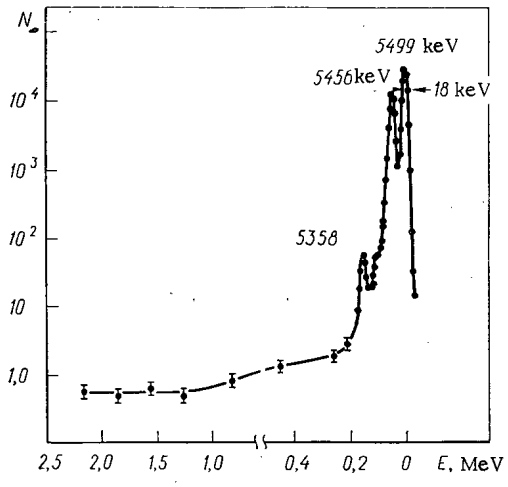

Fig. 1. α-Particle spectrum of Pu^{238}.

In this work we have selected silicon samples with parameters providing good energy resolution and low probability of pulses with reduced amplitudes. Two types of silicon were used. One had a lifetime $\tau = 1700$ μsec, a resistivity $\rho = 1300$ $\Omega \cdot$ cm, and a dislocation density $N_\alpha = 10^4$ cm^{-2}; the second type was free of dislocations and had a lifetime $\tau = 300$ μsec and a resistivity $\rho = 500$ $\Omega \cdot$ cm. The detectors were prepared by the usual method except at the

Translated from Atomnaya Énergiya, Vol. 34, No. 1, p. 34, January, 1973. Original article submitted January 13, 1972.

step of chemical etching when instead of protecting the back contact by a chemically inert layer of varnish the contacts were covered by a vacuum attached cap of Teflon and silicon rubber. Better detectors of both types with an active surface of 0.25 and 0.50 cm^2 had inverse currents of about 0.12 $\mu A/cm^2$ with an applied voltage of 100-200 V and provided a resolution of 15-18 keV.

The detectors used in the spectrometer had an area equal to 0.50 cm^2. An aluminum diaphragm with a polished inner edge was placed near the detector at a distance of 8 cm from the source. A Teflon diaphragm was placed between the source and detector for protection against α-particles scattered from the chamber walls.

The spectrum of Pu^{238} α-particles is shown in Fig. 1. The source was prepared by vacuum sputtering on a glass backing, the active spot having a diameter of 1 cm. The N_α/N_x ratios found with a detector made of the first type of silicon were found to be 14,000, 28,000, 45,000, and 70,000 for ΔE = 200, 400, 800, and above 1200 keV, respectively. The second type of silicon gave somewhat poorer figures.

As an illustration of the spectrometer performance we have taken the spectrum of Th^{229} and Th^{228} isotope mixture with their daughter products and determined the relative content of Th^{229} whose activity was 2.20 ± 0.01% of the overall target activity.

LITERATURE CITED

1. W. Hofker et al., Philips Techn. Rev., 30, 13 (1969).

SPATIAL DISTRIBUTION OF IONIZATION INTENSITY NEAR RADIOISOTOPIC NEUTRALIZERS OF STATIC ELECTRICITY

A. S. Rozenkrantz

UDC 621.317.7

For proper use of a radioisotopic static-electricity neutralizer it is necessary to calculate the electric fields and the volt–ampere characteristics of interelectrode gaps ionized by radiation. Among others, such calculations require the knowledge of the spatial distribution of the number of ionization events N_i per unit volume and time. For surfaces covered with α-and β-active isotopes the spatial distribution of N_i can be calculated by the method based on the thickness of the active layer d_a and of the protective layer d_p which can be represented in relative units:

$$d_a^* = \frac{d_a}{l_{am}}; \quad (1)$$

$$d_p^* = \frac{d_p}{l_{pm}}, \quad (2)$$

where l_{am} and l_{pm} are the total ranges of the given particle in the active and protective layers.

For α-active sources the path x' to the end of the range of a particle produced in the active layer at a depth $x_a = x_a^* l_{am}$ is given by

$$x' = \left(1 - \frac{x_a^* + d_p^*}{\cos\alpha}\right) l_m - R, \quad (3)$$

where l_m is the full range of the particle in air; α is an angle between the particle trajectory and a normal to the active layer surface at the point of escape; R is the distance from this point to the point where N_i

Translated from Atomnaya Énergiya, Vol. 34, No. 1, p. 35, January, 1973. Original article submitted January 11, 1972.

is determined. The factor x' is used as an argument in the Bragg function $F_B(x')$ and in its primitive $N(x')$:

$$N_\alpha(x') = \int_0^{x'} F_B(x')\,dx'. \tag{4}$$

Since $F_B(x') = 0$ when $x' < 0$, expression (3) indicates that particles for which $\alpha > \alpha_{lim} = \arccos d_p^*$ will not leave the active layer.

It is shown that the intensity of ionization at any point is equal to

$$N_i = \frac{1}{4\pi l_m d_a^*} \int_{S_0} \frac{\tau \Delta N_\alpha \cos\alpha}{R^2}\,dS_0, \tag{5}$$

where

$$\Delta N_\alpha = \int_{x'_{max}}^{x'_{max}} F_B(x')\,dx' = N_\alpha(x'_{max}) - N_\alpha(x'_{max}); \tag{6}$$

$$x'_{max} = \left(1 - \frac{d_p^*}{\cos\alpha}\right) l_m - R; \tag{7}$$

$$x'_{max} = \left(1 - \frac{d_a^* + d_p^*}{\cos\alpha}\right) l_m - R; \tag{8}$$

where τ is the total relative surface activity of the layer (the number of disintegrations per unit surface and time).

The results are given of calculating the spatial distribution near a plane active surface of Pu^{239} for a very thin ($d_a^* = 0.09$, $d_p^* = 0.01$) and a very thick ($d_a^* = 0.5$, $d_p^* = 0.5$) layer; experimental and theoretical results were compared for a practical active layer with $d_a^* = 0.3$ and $d_p^* = 0.1$ and were found to be in good agreement.

The obtained results indicate that the layer thickness has a significant effect on the spatial distribution of N_i. The effect of external contamination of the active surface can be allowed for in the same number.

The method is extended to β-active isotopes by taking into account their energy spectrum.

NEUTRON ACTIVATION DETERMINATION OF THE CONTENT OF OXYGEN AND FLUORINE IN SAMPLES OF ZIRCONIUM AND TANTALUM

V. I. Melent'ev, V. V. Ovechkin, and V. S. Rudenko

UDC 543.53

A neutron activation method for the separate determination of the content of oxygen and fluorine, present in test samples based on zirconium and tantalum, is described. The samples were alternately irradiated with 14 MeV neutrons and neutrons of a Pu^{238}–Be isotope source ($\bar{E}_n \approx 5$ MeV), then the ~6 MeV γ-radiation of the isotope N^{16}, which is formed in the reactions $O^{16}(n, p)$ and $F^{19}(n, \alpha)$, was recorded.

In this case a neutron generator with a yield of $\sim 5 \cdot 10^9$ neutrons $\cdot$ sec^{-1}, an isotopic source with a yield of $1 \cdot 10^8$ neutrons $\cdot$ cm^{-1}, and a scintillation γ-spectrometer with NaI(Tl) crystal with dimensions

Translated from Atomnaya Énergiya, Vol. 34, No. 1, pp. 35-36, January, 1973. Original article submitted June 12, 1972.

150 × 150 mm with a depression were used. The results of the determination of the oxygen content are in good agreement with the results of an independent method.

The method and apparatus described provide for a threshold of sensitivity of the determination of fluorine of 1 mg in a system of repeated irradiation after 5 min. The calculated dependence of the threshold of sensitivity of the determination of the oxygen content on the fluorine content in the analyzed samples was obtained. For a sample weighing ~10 g, the method permits measurement of oxygen concentrations $\geq 10^{-2}\%$ by weight even in those cases when the ratio of F : O contained in it is > 10.

EXPERIMENTAL INVESTIGATIONS OF MODULAR OR SECTIONAL CONCRETE BIOLOGICAL SHIELDING

V. B. Dubrovskii, V. N. Ivanov, and I. N. Martem'yanov

UDC 699.8

The article goes into the shielding characteristics of modular concrete structures consisting of blocks fabricated to different tolerances, and to be laid in place dry.

Experimental investigations were carried out in the caster-mounted tote box servicing a recess in the IR-100 reactor, and using a shielded halogen β-counter (to detect the γ-radiation), as well as aluminum threshold indicators, indium resonance indicators, and URSa-7 scintillation detectors for neutron detection. Modular concrete blocks were sized 100 × 200 × 400 mm, and the thickness of the shields investigated was 800, 1200, and 1600 mm.

It was found that the shape and dimensions of the planar horizontal joints which have a decisive effect on the shielding effectiveness of the modular structure depend on the precision to which the modular blocks are fabricated, and that is limited by the band of linear tolerances. Blocks with specified linear tolerancing of ±2 mm, ±5 mm, and ±7 mm were used in the experiments in order to ascertain the effect of dimensional tolerances on passage of radiation through the structures investigated.

Relationships between attenuation of neutron flux density and the γ-radiation dose rate throughout the thickness of the shielding, on the one hand, and the tolerances, on the other, were determined. The experimental data indicate an exponential attenuation of neutrons and γ-radiation by small-block modular shielding when the thicknesses are greater than five fast-neutron mean free path lengths (through monolithic concrete shields).

The contribution made by neutrons belonging to different energy groups, and by γ-radiation, to the total dose on the other side of the shielding was determined experimentally for the modular small-block structures, when high-energy neutrons show large anisotropy in their scattering behavior, transport of such high-energy neutrons through attenuating regions of the shielding occurs with negligible energy loss. As the probability of radiation leakage increases, as it does with decreasing tolerances on the modular blocks in the modular construction, the contribution made by high-energy neutrons to the total dose rate increases.

It was found that the shielding effectiveness of the modular concrete structures improves with respect to the monolithic variant when the tolerances on the modular blocks are large within the range in question. That is accounted for by the formation of steps in the horizontal joints of the reactor stacking that are open all the way through (the height of the steps is proportional to the tolerances). When the steps in the joint are increased, we observe a fall-off in the neutron flux density and in the γ-radiation, because of attenuation by the concrete at the site of the displacement.

Translated from Atomnaya Énergiya, Vol. 34, No. 1, p. 36, January, 1973. Original article submitted May 22, 1972.

It was found that the fabrication technology of the concrete blocks manufactured for modular concrete biological shielding must correspond to current standards and engineering specifications for the fabrication and acceptance of modular concrete and reinforced-concrete structural members, with no special requirements imposed with respect to fabrication of blocks in special casing or scaffolding, nor any special requirements on the finish of the surface.

PASSAGE OF RADIATIONS THROUGH JOINTS IN MODULAR CONCRETE SHIELDING

V. B. Dubrovskii and V. N. Ivanov

UDC 699.8

The article cites results of measurements of neutron flux and γ-radiation dose rate on the far side of shielding made up of sectional concrete blocks, with measurements taken at the outer surface of the blocks. The dependence of the far-side radiation field on the length of the joint, at constant height and width, and also on the height of the step in a plane joint, formed in vertical shear displacement of adjacent blocks, was investigated. The results obtained are compared to measurements taken under similar conditions on monolithic shielding made of the same concrete.

Eleven distinct compositions of monolithic and sectional modular shielding made from ordinary concrete (ρ = 2.3 ton/m^3) were investigated. The source of neutrons and γ-radiation was the core of an IR-100 reactor. The experimental assemblies were installed in a recess of the reactor adjacent to the outer course of blocks forming a graphite reflector. The dimensions of the recess were such that measurements could be taken on concrete structures of thickness 80, 100, 120, and 160 cm. Radiations were recorded by a threshold indicator on the basis of the reaction $Al^{27}(n, p)Mg^{27}$, by a $In^{115}(n, \gamma)In^{116}$ resonance indicator, by scintillation detectors responding to fast and intermediate-spectrum neutrons, by the URSa-7 general-purpose thermal neutron radiometer, and by a shielded SBM-10 halogen β-counter employed to detect γ-radiation.

Experimental findings are presented for attenuation of radiations on the far side of a plane "dry" joint. The amount of buildup on the far side of the joint is estimated by the number of times the radiation field was increased, as characterizing the increase in the flux or exposure dose rate beyond the joint, in comparison to the situation on the shielded side of a monolithic integral concrete shield. It is demonstrated experimentally that attenuation of thermal flux, epithermal flux, and of the γ-radiation dose rate in "dry" plane joints takes place at a more intense rate than attenuation of fast flux. Increases in the radiation field are entered in Table 1.

TABLE 1. Enhancement of Radiation Field (in relative units)

Shielding thickness, cm	Modes of radiations recorded*		
	Φ_f	Φ_{th}	D_γ
80	3,32	2,74	3,28
100	5,18	4,80	3,44
120	13,85	5,08	5,96
160	79,40	22,40	19,30

* Φ_f and Φ_{th} are respective flux densities of fast and thermal neutrons; D_γ is dose rate of γ-radiation.

The effect of the size of the step T in the plane "dry" joint on transmission of radiations was studied. The introduction of this step exerted a pronounced effect on transmission of high-energy neutrons, as compared to low-energy neutrons and γ-radiation. It is demonstrated that blocks must be offset (relative to one another) in the vertical direction not less than 30 mm when designing modular concrete biological shielding with spatial bonding of "dry" concrete joints, since an increase T > 30 mm would not bring about any substantial decrease in the field on the far side of the shield.

Translated from Atomnaya Énergiya, Vol. 34, No. 1, pp. 36-37, January, 1973. Original article submitted June 14, 1972.

ESTIMATION OF DIMENSIONAL-WEIGHT AND ENERGY CHARACTERISTICS OF ELECTRON ACCELERATORS FOR EXPERIMENTAL AND INDUSTRIAL RADIATION INSTALLATIONS

V. S. Karmaza, I. F. Malyshev, and I. A. Prudnikov

UDC 621.384.6

The last 15-20 years have seen considerable improvement in low energy accelerators [1, 2], related to the continuous broadening of their areas of application. At the same time, the experiments conducted in accelerators, for a long time, fell outside the limits of laboratory investigations, but to date have already resulted in a whole series of industrial radiation procedures [3, 4]. Beams of accelerated electrons with energies from a fraction to 10 MeV are utilized and different types of accelerators are applied in these procedures.

It is known that prior to the development of commercial or research radiation apparatus there already arises, during preliminary design, the question of the choice of the type and basic characteristics for the ionizing radiation source. A recommended procedure for this choice is presented in the article.

As the basic characteristics of the accelerators, there are taken: the energy of the electrons, average strength of the beam, specific weight (ton/kW), density (ton/m^3), efficiency, electron energy increase per unit length, and overall dimensions.

The distribution of the "spheres of influence" among the most diversified types of operative accelerators results from an analysis of their parameters.

Graphs, allowing one to estimate the characteristics mentioned for present-day electrostatic and cascade generators, resonance transformers, and linear accelerators, are presented.

As an example of mobile radiation apparatus, two flaw detectors are considered on the basis of LUÉ-15/1.5 and LUÉ-10/1 type linear accelerators.

LITERATURE CITED

1. H. Gordon and G. Behman, Particle Accelerators, Univ. Calif. Radiat. Laboratory, UCRL-9876 (1960).
2. E. Berill, Atomnaya Tekhnika za Rubezhom, No. 1, 26 (1971).
3. P. Parker, Particle Accelerators, 1, No. 4, 285 (1970).
4. Information of the All-Union Scientific-Engineering Conference on the Use of Accelerators in the National Economy, NIIEFA im. D. V. Efremova, Leningrad (1971).

Translated from Atomnaya Énergiya, Vol. 34, No. 1, p. 37, January, 1973.

LETTERS TO THE EDITOR

LEAKTIGHTNESS MONITORING OF THE PRIMARY LOOP IN STEAM GENERATORS AT NUCLEAR POWER STATIONS USING WATER-MODERATED WATER-COOLED POWER REACTOR

T. K. Fedchenko and A. A. Il'khman

UDC 621.039.587

The process flowsheet that has been accepted, and the principles agreed upon for organizing testing and monitoring of pressuretightness, allow us to consider the two-stage structure of the nuclear power station as an acceptable engineering solution: information on the appearance of leaks in the primary loop is obtained on the first level in the secondary loop, and which steam generator unit is at fault is determined at the second level.

The arrangement of monitoring points is shown in Fig. 1, and results of calculations are entered in Table 1.

Detection of Primary Loop Leaks in the Secondary Loop. The concentration of radioactive gases can be measured in the main steam line upstream of the turbine (point 1), and at blowdown points from the main ejectors of the turbines (point 2). A conventional ejector is employed in order to bleed steam upstream of the turbine and in order to prepare specimens for monitoring. Calculations of the effectiveness of these monitoring techniques, based on the standard procedure, demonstrated the feasibility of carrying out the monitoring operation at point 2, i.e., monitoring at the principal ejector stations, which is a technique roughly 400 times more sensitive than monitoring in the steam line upstream of the turbine.

TABLE 1. Sensitivity of Different Techniques for Monitoring Leaks in Primary Loop in Steam Generator Units

Number of monitoring point	Variable monitored	Monitoring site	Instrument sensitivity	Calculated leakage of primary loop (liters/h) at primary-loop activity:	
				$\cdot 10^{-1}$ Ci/liter	$\cdot 10^{-5}$ Ci/liter
1	Concentration of radioactive noble gases	In steam line upstream of turbine	$5 \cdot 10^{-10}$ Ci/liter	0.32	3200
2	Concentration of radioactive noble gases	At points of blowdown from chief ejectors serving turbines	$5 \cdot 10^{-10}$ Ci/liter	8.10^{-4}	8
3	γ-radiation	Above blowdown water pipe (ϕ 8.9 x 4.5 mm)	0.01 μR/sec	74	520
4	N^{16} β-radiation	In blowdown water	3 pulses/sec	1.5	
5	γ-radiation	Above steam line (ϕ 450 x 16 mm)	0.01 μR/sec	1600	5800
6	N^{16} β-radiation	In steam line	3 pulses/sec	74	—
7	Activity of steam generator blowdown water	Downstream of expansion tank and heat exchanger	$5\ 10^{-10}$ Ci/liter	0.15	1500

* Minimum leakage monitorable by this method is independent of the primary-loop fission-fragment activity.

Translated from Atomnaya Énergiya, Vol. 34, No. 1, pp. 39-40, January, 1973. Original article submitted June 13, 1972.

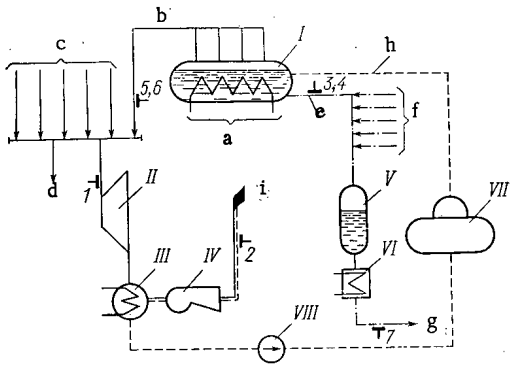

Fig. 1. Disposition of radiation leak monitoring points: I) steam generator; II) turbine; III) condenser; IV) ejector; V) expansion tank; VI) heat exchanger; VII) deaerator; VIII) pump; a) primary-loop coolant; b) steam; c) steam from other steam generators; d) steam to other turbine(s); e) water from continuous blowdown of steam generator; f) water from continuous blowdown of other steam generators; g) water to filters of cleanup facility; h) feedwater; i) vent to atmosphere. 1-7) Leak monitoring points.

The method of measuring the total activity of the primary-loop water (point 7) is a sufficiently sensitive technique [1]. But this method shows a slower response to changes than monitoring carried out at the principal ejector stations (it takes anywhere from 5 to 9 min to deliver the sample from the steam generator unit to the sensing device).

The methods of radiation monitoring at points 2 and 7 enable us to establish, quite reliably, the fact of appearance of a leak in the secondary loop, but not to find out which steam generator unit is responsible for the leak.

Accordingly, measurements of the specific activity of the secondary-loop water and of the concentration of radioactive gases at blowdown points from the chief ejectors serving the turbines must be backed up by monitoring the activity of the blowdown water purged from the steam generators, or of the steam directly downstream of each steam generator unit.

Detection of Damaged Steam Generator. The activity of the secondary-loop water and of the steam in the damaged (leaky) steam generator unit have been calculated within 100 sec after the damage occurred, e.g., in the case of failure or rupture of a secondary-loop pipe, and at a coolant specific activity of 10^{-1} Ci/liter. This time was arrived at on the basis of the allowable time that can be allotted for pinpointing which steam generator is damaged. The isotope composition of the fission-fragment activity in the primary loop when 1% of the fuel elements are unsound has been calculated theoretically [2].

The mechanism by which nongaseous fission fragments disseminate through the secondary-loop piping in response to leaks appearing in the primary loop in one of the steam generator units has been discussed elsewhere [3]. Here we take up calculations of the specific activity of the water and steam, using a similar procedure. The carryover coefficients for radioactive products entering the steam stream were assigned the following values in the calculations: 1 for radioactive noble gases, 0.1 for compounds containing the isotope N^{16}; $2 \cdot 10^{-3}$ for nongaseous fission products. The assumption that radioactive gases carried out entrained in the steam do not return to the condensate was entertained. When the specific fission-fragment activity of the coolant is 10^{-5} Ci/liter, the sensitivity of the methods falls off markedly.

Induced isotopes whose concentration in the loop remains constant at any given reactor output level were considered in the analysis. The analysis we carried out indicated that the maximum contribution to the amount of induced activity of the coolant proper is made by the isotope N^{16}. In calculating the N^{16}-induced activity, it was assumed that only 10% of the isotope formed would end up in the composition of the gaseous compounds present, and that it would take 10 sec to transport the isotope from the point of damage in the affected steam generator unit to the site where the sensing device was located. The γ-radiation dose rate was determined for the fission-fragment activity and for the induced activity at a distance of 10 cm from the surface of the piping, while the γ-radiation was calculated for the case where the sensing device is accommodated in the interior of the piping [4].

As is evident from the calculations, the most sensitive method for determining which steam generator is affected in the leakage is the method in which the β-emission of the Na^{16} isotope in the blowdown water pipe (point 4) is measured. By taking the half-life of the nuclide ($T_{1/2}$ = 7.35 sec) and the velocity at which the water advances through the piping (0.2 m/sec) into account it is found that the β-sensing device must be placed in the immediate vicinity of the steam generator. The disadvantages inherent in this method, based on measuring the γ-radiation dose rate above the blowdown piping (point 3), are: 1) the inaccessibility of the sensing deviced for servicing and maintenance while the loop is in service; 2) the need to provide additional shielding for the device. Placement of the radiation-sensing devices in the zone accessible to servicing lowers the sensitivity of these methods appreciably, however.

The variant of positioning β-radiation sensors in the piping downstream of the steam generators is interesting from this standpoint. Sampling specimens of blowdown water downstream of each of the steam generators is a sufficiently exact method, but is not helpful in keeping up to date on recent changes in the system.

Consequently, it is the method of measuring the concentration of radioactive gases at points of blowdown from the chief ejectors serving the turbines (point 2), backed up by measurements of the total activity of the secondary-loop water (point 7), that is the most sensitive, most reliable, and most convenient in use. In the case of a major breakdown (rupture of a pipe in the primary loop in a steam generator), it is advised to use a γ-radiation sensor situated above the pipe (point 5). Detection of smaller damage in a steam generator would be best served by supplementing these methods with one of the suggested techniques for monitoring directly at each steam generator unit.

The selection of the specific method depends on the presence of sufficiently reliable and inexpensive sensing devices.

LITERATURE CITED

1. M. I. Arsaev et al., Proc. SNIIP, Nuclear Instrumentation [in Russian], Atomizdat, Moscow (1970).
2. L. M. Luzanova and B. G. Pologikh, Symposium on Planning Measures to Cope with Radiation Accidents, Vienna (1969), paper Sm119/44.
3. E. Smith et al., Trans. Amer. Nucl. Soc., 11, No. 1, 371 (1968).
4. Rockwell (editor), Nuclear Reactor Shielding [Russian translation], Izd-vo Inostr. Lit (1958).

FUEL-ELEMENT TESTING CHANNEL LOOP WITH NATURAL COOLANT CIRCULATION

G. A. Klochko, V. A. Kurov,
V. I. Maksimenko, A. D. Martynov,
V. G. Potolovskii, M. G. Bul'kanov,
and V. M. Selivanov

UDC 621.039.54

One way to solve the problem of how to test new types of fuel-elements is to build special-purpose stationary experimental loop devices at research reactor facilities. The design, construction, and operation of loops with complex technological equipment and fixturing, all accommodated in special separate rooms with total biological shielding, is an expensive undertaking. One of the prominent shortcomings of stationary loops is the impossibility of easily retooling and modifying the loop device to handle a different type of coolant or to adjust to different conditions [1].

A design of a compact loop facility (Fig. 1) has been worked out to facilitate research on several different types of fuel-elements at comparatively low costs.

The channel loop (Fig. 2) was designed for an official cell of the reactor in the world's first nuclear power station [2, 3]. The channel, which is designed for natural circulation of coolant, has an external cylindrical body within which the fuel assembly, a compact shell-and-tube heat exchanger with floating twin-chamber head, and lifting and lowering tubes for the thermocouple, are accommodated. The heat exchanger is located at the top of the channel. The heat transfer surface is formed by a bundle of straight tubes sized 6 × 1 mm. Coolant water flows inside the tubes in a U-shaped circuit, and the collecting and distributing headers for the coolant are built into the head of the channel. The rotary chambers are staggered in height. Baffles are placed on the shell side of the heat exchanger to bring about transverse flow of coolant from the natural circulation loop over the tubes. The fuel assembly is accommodated within the lifting tube (dimensions 63 × 3.5 mm).

Steel foil screens are provided in order to diminish the influx of heat from the graphite stacking of the reactor over the length of the reactor, and in order to diminish recuperative heating of the coolant in the lowering branch. Supply of coolant water to the heat exchanger, and withdrawal of coolant water, as well as filling of the natural circulation loop, are achieved through ball-on-cone nipple type pipe connections.

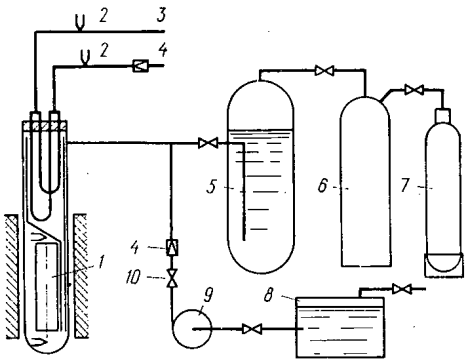

Fig. 1. Fuel-element testing loop design: 1) channel loop with fuel assembly; 2) thermocouples; 3) intermediate loop in station; 4) flowmeter; 5) pressure compensation device; 6) receiver tank; 7) compressed-gas cylinder; 8) distillate preparation tank; 9) feedwater pump; 10) shutoff valves.

Translated from Atomnaya Énergiya, Vol. 34, No. 1, pp. 40-42, January, 1973. Original article submitted April 20, 1972.

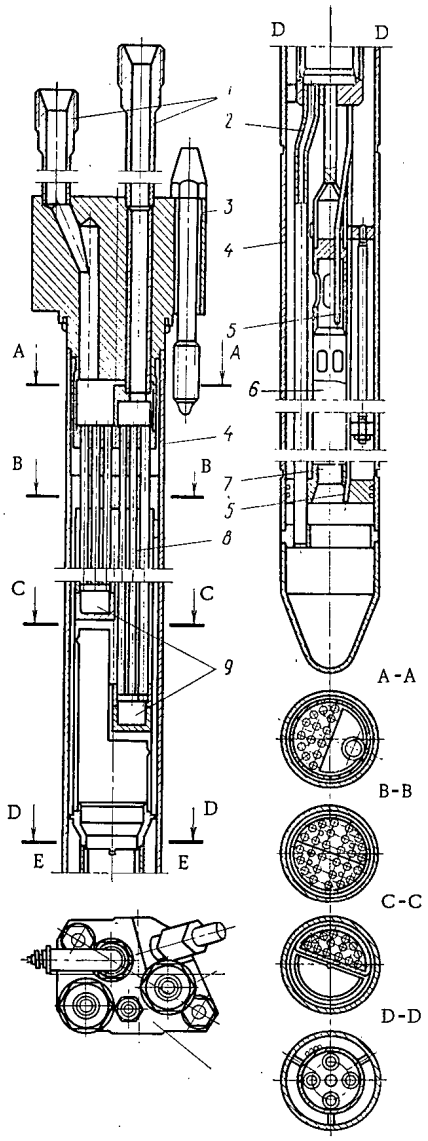

Fig. 2. Design of channel loop: 1) pipe outlets for coolant water; 2) lowering tube; 3) channel head; 4) outer casing; 5) thermocouple; 6) fuel assembly to be tested; 7) lifting tube; 8) built-in tube-and-shell heat exchanger; 9) floating heads of heat exchanger.

The water pressure in the natural circulation loop is maintained by a gas pressure compensation device. Coolant water makeup is handled by one of the feedwater pumps in the reactor experimental loops. The water temperature at the channel exit and entrance is monitored by four Chromel–Copel thermocouples in Kh18N10T steel capillary sized 0.8 × 0.15 mm. The following parameters are measured as part of the job of monitoring channel operating conditions: the pressure and the fill level in the pressurizer, the coolant temperature in the natural circulation loop at the exit and entrance; the rate of coolant water flow through the heat exchangers; the temperature of the coolant water at the heat exchanger entrance and exit. All of the devices installed to monitor the parameters of the loop channel are connected to advance-warning and alarm annunciation systems. Deviations from set points that are not likely to lead to dangerous consequences are registered in a visual and audible signal. A drastic change in parameters (such as a steep rise in the temperature of the coolant water at the exit from the heat exchanger to excessive levels, a drop in pressure in the natural circulation loop) bring the scramming system of the reactor into action [2].

The channel capacity was computed with the heat source distribution over the height of the reactor core, the effective length of the fuel element being studied, and changes in the uniformity of the heat release pattern over the radius of the unperturbed reactor, all taken into account.

The experiments were conducted with a fuel assembly consisting of four ribbon type fuel elements used in the reactor of the Sever plant [4-6]. Uranium–aluminum alloy (UAl_3) 90% enriched with U^{235}, or 4.5 times the uranium enrichment in the Sever plant, was used in the fuel assembly. The high enrichment in the loop specimens of fuel elements was brought about with the object of stepping up the rate of accumulation of fission products. Stainless steel cladding 0.3 mm thick was used.

The channel loop was operated at the rated reactor output level for 11,142 h, and at 50% of the reactor power rating for 2937 h.

The parameters of the natural circulation and coolant water loop are cited in Table 1.

Water conditions generally accepted for nuclear power station performance were maintained [7] throughout the experiment in the natural circulation loop: dry residues content 1 to 5 mg/liter; chlorine content 0.02 mg/liter; oxygen content 0.02 mg/liter; pH 6.5 to 7.5; water hardness 10 to 20 μg-equivalents /liter; total activity 2.2 to 5.5 Ci/liter; iodine activity $2 \cdot 10^{-8}$ Ci/liter. Samples of water were taken periodically, throughout the experiment, from the natural circulation loop, and their total activity and iodine content were measured. No activity was detected in the coolant water during the experiment. Because of the low volume of coolant present in the natural circulation loop, the specific weight of the coolant did not result in any appreciable change in the fill level in the gas pressurizer during the startup to shutdown period, so that dumping and makeup of coolant were eliminated in that case.

The operating history of the loop channel over the course of two years and more demonstrated the reliable performance and ease of maintenance of the facility; natural circulation could be used to remove heat from the fuel assembly at heat fluxes in the neighborhood of $1.3 \cdot 10^{-6}$ W/m^2; the cost feasibility and effectiveness of using that type of experimental channels, eliminating the need to build expensive special loops, was also demonstrated.

TABLE 1

Natural circulation loop	
Channel output level	28 kW
Maximum heat flux from fuel element surface	$1.3 \cdot 10^6$ W/m^2
Cladding temperature	592° K
Heating of water in assembly	50° K
Average water flowspeed through assembly	0.38 m/sec
Average water flowspeed through heat exchanger	0.35 m/sec
Loop pressure	$9 \cdot 10^6$ N/m^2
Coolant water loop	
Pressure	$2.45 \cdot 10^6$ N/m^2
Flowrate	$2.5 \cdot 10^3$ kg/h
Entrance water temperature	300-350° K

At the present time, the underlying principle in the design of the channel loop is being developed in various projects.

LITERATURE CITED

1. V. A. Tsykanov et al., At. Énerg., 29, 169 (1970).
2. L. A. Kochetov and G. N. Ushakov, in: Ten Years of Service of the World's First Nuclear Power Station in the USSR [in Russian], Atomizdat, Moscow (1964), p. 20.
3. G. A. Klochko et al., USSR report presented at the Anglo-Soviet seminar on "Operation and use of research and test reactors," Harwell, 1969.
4. V. A. Zhil'tsov et al., At. Énerg., 26, 403 (1969).
5. N. M. Sinev et al., III Geneva Conference on the Peaceful Uses of Atomic Energy (1964), Paper P/310 (USSR).
6. E. I. Inyutin et al., Énerg., 26, 445 (1969).
7. G. N. Ushakov, The World's First Nuclear Power Station [in Russian], Gosénergoizdat, Moscow–Leningrad (1959).

EQUATION OF STATE OF UF_6 FOR DENSITIES UP TO 0.01180 g/cm^3 AND TEMPERATURES UP TO 367°K

V. V. Malyshev

UDC 533.12

We studied the equation of state of UF_6 for densities up to 0.01180 g/cm^3, pressures up to 750 mm Hg, and temperatures up to 367°K, and also determined the saturated vapor density of UF_6 and the heats of sublimation at 296.3-327.6°K.

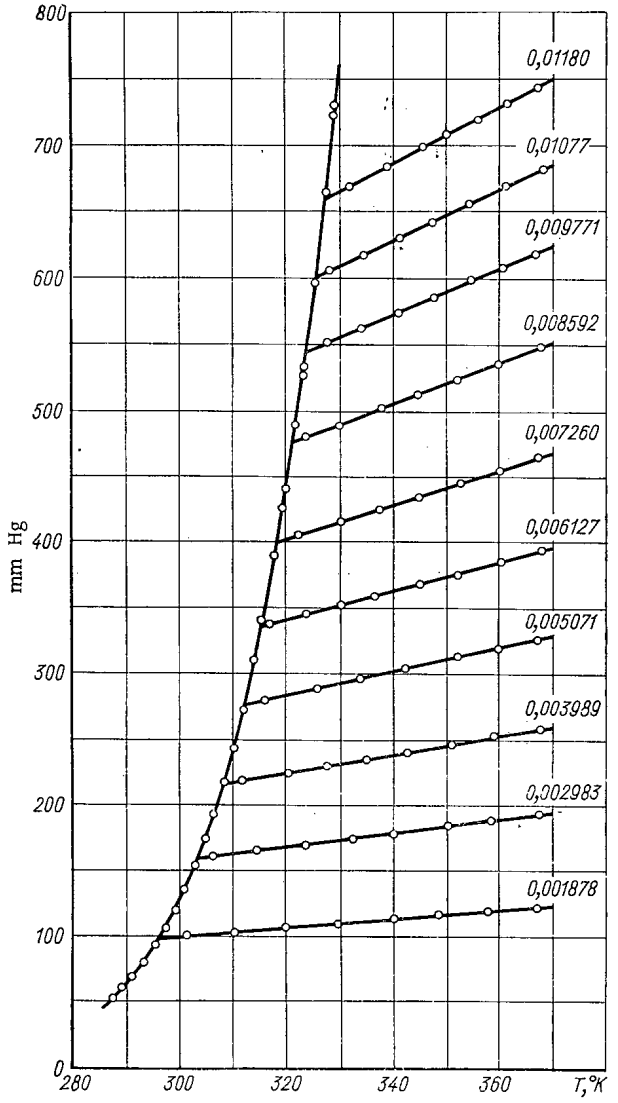

Fig. 1. Isochoric curves relating the UF_6 pressure to temperature (the figures give the density values in g/cm^3 averaged over the isochores).

The measurements were made by means of a constant-volume piezometer. The capacity of the nickel ampoule, with its inner surface passivated by fluorine was 3227 cm^3 at t = 23°C, with an error of 0.06%. The pressure of the UF_6 in the piezometer was measured by a compensation method, using a sensitive membrane separator between the media [1]. The error in the counterpressure was no greater than 0.3 mm Hg, and the temperature error 0.2°K. We used UF_6 of purity no worse than 99.98%. The amount of UF_6 in the piezometer was determined by weighing, allowing for corrosion losses not exceeding 0.1% of the charge.

We studied fourteen isochoric relationships between the pressure p and the temperature, and also the vapor tension curve $p_s(T)$ (Fig. 1). For each temperature value the piezometer was held for 60-90 min (two-phase system) and 30-40 min (gas state) in order to establish equilibrium.

The experimental data for the saturated vapor pressure of UF_6 (in mm Hg) were approximated by the equation:

TABLE 1. Dependence of ρ_v and r on Temperature

T°, K	$\rho_v \times 10^3$, g/cm^3	r, kcal/mole
296,3	1,881	11,80
303,6	2,987	11,75
308,4	3,993	11,68
312,5	5,077	11,63
315,7	6,136	11,50
318,4	7,190	11,38
318,6	7,270	11,38
321,1	8,322	11,36
321,7	8,597	11,35
323,3	9,388	11,31
324,0	9,780	11,26
324,8	10,22	11,23
325,8	10,77	11,24
327,6	11,81	11,21

Translated from Atomnaya Énergiya, Vol. 34, No. 1, pp. 42-44, January, 1973. Original article submitted February 2, 1972; revision submitted August 15, 1972.

$$\lg p_s = 12.2250 - \frac{2808.8}{T} - 0.0025309\ T, \quad (1)$$

which described the experimental data with an error under 0.5%. The differences between the results and those of [2] were no greater than 1-2%.

By extrapolation of the isochores to the vapor tension curve we determined the saturated vapor pressure ρ_V (Table 1). The same table gives the heats of sublimation of solid UF_6 calculated from the Clapeyron–Clausius curve, using Eq. (1). The errors in the values of r are less than 0.7%; the values average 1-2% lower than those of [3].

Since the range of parameters of state under consideration lay in a region remote from the critical point [4], the experimental $p-\rho-T$ data obtained for gaseous UF_6 were approximated by an equation which, in contrast to the equation of state in the region close to the critical point [4], contained only the first term with respect to density

$$Z = \frac{p\mu}{\rho RT} = 1 + B(T)\rho. \quad (2)$$

In this case the coefficient B(T) is identical with the second virial coefficient.

The following are the values of the second virial coefficient calculated by the method of least squares, using an electronic computer (the error is ±4%):

T^0, K	320	330	340	350	360	370
$-B$, $cm^3 \cdot g$. .	2.93	2.73	2.51	2.31	2.15	2.05

The equation of state of UF_6 finally takes the form

$$p\mu/\rho RT = 1 + \left(3.94 - \frac{2.197 \cdot 10^3}{T}\right)\rho. \quad (3)$$

The mean deviation between the experimental data and those calculated from Eq. (3) never exceeds 0.2-0.3% over the whole range of parameters of state studied.

The second virial coefficient values obtained from the present investigation and [4] were approximated by a Lennard–Dyson potential. The calculated values of the intermolecular parameters of UF_6 were $\varepsilon/R = 224°K$, $\sigma = 8.3$ Å.

In conclusion, the author wishes to thank Academician I. K. Kikoin for advice and a number of useful comments.

LITERATURE CITED

1. V. V. Malyshev, Teplofiz. Vys. Temp., No. 6 (1972).
2. B. Weinstock and R. Crist, J. Chem. Phys., 16, No. 5 (1948).
3. J. Masi, J. Chem. Phys., 17, No. 9 (1949).
4. V. V. Malyshev, At. Énerg., 32, No. 4, 313 (1972).

SOME DOSIMETRIC MONITORING RESULTS AT THE ITR-2000 NUCLEAR REACTOR IN SOFIA

I. T. Mishev and M. G. Gelev

UDC 539.12.08: 621.039.538.7

The basic biological shielding of the core of the IRT-2000 nuclear reactor in Sofia consists of water and heavy concrete, as in other reactors of its type. In addition, in addition to the experimental channels there is additional biological shielding consisting of water, paraffin, boric acid, and heavy concrete. Since the thickness and the composition of this shielding vary in different experiments, the dose rate on the far side of the shielding will also vary. As a rule, it will not be in excess of the maximum permissible dose rate. Dosimetric monitoring in the main reactor hall is carried out with the aid of both stationary and portable instrumentation capable of measuring the dose rate of γ-radiation, fast neutrons $E > 0.5$ MeV, thermal neutrons $E < 0.4$ eV, and the activity of gas and aerosols. Clearly, the measured dose will differ from the real dose because of the dose of neutrons with energies in the 0.4 eV to 0.5 MeV range. The difference between the real and measured individual doses will be even greater, because personnel monitoring at the ITR-2000 facility has been carried out over a long period with respect to γ-radiation and thermal neutrons only.

In 1966-1967, a team of radiobiologists carried out a medical and biological examination and study of personnel working at the IRT-2000 reactor facility in Sofia. Several groups of persons working in the main hall over protracted periods were studied, as well as persons working for protracted periods in the radiochemical laboratory, and directly at the experimental channels at the reactor face in the main reactor hall. Chromosomal aberrations were detected in some of those persons exposed.

Comparison of the data resulting from this survey and acquired through the regular personnel dosimetric monitoring service brought the radiobiologists to the conclusion that chromosomal aberrations appear in the human subjects not only after exposure to doses of several tens of rem units, but even in the case of exposures to a dose of 1 rem/year [1].

Since this conclusion could lead to doubts as to the reliability of the recorded exposure dose in the persons examined, it was decided to determine the greatest possible individual exposure doses that can be acquired by persons working at the reactor.

TABLE 1. Maximum Possible Annual Exposure Dose beyond Second-Echelon Reactor Shielding

Dose, rem	Horizontal channel number *								
	1			2	4	9			11
	opposite beam	60 cm above beam	60 cm below beam	opposite beam	opposite beam	opposite beam	60 cm above beam	60 cm below beam	opposite beam
Thermal neutrons	$\leqslant 0{,}17$	$\leqslant 0{,}17$	$\leqslant 0{,}17$	$\leqslant 0{,}17$	$\leqslant 0{,}17$	1,2	$\leqslant 0{,}17$	$\leqslant 0{,}17$	0,4
Fast neutrons	2,0	2,6	2,4	$\leqslant 0{,}15$	$\leqslant 0{,}15$	2,6	3,0	1,0	2,6
γ-Radiation	$\leqslant 0{,}05$	$\leqslant 0{,}05$	$\leqslant 0{,}05$	$\leqslant 0{,}05$	0,1	1,0	0,1	0,1	0,2
Total dose	2,0—2,2	2,6—2,8	2,4—2,6	$\leqslant 0{,}04$	0,1—0,4	4,8	3,1—3,3	1,1—1,3	3,2

* Site of exposure located beyond second-echelon biological shielding of horizontal channel.

Physics Institute of the Bulgarian Academy of Sciences. Translated from Atomnaya Énergiya, Vol. 34, No. 1, pp. 44-46, January, 1973. Original article submitted February 28, 1972.

TABLE 2. Exposure Dose Rate beyond Permanent Biological Shielding

Dose rate, mrem/h	Exposure site						
	basic biological shielding, 30 cm from center of horizontal channel beam				reactor operations area and platform		
	1	2	9	11	on reactor top	at plug of No. 5 vertical channel	on electric drive motors of scram rod
Thermal neutrons	$\leqslant 0,4$	$\leqslant 0,4$	—	12	$\leqslant 0,4$	$\leqslant 0,4$	$\leqslant 0,4$
Fast neutrons	1540	$\leqslant 0,4$	—	100	$\leqslant 0,4$	1,4	$\leqslant 0,4$
γ-Radiation	250	$\leqslant 0,2$	1160	$\leqslant 0,2$	36	36	20
Total dose	1790	$\leqslant 1$	1160	112	36	37,4	20

TABLE 3. Recorded Annual Exposure Dose Acquired by Some Colleagues Present at Most Dangerous Sites

Dose, rem	Individual number assigned to colleague									
	1	2	3	4	5	6	7	8	9	10
Thermal and intermediate-spectrum neutrons	$\leqslant 0,1$	0,3	$\leqslant 0,1$	$\leqslant 0,1$	0,3	$\leqslant 0,1$	$\leqslant 0,1$	0,4	0,3	$\leqslant 0,1$
Fast neutrons	$\leqslant 0,1$	$\leqslant 0,1$	$\leqslant 0,1$	$\leqslant 0,1$	$\leqslant 0,1$	$\leqslant 0,1$	$\leqslant 0,1$	$\leqslant 0,1$	$\leqslant 0,1$	$\leqslant 0,1$
γ-Radiation	0,4	0,1	0,1	0,1	0,1	0,1	0,1	0,1	0,1	0,8
Total dose	0,4—0,6	0,4—0,5	0,1—0,3	0,1—0,3	0,4—0,5	0,1—0,3	0,1—0,3	0,5—0,6	0,4—0,5	0,8—1,0

The neutron dose was measured, except for the neutron group of energies 7 to 500 keV, with the aid of MKT-20 film with a correcting pack [2,3]. The thermal neutron does ($E < 0.4$ eV) and the fast neutron dose (0.5 MeV < E < 15 MeV), principally, were measured beyond the reactor shielding (here the emulsions were irradiated without a phantom). The γ-radiation dose was determined with the aid of Adox and ORWO x-ray films. The concentration of radioactive gases was determined with the aid of a high-sensitivity device [4], while the aerosol concentration was determined by the method of suctioning air through a filter.

In order to determine the greatest possible individual exposure we measured the neutron dose and the γ-radiation dose, and also the concentration of aerosols and radioactive gas at places accessible to personnel, wherever those variables attained their highest values. Those sites were selected directly on the other side of the biological shielding near the experimental channels, which were most often left open while the reactor was in service. On the basis of those measurements, and with the recommendations made by the International Radiological Protection Commission taken into account, we determined the total exposure dose in rem units. The following assumptions were entertained: 1) the reactor was operating only at its peak power output of 1500 kW; 2) horizontal channels which we examined were open continuously while the reactor was in service; 3) the personnel were present at the sites surveyed throughout their working time (46 weeks out of the year). The resulting dose was the maximum possible yearly exposure dose. The results of the exposure dose determination are listed in Table 1.

In addition, sites beyond the reactor shielding where any staffmember might conceivably spend some time without infringing on saftey rules were also investigated. Those sites are located at the exit of open horizontal channels. Results of the dose rate determination at those sites are entered in Table 2. It is clear from the tabular data that, if any of the servicing personnel were to remain some length of time in such dangerous zones, say not more than 30 minutes out of a year, than the total individual dose accumulated would be not greater than one rem.

According to our measurements, the concentration of radioactive gas (mostly Ar^{41}) and radioactive aerosols never exceeded 1/10 of the maximum permissible dose stipulated for the work rooms. It is evident from the data in Table 1 and from the results of measurements taken of the concentrations of radioactive gases and aerosols that there is no place beyond the second-echelon reactor shielding where

the total dose would be greater than one maximum permissible annual dose, i.e., 5 rem. That is also confirmed by measurements of the individual exposure dose (Table 3). The fast neutron dose was determined from the number of tracks in the emulsion in a dosimeter enclosed in a cadmium shield. The thermal neutron dose and the dose of intermediate-spectrum neutrons (with the exception of neutrons whose energies fell within the range from 7 to 500 keV) were determined from the difference between the tracks registered in dosimeters with or without the cadmium shield.

We are led to infer, on that account, that the individual exposure dose to which one worker is subjected in the course of ordinary duties at the IRT-2000 reactor facility in Sofia is not greater than 1 rem ± 30% in the course of a year (neutrons of energies from 7 to 500 keV are not covered by that statement).

The annual exposure dose was less than that in the case of most of the staff colleagues examined. That is also confirmed by regular personnel monitoring data.

The authors are indebted to M. M. Komochkov and M. I. Salatskaya (JINR–Dubna) for their kind and essential assistance in obtaining the experimental results and discussing them.

LITERATURE CITED

1. I. Donev et al., Strahlentherapie, 138/2, 196 (1969).
2. L. S. Zolin, V. B. Lebedev, and M. I. Salatskaya, At. Énerg., 13, No. 5, 467 (1962).
3. M. I. Salatskaya, V. N. Lebedev, and L. S. Zolin, Radiatsionnaya Fizika, 2, 107 (1964).
4. M. G. Khristova and I. T. Mishev, Izv. na Fiz. Inst. s ANEB, Bulgar. Akad. na Naukite, 17, 165 (1968).

POSSIBLE SUPPRESSION OF A PLASMA CYCLOTRON INSTABILITY BY ELECTRON BEAM MODULATION

A. N. Karkhov

UDC 533.9

It is known that a magnetized plasma with an anisotropic velocity distribution of ions ($T_\perp/T_\parallel > 1$, $T_\perp$ and $T_\parallel$ are the "transverse" and "longitudinal" temperatures) must be unstable at an ion cyclotron frequency and its harmonics $\omega \approx m\omega_{Hi}$, m = 1, 2, . . .(see, for example, the review [1]). Experiment and theory indicate that Landau damping has a great influence on the electrons during the buildup of cyclotron oscillations. It is shown in [2] that even the calculation of a simple, local equation for the appearance of this damping $v_{Te} \gtrsim \omega/k_\parallel$ (v_{Te} is the thermal velocity of the electrons, $k_\parallel$ is the projection of the wave vector in the direction of the external magnetic field H_z) permits a good explanation of the experimental results. One can represent the condition on the wavelengths, which can be excited in a plasma having a longitudinal length L, in the form

$$\frac{2\pi v_{Te}}{m\omega_{Hi}} < \lambda_\parallel < 2L. \tag{1}$$

It is shown in [3] that one can suppress the cyclotron instability, removing the oscillational energy by means of external electrons incorporated into a feedback system. However, apparently this method can be utilized only for the suppression of large-scale (compared to L) oscillations.

In the present work, it is proposed that one utilizes a density modulated electron beam, transmitted along H_z and controlled by a feedback system. The particle velocity v_p and the beam modulation law were of necessity chosen so that the beam electrons could compensate the separation of the changes caused by the instability, i.e. $v_p = \omega/k_\parallel$, where $\omega \approx m\omega_{Hi}$ is the beam modulation frequency. Let us show that, in this case, one can in fact expect the suppression of the cyclotron instability.

Let us consider an ideal case. Initially, all of the ions (protons) move with a uniform velocity $v_0 \perp H_z$, $v_{Te} = 0$. It is assumed that the plasma is contained in a conducting cylinder of radius a, unbounded with respect to z. An ion compensated electron beam passes through the plasma along z, in which there occurs, by means of a feedback system, a density modulation of the form

$$n_p = \alpha' \psi e^{-i\omega(t-\tau)-i\theta-im\varphi+ik_\parallel z}, \tag{2}$$

where α' is the transmission coefficient of the feedback system, which is taken to be frequency independent; ψ is the oscillation potential, θ is the phase angle which is arbitrarily specified in the feedback system; τ is the time of flight of the beam from the electron gun up to the plasma; φ is the azimuthal angle.

Utilizing Eq. (2), we obtain from Poisson's equation a dispersion relation for the cyclotron oscillations:

$$1+\frac{\alpha e^{-i(\theta-\omega\tau)}}{k_\parallel^2}+\frac{k_r^2}{k_\parallel^2}\left(1+\frac{\omega_{0i}^2}{\omega_{Hi}^2}\right)-\frac{\omega_{0e}^2}{\omega^2}=\frac{\omega_{0i}^2}{(\omega-m\omega_{Hi}^2}, \tag{3}$$

where ω_{0i}, ω_{0e} are the plasma ion and electron frequencies; $\alpha = 4\pi\alpha'$, $k_r^2 = \mu_{ml}^2/a^2$ (μ_{ml} is the l-th zero of the m-th Bessel function). It is assumed that $\omega^2 \ll \omega_{He}^2$, $\omega_{0e}^2 \ll \omega_{He}^2$. When $\alpha = 0$, Eq. (3) passes over into a known dispersion relation for the cyclotron oscillations from which it follows that when $\omega_{0i}^2 \leq \omega_{Hi}^2$, the oscillations are excited at frequencies $\omega \approx m\omega_{Hi}$ and an increment $\gamma_{max} \ll \omega$. On the basis of this result, let us simplify Eq. (3), replacing ω by $m\omega_{Hi}$ in the left-hand member and assuming that $\gamma_{max}\tau \ll 1$. As a result, we obtain a simplified dispersion relation:

Translated from Atomnaya Énergiya, Vol. 34, No. 1, pp. 46-47, January, 1973. Original article submitted May 10, 1972.

$$\omega = m\omega_{Hi} \pm \omega_{0i} \sqrt{\frac{1}{A + \frac{\alpha e^{-i(\theta - m\omega_{Hi}\tau)}}{k_{\|}^2}}}, \tag{4}$$

where

$$A = 1 + \frac{k_r^2}{k_{\|}^2}\left(1 + \frac{\omega_{0i}^2}{\omega_{Hi}^2}\right) - \frac{\omega_{0e}^2}{m^2\omega_{Hi}^2}, \quad \omega_{0i}^2 \ll \omega_{Hi}^2.$$

Let us assume at first that one can choose a θ such that, for a given m, $\theta - m\omega_{Hi}\tau = 0$ is satisfied. Then one can write the condition for the instability of cyclotron oscillations in the form

$$k_{\|}^2 > (k_{\|}^2)_{\text{crit}} \equiv \frac{k_r^2\left(1 + \frac{\omega_{0i}^2}{\omega_{Hi}^2}\right) + \alpha}{\frac{\omega_{0e}^2}{m^2\omega_{Hi}^2} - 1}. \tag{5}$$

If one now takes into account that actually $v_{Te} \neq 0$ (at the same time, oscillations are sustained at a frequency $\omega \approx m\omega_{Hi}$ with an increment $\gamma < \gamma_{max}$), then Landau damping appears and the region of unstable wave numbers will be determined by the inequality

$$(k_{\|})_{\text{crit}} < k_{\|} < \frac{m\omega_{Hi}}{v_{Te}}. \tag{6}$$

It is clear that when $(k_{\|})_{crit} > m\omega_{Hi}/v_{Te}$, the plasma becomes stable with respect to the cyclotron oscillations. This is necessary so that the condition

$$\alpha > \frac{\omega_{0e}^2 - m^2\omega_{Hi}^2}{v_{Te}} - k_r^2\left(1 + \frac{\omega_{0i}^2}{\omega_{Hi}^2}\right)$$

is satisfied or that the amplitude of the density modulation for the beam is

$$n_p^0 > \frac{\psi_0}{2\pi e}\left[\frac{m^2\omega_{Hi}^2(\varkappa^2 - 1)}{v_{Te}^2} - k_r^2\left(1 + \frac{\omega_{0i}^2}{\omega_{Hi}^2}\right)\right], \tag{7}$$

where ψ_0 is the minimum amplitude of the oscillations in the potential which can be registered by a detector; $\varkappa = \omega_{0e}/m\omega_{Hi}$.

Let us consider the case when $\delta = \theta - m\omega_{Hi}$, $\tau \neq 0$. Assuming that $k_{\|}$ is real, let us seek a solution of Eq. (4) in the form $\omega = \omega_{1,2} + \gamma_{1,2}$. As a result, we obtain

$$\Delta\omega_{1,2} = \pm\omega_{0i}\sqrt{\frac{A + \frac{\alpha}{k_{\|}^2}\cos\delta + \sqrt{A^2 + \frac{\alpha^2}{k_{\|}^4} + 2A\frac{\alpha}{k_{\|}^2}\cos\delta}}{2\left[\left(A + \frac{\alpha}{k_{\|}^2}\cos\delta\right)^2 + \frac{\alpha^2}{k_{\|}^4}\sin^2\delta\right]}}; \tag{8}$$

$$\gamma_{1,2} = \frac{\alpha\omega_{0i}\sin\delta}{2k_{\|}^2\left[\left(A + \frac{\alpha}{k_{\|}^2}\cos\delta\right)^2 + \frac{\alpha^2}{k_{\|}^4}\sin^2\delta\right]\Delta\omega_{1,2}}, \tag{9}$$

where $\Delta\omega_{1,2} \equiv \omega_{1,2} - m\omega_{Hi}$. It follows from Eq. (9) that, in the presence of feedback and the appropriate θ, even previously stable oscillations can commence instability. Both waves $\omega_{1,2}$ are damped, if, when $\Delta\omega < 0$ $\delta > 0$, and vice versa.

The damping of the oscillations in this case occurs because of their collisionless absorption by the electrons in the beam. However, for small phase shifts, i.e., when $\theta - m\omega_{Hi}\tau \approx 0$, Landau damping in the plasma electrons must evidently play a key role in the suppression of the instability. At the same time, the energy will not be removed from the plasma, but only redistributed among the ions and electrons.

In conclusion, let us cite an estimate of the beam currents necessary for the suppression of the instability and the amplification factors of the feedback system. When $\omega_{Hi} = 6 \cdot 10^7$ sec^{-1}, $\omega_{0i}^2 \ll \omega_{Hi}^2$, m = 1, $\varkappa = 5$, $k_r = \pi/a$, $a = 10$ cm, L = 20 cm, $T_e = 10$ eV and $\psi_0 = 1$, we have $n_p^0 \gtrsim 1.5 \cdot 10^8$ cm^{-3}. The energy of the beam electrons must be 400 eV, while the current density guaranteeing stability is about 30 mV/cm^2.

The amplification factor k_0 is determined by the expression

$$k_0 \equiv \frac{V}{\psi} \geqslant 5.5 \cdot 10^2 l^{4/3} \psi_0^{-1/3},$$

where l is the distance between the cathode and the accelerating electrode of the electron gun, cm; V is the accelerating potential. When $l = 0.3$ cm and $\psi_0 = 1$, we have $k_0 \approx 10^2$.

The author thanks V. V. Arsenin, V. A. Chuyanov, V. A. Zhil'tsov, and D. A. Panov for helpful discussions of the work.

LITERATURE CITED

1. A. V. Timofeev and V. I. Pistunovich, in: Problems in Plasma Theory [in Russian], No. 5, Gosatomizdat, Moscow (1967), p. 351.
2. C. Damm et al., Phys. Rev. Letters, 24, No. 10 (1970).
3. V. V. Arsenin et al., ZhÉTF Pis'ma, 8, No. 2 (1968).

BUILDUP FACTORS OF SCATTERED γ-RADIATION FROM A POINT SOURCE IN AN UNBOUNDED AIR MEDIUM

M. N. Vrubel', S. N. Sidneva, and A. S. Strelkov

UDC 539.166.3

The nonstationary problem of propagation of γ-radiation from a prompt point isotropic monoenergetic source through a homogeneous air medium is solved in the present article, with the aid of the Monte Carlo method (method of statistical tests). A modification of this method, proposed in [1], was employed in the calculations. Time-dependent spectral–angular fluxes of the energy of scattered γ-radiation I_E (E_0, E, Ω, t, R) were found for sources with photon energy E_0 = 20 keV to 6 MeV, and time distributions of absorbed energy I_a (E_0, t, R) were found for initial photon energies E_0 = 20 to 500 keV. On the basis of those differential energy characteristics, buildup factors B_E on the energy flux and buildup factors B_a of the absorbed energy, related to I_E and to I_a by the formulas

$$B_E(E_0, \mu_0 R) = 1 + \frac{1}{E_0} 4\omega R^2 e^{\mu_0 R} \int dE\, dt\, d\Omega I_E \times (E_0, E; \Omega, t, R);$$

$$B_a(E_0, \mu_0 R) = 1 + \frac{1}{\mu_0^a E_0} 4\pi R^2 e^{\mu_0 R} \int dt I_a(E_0, t, R),$$

where μ_0 and μ_0^a are the linear coefficients of the total interaction and of absorption of the γ-radiation energy with energy E_0 in air, were determined.

Compton scattering and Rayleigh scattering, as well as photoabsorption and pair production, were taken into account when calculating the propagation of the radiation. Annihilation radiation and fluorescent radiation were assumed absorbed at the point of interaction.

TABLE 1. Value of Buildup Factors of Energy Flux and of Absorbed Energy of Scattered γ-Radiation in Air from a Point Isotropic Source

E_0, keV	$\mu_0 R$											
	1		2		3		4		6		8	
	B_E	B_a	B_E	B_a	B_E	B_a	B_E	B_a	B_E	B_a	B_E	B_a
20	1,42	1,50	1,73	1,85	2,0	2,15	2,37	2,57	2,77	3,00	3,36	3,60
30	1,91	2,32	2,73	3,50	3,56	4,65	4,54	5,88	6,50	8,50	8,50	11,2
40	2,53	3,38	4,12	5,98	6,03	9,14	8,03	12,5	15,1	23,8	18,9	31,0
50	2,95	4,14	5,52	8,80	8,60	14,5	12,6	21,8	22,4	41,0	38,1	69,2
60	3,25	4,54	6,50	10,4	10,9	18,9	16,6	30,0	32,3	62,0	53,6	106
70	3,41	4,50	7,15	10,8	12,3	20,1	19,3	33,2	42,8	78,0	71,8	139
80	3,48	4,60	7,50	11,3	13,3	21,9	21,7	37,7	45,8	84,4	83,2	162
90	3,55	4,37	7,74	10,9	14,1	21,6	22,9	37,4	49,1	86,1	90,0	163
100	3,56	4,25	7,60	10,6	14,4	21,3	23,5	36,5	52,6	89,0	99,4	175
150	3,41	3,70	7,57	9,10	13,8	18,0	22,8	31,9	51,2	77,0	101	158
250	3,05	3,00	6,50	6,73	11,6	12,7	19,0	21,5	40,0	48,0	71,2	88,0
500	2,47	2,44	4,84	4,80	8,00	8,10	12,1	12,4	23,3	23,9	40,7	41,0
1000	2,03	—	3,47	—	5,21*	—	7,24	—	12,3	—	19,3	—
2000	1,71	—	2,54	—	3,46*	—	4,36	—	6,60	—	9,00	—
4000	1,41	—	1,95	—	2,34*	—	2,92	—	4,00	—	5,24	—
6000	1,33	—	1,65	—	1,94*	—	2,22	—	2,73	—	3,88	—

*Data obtained by interpolation with respect to $\mu_0 R$.

Translated from Atomnaya Énergiya, Vol. 34, No. 1, pp. 47-49, January, 1973. Original article submitted May 18, 1972.

TABLE 2. Values of Parameters in Berger Formula for Calculating Buildup Factors of Energy Flux and Absorbed Energy of γ-Radiation Scattered in Air

E_0, keV	C_E	D_E	Error, %		C_a	D_a	Error, %	
			mean	maximum			mean	maximum
20	0,410	—0,047	2,2	3,5	0,048	—0,055	2,5	4,0
30	0,86	0,0089	1,5	2,0	1,26	—0,0016	2,5	7,0
40	1,40	0,0066	4,0	1,2	2,19	0,074	3,5	11,0
50	1,80	0,120	1,5	3,5	2,90	0,138	2,5	3,5
60	2,00	0,158	3,0	7,0	3,20	0,188	5,0	6,5
70	2,10	0,183	4,0	10	3,18	0,228	5,0	12,0
80	2,17	0,201	4,0	6,0	3,08	0,247	6,5	10,0
90	2,21	0,210	4,5	7,0	2,90	0,258	7,5	11,0
100	2,20	0,222	4,0	5,5	2,75	0,270	7,0	9,0
150	2,05	0,232	3,0	5,0	2,30	0,278	9,0	10,0
250	1,83	0,205	5,0	7,0	1,78	0,238	6,0	10,0
500	1,37	0,160	4,0	6,0	1,33	0,173	4,0	7,0
1000	0,96	0,107	3,0	5,0	1,05*	0,097*	—	—
2000	0,67	0,058	2,0	5,5	0,8257†	0,02407†	—	5,0
4000	0,43	0,023	2,0	2,5	0,6020†	0,00323†	—	1,0
6000	0,30	0,012	4,0	7,0	0,5080†	—0,00289	—	1,0

*Obtained from $C_a(E_0)$ and $D_a(E_0)$ curves by interpolation.

† Data borrowed from [7].

Interaction coefficients for air of normal composition at density $1.293 \cdot 10^{-3}$ g/cm^3 [2, 3] were used. The distances at which the characteristics of the fields of scattered radiation were calculated were selected on the basis of the mean free path length of the original radiation from the source, and were found to conform to the optical thicknesses $\mu_0 R = 1, 2, 3, 4, 6, 8$.

In each variant, calculations were performed on 40,000 trajectories, so that buildup factors could be obtained with statistical error smaller than 10% for the maximum distances from the source. The statistical error in the calculations was checked by finding the rms error and the convergence of the results after 10,000, 20,000, 30,000, and 40,000 trajectories had been examined. The two estimates were in close agreement.

The resulting energy buildup factors and buildup factors of absorbed energy are listed in Table 1. It is evident from the tabular data that the energy buildup factors peak at the energy of the initial radiation ≈ 150 keV. The maximum in the buildup factors of absorbed energy ends up shifted in the direction of lower original energies, and is observed at $E_0 \approx 90$ to 100 keV, on account of the tendency of the absorption coefficient to increase with decreasing energy. On the whole, the behavior exhibited by $B_E(E_0)$ and by $B_a(E_0)$ is in agreement with that disclosed earlier [4] in solving the age equation for γ-photons.

The B_E and B_a values found in this article for air are in close agreement with the data reported by Goldstein and Wilkins for water [5] at energies from 250 keV to 1 MeV. The scattering and absorbing properties of the media in question are practically coincident over the range of energies in question.

The buildup factors B_E and B_a were approximated by Taylor formulas [6] and Berger formulas in order to render them more convenient for applications. It was found that the Berger formula $B_{a,E}(E_0, \mu_0 R) = 1 + C_{a,E}(E_0)\mu_0 R \exp\{D_{a,E}(E_0)\mu_0 R\}$ yields more accurate results. The values of the parameters $C_{a,E}(E_0)$, $D_{a,E}(E_0)$ found by the method of least squares, using a standard program for the NAIRI-2 digital computer, are listed in Table 2.

Similar behavior on the part of the buildup factors of absorbed energy in air has been reported [7] for radiation energies from 0.5 to 10 MeV. Comparison of the B_a values arrived at in the present article ($E_0 = 500$ keV) and the data reported in [5, 7] showed that the buildup factors of absorbed energy obtained by using C_a and D_a from [7] are depressed markedly for $E_0 = 0.5$ MeV and $E_0 = 1$ MeV (to 40% approximately, in the case $\mu_0 R = 8$ at $E_0 = 0.5$ MeV, both in relation to the present article and in relation to [5]). At still higher initial energies of γ-radiation ($2 \leq E_0 \leq 6$ MeV), the B_a values reported in [7] and [5] coincide, within the limits of error of the approximation, with those reported in [7]. Under the assumption that the B_a values obtained with the use of the data reported in [7] are true values over the 2-6 MeV energy range, we constructed the entire dependence $C_a(E_0)$, $D_a(E_0)$ for the energy range from 20 keV to 6 MeV.

Values of the parameters C_a and D_a for radiation energy 1 MeV were determined on the basis of that dependence (see Table 2). The values obtained for parameters C_a and D_a (respectively 1.05 and 0,0097) are in agreement with the values computed by Chilton for water at $E_0 = 1$ MeV [8].

The general form of the description of buildup factors of the energy flux and of absorbed energy for γ-radiation scattered in air, at energies from 20 keV to 6 MeV, was found in that manner, and then utilized to calculate the basic characteristics of γ-ray fields in air.

LITERATURE CITED

1. A. S. Frolov and N. N. Chentsov, in: Monte Carlo Method in Radiative Transfer Problems [in Russian], G. I. Marchuk (editor) Atomizdat, Moscow (1967), p. 25.
2. K. Siegbahn (editor), Alpha-Ray, Beta-Ray, and Gamma-Ray Spectroscopy [Russian translation], No. 1, Appendix 1, Atomizdat, Moscow (1969).
3. E. Storm and H. Israel, Nuclear Data Tables, Section A, 7, No. 6, 565 (1970).
4. V. Ch. Pal'vanov and A. S. Strelkov, in: Advances in Dosimetry and Radiation Shielding [in Russian], L. R. Kimel' (editor), No. 7, Atomizdat, Moscow (1969), p. 139.
5. H. Goldstein and I. Wilkins, "Calculation of the penetration of gamma-rays," USAEC Rep. NYO-3075 (1954).
6. S. G. Tsypin (editor), Nuclear Reactor Shielding [Russian translation], Izd-vo Inostr. Lit., Moscow (1958), p. 300.
7. D. Trabi, Atomnaya Tekhnika za Rubezhom, No. 10, 25 (1971).
8. A. Chilton, Nucleonics, 23, No. 8, 92 (1965).

USE OF Pa^{231} AND U^{236} IN MEASURING FAST NEUTRON SPECTRA

K. K. Koshaeva and S. N. Kraitor

UDC 539.125.164

One method of measuring fast neutron spectra consists of using threshold detectors which record the neutron yield in fission reactions of the type (n, p), (n, α), etc. By proper interpretation of the detector readings [1-4], it is possible to reestablish fast neutron spectra with a certain degree of accuracy. The largest error in reestablishing the spectra lies in the 0.5-1.5 MeV range, since there are no detectors that can furnish adequate spectrometric data in this voltage range.

It is possible to increase the accuracy of spectra measurement by using fissionable isotopes Pa^{231} and U^{236} in a set of threshold detectors. The effective cross section σ_{eff} and the threshold energy E_{th} for these isotopes were calculated with the following formula:

$$\sigma_{eff} \int_{E_{th}}^{\infty} \varphi(E)\, dE = \int_{0}^{\infty} \sigma(E)\, \varphi(E)\, dE, \qquad (1)$$

where $\sigma(E)$ is the fission cross section and $\varphi(E)$ is the differential neutron flux.

Calculations were made for the neutron spectra of various critical components, reactors, and shields described in [5]. Data on the fission cross section was obtained from [6, 7]. Results of the calculations for Pa^{231} and U^{236} are shown in Figs. 1 and 2, respectively. Threshold energy values are seen at which

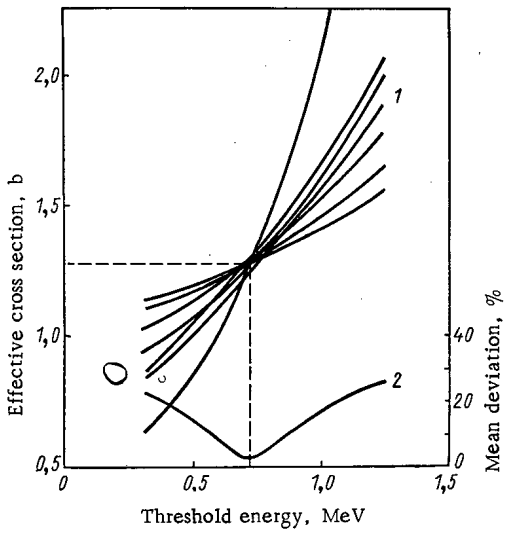

Fig. 1

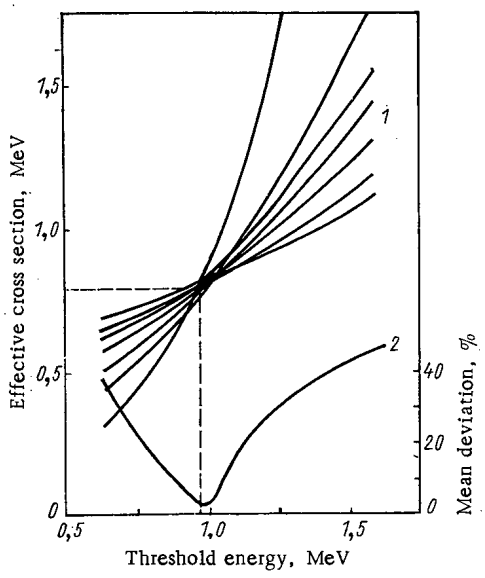

Fig. 2

Fig. 1. Behavior of the effective cross section fission of Pa^{231} (curve 1) and its maximum mean deviation (curve 2) from the threshold energy selected.

Fig. 2. Behavior of the effective cross section fission of U^{236} (curve 1) and its maximum mean deviation (curve 2) from the threshold energy selected.

Translated from Atomnaya Énergiya, Vol. 34, No. 1, pp. 49-52, January, 1973. Original article submitted May 22, 1972.

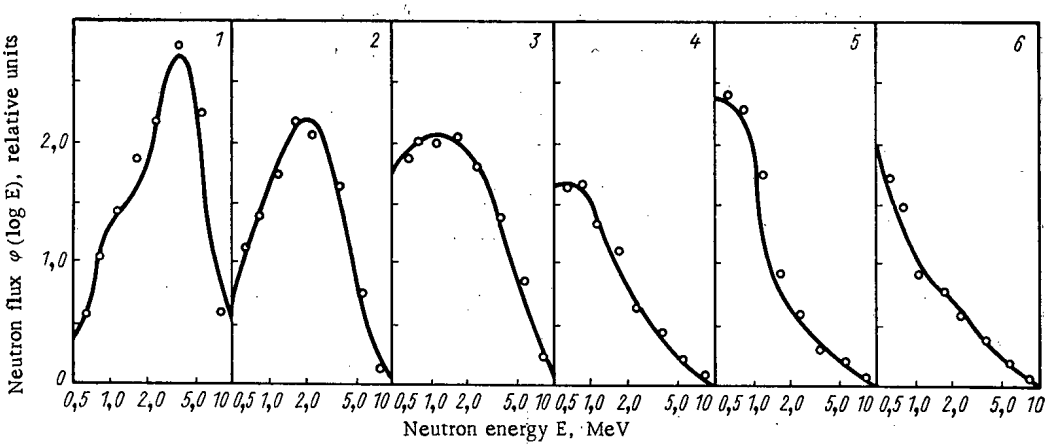

Fig. 3. Reestablishment of spectra from a Pu–Be source (1), from neutron fission without shielding (2), from neutron fission with water shielding (3), from VVR (4), Br-5 (5), and Br-1 (6) reactors, with a set of threshold detectors using Pa^{231} and U^{236}. Solid lines indicate the given spectra and the small circles indicate the reestablished neutron flux values.

the deviation of the effective cross section from the mean value is the least. For Pa^{231} the optimal values are 0.72 MeV and 1.28, and for U^{236} they are 0.95 MeV and 0.79. The threshold energies for these isotopes lie between the threshold energies for Np^{237} and U^{238}, which are 0.56 and 1.4 MeV, respectively [5]. The variance of the effective cross sections at optimal threshold energy values does not exceed 2-4%.

The spectrometric potentialities represented in the detectors were investigated, for example, in a set of detectors used for measuring fast neutron spectra. This set of detectors used Np^{237} (n, f), U^{238} (n, f), S^{32} (n, p), Al^{27} (n, p), and Al^{27} (n, α) to which Pa^{231} (n, f) and U^{236} (n, f) were added. The neutron spectra reestablished with this modified set of detectors differed markedly in form from those usually found in the low-energy area. As examples of the latter, the spectra of the following were chosen: Pu–Be source, neutron fission without shielding and with water shielding [8], VVR, Br-5, and Br-1 reactors [9-11].

The exponential approximation method was used to reestablish the spectra [12-13]. In this method the 0.5-1.5 MeV range is divided into intervals corresponding to the threshold energies of the detectors selected and the neutron spectra in the i-th interval were approximated by using the following expression:

$$\varphi(E) = A_i e^{-\alpha_i (E_i - E)}, \tag{2}$$

where A_i and α_i are constants, determined from the conditions of the continuous spectra at the interval boundaries. The values of the effective cross section and threshold energy, necessary for reestablishing the spectra, were taken from [5] or calculated using formula (1).

The reestablished neutron spectra are compared with the given spectra in Fig. 3. The data indicate that even such a simple and approximate method as exponential approximation permits adequate reproduction of the low-energy part of the spectrum. The error in reproducing the given spectra η_φ was calculated and averaged out in the 0.5-1.5 MeV range. The calculation was performed with the following formula:

$$\eta_\varphi = \frac{\int_{0.5\,\text{MeV}}^{1.5\,\text{MeV}} \left| 1 - \frac{\varphi(E)}{\varphi_0(E)} \right| \varphi_0(E)\, dE}{\int_{0.5\,\text{MeV}}^{1.5\,\text{MeV}} \varphi_0(E)\, dE}, \tag{3}$$

where $\varphi_0(E)$ is the given spectrum and $\varphi(E)$ the reestablished spectrum.

The error was determined for two cases. In the first case, Pa^{231} and U^{236} were included in the set of detectors; in the second case, these isotopes were excluded. In the present work, the measurement errors for the activated integrals and cross sections of the corresponding reactions were not investigated because their effect on the error in reestablishing the spectra by the exponential approximation method was described in [12]. The results of the calculation, listed in Table 1, indicate that the inclusion of Pa^{231} and

TABLE 1. Errors in Reestablishing Fast Neutron Spectra and Calculation of the Tissue Kerma in the 0.5-1.5 MeV Range with a Set of Threshold Detectors

Spectra	Error, %			
	neutron flux		tissue kerma	
	with isotopes Pa^{231} and U^{236}	without isotopes Pa^{231} and U^{236}	with isotopes Pa^{231} and U^{236}	without isotopes Pa^{231} and U^{236}
Pu–Be	5,9	25	5,8	14
Fission	3,1	14	2,8	11
Water	2,0	9,0	0,1	7,7
VVR	4,2	17	2,0	17
BR-5	7,0	26	5,8	18
BR-1	4,6	19	0,1	12
Median error	4,5	17,5	2,9	18

U^{236} in the set of detectors permit a decrease of three to four times in the error of reestablishing spectra in the 0.5-1.5 MeV range.

In the same two cases, the error in calculating the tissue kerma η_k during reestablishment of neutron spectra was computed. The error in η_k was determined using the following formula:

$$\eta = \left| 1 - \frac{\int_{0.5\,\text{MeV}}^{1.5\,\text{MeV}} \delta_k(E)\,\varphi(E)\,dE}{\int_{0.5\,\text{MeV}}^{1.5\,\text{MeV}} \delta_k(E)\,\varphi_0(E)\,dE} \right|, \quad (4)$$

where $\delta_k(E)$ is the relationship of the specific tissue kerma to neutron energy [14]. The results obtained are presented in Table 1. The data indicate that use of fissionable isotopes Pa^{231} and U^{236} significantly increase the accuracy of dosimetric measurements.

The authors are grateful to I. B. Keirim-Markus for his interest in the work and for his helpful comments, and to G. A. Frolovaya for assistance in carrying out the calculations.

LITERATURE CITED

1. M. Bresesti et al., Neutron Dosimetry, Proc. Symp., Vol. I, IAEA, Vienna (1963), p. 27.
2. R. Dierkx, ibid, p. 235.
3. G. Cola and A. Rota, Nucl. Sci. and Engng., 23, 344 (1965).
4. E. A. Kramer-Ageev, E. G. Tikhonov, and V. S. Troshin, in: Problems in Dosimetry and Radiation Shielding [in Russian], Vol. 9, Atomizdat, Moscow (1969), p. 139.
5. K. K. Koshaeva, S. N. Kraitor, and L. B. Pikel'ner, Preprint RZ-5421, OIYaI (1970).
6. W. Hart, UK–USSR Seminar, Paper UK-10 (1968).
7. E. Hyde, I. Perlman, and G. Seaborg, Nuclear Fission [Russian translation], Atomizdat, Moscow (1969).
8. I. A. Bochvar et al., Neutron Monitoring, Proc. Symp., IAEA, Vienna (1967), p. 459.
9. Yu. A. Egorov, V. I. Zharkov, and Yu. V. Orlov, At. Énerg, 28, 170 (1970).
10. Yu. S. Ryabukhin et al., Med. Radiologiya, 14, 66 (1969).
11. A. I. Leipunskii et al., At. Énerg, 5, 277 (1958).
12. R. D. Vasil'ev et al., in: Measurement of Neutron Radiation in Reactors and Accelerators [in Russian], VNIIFTRI, Moscow (1971), p. 130.
13. A. A. Chernoyarskii, V. I. Kukhtevich, and V. S. Medik, in: Problems in Shielding from the Penetrating Radiation of Reactor Apparatus [in Russian], Vol. 7, Melekess (1969), p. 5.
14. J. Dennis et al., AERE-R (1970), p. 6498.

ASYMMETRY OF THE PHOTOFISSION OF Np^{237} AS A FUNCTION OF THE MAXIMUM BREMSSTRAHLUNG ENERGY

M. Ya. Kondrat'ko, V. N. Korinets, and K. A. Petrzhak

UDC 537.531.9

We measured the yields of several products of the symmetrical and approximately symmetrical fission of Np^{237} by bremsstrahlung for maximum energies ranging between E_γ^{max} = 10 and 24 MeV. The work was carried out by the radiochemical method. Irradiation took place in a betatron with a maximum electron energy of 30 MeV. The target was irradiated in a special cylindrical vessel mounted in the accelerator chamber in such a way as to facilitate the insertion and extraction of samples without breaking the vacuum [1]. The electron beam was deflected to the bottom part of the vessel; the bremsstrahlung was generated in a tungsten radiator and in the irradiated sample.

Energy calibration of the betatron was carried out on the basis of photoneutron reactions with known thresholds. The error in measuring the energy, allowing for the voltage instability in the magnet windings, was 0.15 MeV. The energy was varied by means of an electronic circuit, introducing a phase shift between the pulse corresponding to the injection of the electrons into the chamber and the deflection of the electrons on to the target.

We used a method based on the collection of the recoil fragments. The target was assembled from thin layers of NpO_2 (200 $\mu g/cm^2$) baked into an aluminum substrate. The layers of fissile material were placed adjacent to collector layers of aluminum foil 5.4 mg/cm^2 thick. After irradiation, the collectors were dissolved in concentrated nitric acid, to which known quantities of stable isotope carriers had previously been added. Then the solution was subjected to standard radiochemical procedures of purification and isotope separation. The final residue was placed on conducting substrates (1.36 mg/cm^2) in uniform layers 1-3 mg/cm^2 thick. The beta activity was measured in flow-type 4π-counters.

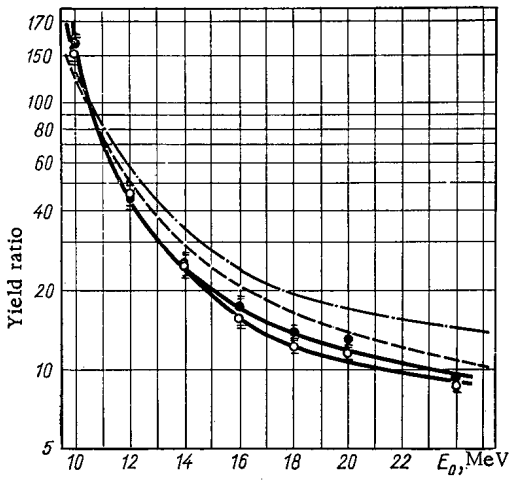

Fig. 1. "Peak to trough" ratio for the photofissions of Np^{237} and U^{235}. Results of the present investigation for the Np^{237} (γ, f) reaction: ●) $Y_{Ba^{140}}/Y_{Cd^{115}}$; ○) $Y_{Ba^{140}}/Y_{Cd^{117}}$. Results of [6] for the U^{235} (γ, f) reaction: -.-.--) $Y_{Ba^{140}}/Y_{Ca^{115}}$; ----) $Y_{Ba^{140}}/Y_{Cd^{117}}$.

Translated from Atomnaya Énergiya, Vol. 34, No. 1, pp. 52-53, January, 1973. Original article submitted May 23, 1972.

TABLE 1. Relative Yields of the Photofission Products

E_γ^{max}, MeV	$\frac{Y_{Pd^{109}}}{Y_{Ba^{140}}}$	$\frac{Y_{Ag^{111}}}{Y_{Ba^{140}}}$	$\frac{Y_{Pd^{112}}}{Y_{Ba^{140}}}$	$\frac{Y_{Ag^{113}}}{Y_{Ba^{140}}}$	$\frac{Y_{Cd^{115}}}{Y_{Ba^{140}}}$	$\frac{Y_{Cd^{117}}}{Y_{Ba^{140}}}$
10	0,044	0,019	0,0062	0,0055	0,0064	0,0055
12	—	0,040	0,029	0,023	0,025	0,023
14	0,138	0,0652	0,0429	0,0433	0,0451	0,0415
16	0,147	0,0950	0,0624	0,0627	0,0657	0,0570
20	0,182	0,109	0,0968	0,0827	0,0877	0,0816
24	0,248	0,145	0,114	0,106	0,116	0,110

In order to introduce small corrections for self-absorption and absorption in the substrate we used the results of a calibration of the same counters based on standard specimens with different radiation energies [2].

As fragments characteristic of symmetrical fission we chose $Cd^{115, 117}$, and as fragments close to symmetrical we chose $Pd^{109, 112}$ and $Ag^{111, 113}$. The yields of all the isotopes were measured relative to the yield of Ba^{140}.

The radioactive decay curves were analyzed by the method of least squares, introducing the known constants [3]. In analyzing the results for mass number 117, the ratios of the Ag^{117} decay branches ($T_{1/2}$ = 1.1 min) leading to the formation of Cd^{117m} ($T_{1/2}$ = 3 h) and Cd^{117} ($T_{1/2}$ = 50 min) were taken as 0.82 : 0.18 [4, 5].

The absolute activities, corrected for the chemical yield, were converted to the saturation activity A_i^∞. The relative yields were determined as the ratio $A_i^\infty/A_{Ba^{140}}^\infty = Y_i/Y_{Ba^{140}}$. The results, averaged over two to four measurements, are presented in Fig. 1 and Table 1. We also measured the relative yields of Ru^{103} and Ru^{105} for maximum energies of 24 MeV (respectively equal to 0.925 and 0.548), 20 MeV (1.011 and 0.594), and 14 MeV (0.867 and 0.584). The relative error in the results presented was 10-15% for an E_γ^{max} of 10 and 12 MeV and 5-7% for higher energies.

Comparison of the results shows that the relative yields of the mass chains 112, 113, 115, and 117 are equal (within the limits of measuring error) and increase rapidly with rising excitation energy of the nucleus undergoing fission. The yields of Pd^{109} and Ag^{111} exhibit a less violent rise with increasing energy. As E_γ^{max} increases from 10 to 24 MeV, the ratio of the yields of Pd^{109} to the average value of the yields of symmetrical fission falls from 8 to 2.2, while for Ag^{111} the analogous quantity changes from 3.4 to 1.3, which indicates a more rapid increase in the yield of the fragments corresponding to the symmetrical fission of Np^{237} with increasing excitation energy. The measured yields of Ru^{103} and Ru^{105} are practically independent of E_γ^{max} in the range 14-24 MeV.

Figure 1 presents data obtained in an analogous manner for the photofission of U^{235} [6]. Comparison of the results indicates a slightly greater asymmetry of the photofission of Np^{237} at E^{max} = 10 MeV and a smaller asymmetry at E_γ^{max} = 12-14 MeV. In the photofission of Np^{237} there is no irregularity in the range of symmetrical fission, such as appears as a systematic increase in the yield of masses 115 and 117 over 111 and 113 in the photofission of U^{235}.

LITERATURE CITED

1. M. Ya. Kondrat'ko, O. P. Nikotin, and K. A. Petrzhak, At. Énerg., 27, 544 (1969).
2. M. Ya. Kondrat'ko, O. P. Nikotin, and K. A. Petrzhak, Pribory i Tekh. Éksper., 3, 47 (1964).
3. B. S. Dzhelepov, L. K. Peker, and V. O. Sergeev, Schemes of the Decay of Radioactive Nuclei. A ≥ 100 [in Russian], Izd. AN SSSR, Moscow (1963).
4. T. Kivikas and B. Forkman, Nucl. Phys., 64, 420 (1965).
5. M. Ya. Kondrat'ko and K. A. Petrzhak, At. Énerg., 23, 559 (1967).
6. M. Ya. Kondrat'ko and K. A. Petrzhak, At. Énerg., 20, 514 (1966).

γ-ACTIVATION ANALYSIS OF CARBON IN THORIUM AND URANIUM

A. F. Gorenko, N. A. Skakun,
G. M. Shevchenko, A. S. Zadvornyi,
N. I. Bugaeva, and A. P. Klyucharev

UDC 543.52:546.21

Interest in analysis of carbon, nitrogen, and oxygen contained in thorium and uranium stems from the profound influence of those impurities on the mechanical and physical properties of uranium and thorium. The greatest effect seems to be that caused by carbon present [1]. Methods of effecting quantitative carbon determinations in uranium and thorium have been known, and are based on combustion of the specimen in an oxygen stream: the carbon dioxide gas released is selectively drawn out of the oxygen stream and the amount is then determined by gravimetric, manometric, conductometric, or other methods [2].

In thorium analysis, and also in analysis of uranium carbides and thorium carbides, the specimens are ashed in the presence of flux. The purity of the flux and the purity of the stream of oxygen employed in the combustion process exert a serious effect on the accuracy of the analysis. The purer the metal, the more pronounced that effect will be. Certain errors are also introduced by superficial contaminations of the specimen, but the principal shortcoming of those methods of analysis is the low sensitivity of the detectors employed: 0.01 to 0.001 wt.%. In some cases, however, carbon impurities must be determined with a higher sensitivity.

The use of more sensitive nondestructive methods of activation analysis is not without its difficulties either, since uranium and thorium nuclei become activated when bombarded by neutrons of γ-photons, and

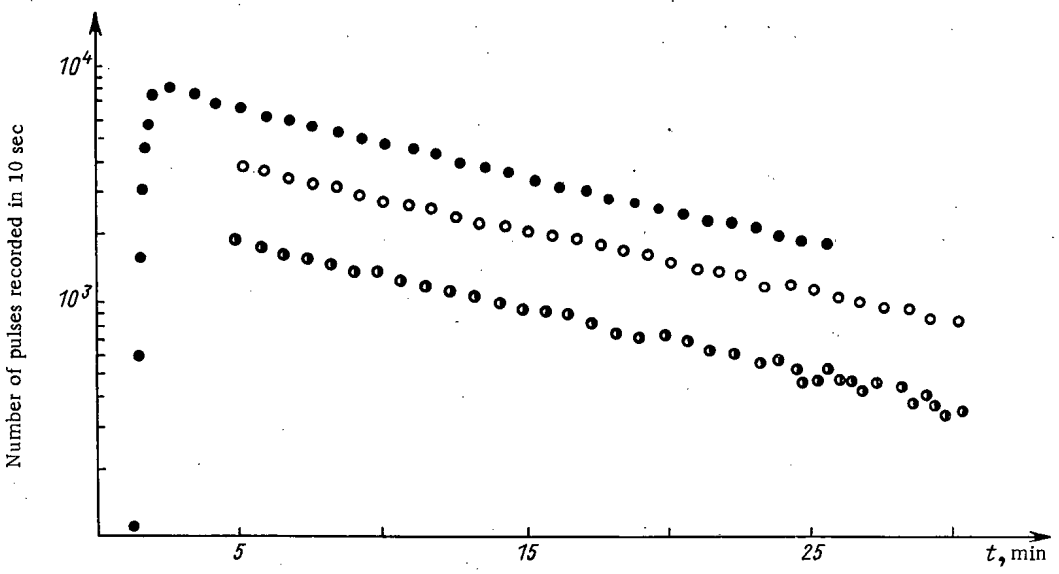

Fig. 1. Buildup and decay of $C^{11}O_2$ molecules obtained in combustion of specimens, in ascarite: ○) uranium; ◑) thorium; ●) lavsan [Dacron].

Translated from Atomnaya Énergiya, Vol. 34, No. 1, pp. 53-54, January, 1973. Original article submitted June 12, 1972.

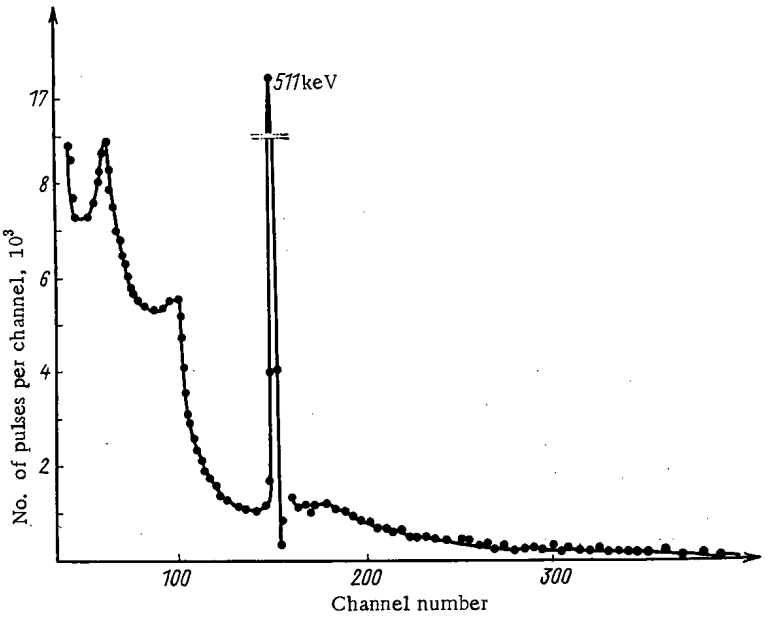

Fig. 2. Spectrum of activity in ascarite.

they undergo fission. Charged particles should be used in the activation analysis. The coulomb barrier is ≈ 10 MeV for protons, which is higher than the threshold of the reaction $C^{13}(p, n)$, and higher than the energy of the first resonance of the reaction $C^{12}(p, \gamma)$. But one disadvantage of this method of analysis for determining carbon present on the surface of specimens is the low sensitivity and limited accuracy [3] due to the noise associated with limited penetration of protons into the bulk of the specimens, and several other reasons.

The high sensitivity in carbon determinations in fissionable elements and materials based on fissionable elements is attained when carbon is burned up in a stream of oxygen from specimens preirradiated by γ-photons. In that case, the C^{11} forming in the reaction $C^{12}(\gamma, n)$ is selectively withdrawn from the active matrix, as is the chemical methods of analysis, and the amount of $C^{11}O_2$ collected is found from the decay of the radioactive carbon isotope, by a sensitive nuclear detector.

We irradiated a test specimen with bremsstrahlung γ-photons generated on a tungsten converter by a beam of 30 MeV electrons. The cross section of the reaction $C^{12}(\gamma, n)C^{11}$ is quite large, and the 20.74 min half-life is convenient for analytical purposes. After the sample was irradiated, it was transferred to a facility [4] for carbon determinations by the method of oxidative fusion. The $C^{11}O_2$ molecules were selectively absorbed in ascarite placed between two photomultiplier tubes with NaI(Tl) crystals sized 150 mm × 100 mm in a fast–slow coincidence spectrometer. That makes it possible to heighten the sensitivity of the carbon determination appreciably over that attainable with more familiar techniques. In addition, no such stringent requirements are imposed on the purity of the oxygen or of the fluxes employed as was the case in [2].

Figure 1 shows the process of accumulation and decay of $C^{11}O_2$ molecules extracted from specimens of uranium, thorium, and Dacron [lavsan] film $(C_{15}H_{12}O_6)_n$. The film was irradiated simultaneously and under identical conditions with the specimens, and was then employed as standard for the determination of the carbon concentration. Clearly, the burnup of carbon and pickup of $C^{11}O_2$ in the ascarite go to completion within 3–4 min after the onset of oxidation, and then the activity built up decays with the half-life $T_{1/2}$ = 20.74 min characteristic of C^{11}.

Figure 2 shows a spectrum of the decay of activity built up in ascarite in a carbon determination in uranium carbide. The spectrum was measured with a Ge(Li)-detector 50 cm^3 in volume. The mean carbon concentration in the uranium and thorium specimens, for the three measurements, was respectively 0.064% for uranium and for thorium. The following results were obtained by the volumetric method in analysis of similar specimens: 0.063% for uranium, 0.21% for thorium.

Under the activation conditions selected (electron energy 30 MeV, current 10 μA, exposure time 20 min), the sensitivity of the carbon determination in uranium and in thorium was $1.3 \cdot 10^{-7}$ g. The method described can be used in analysis of carbon in other heavy elements as well.

LITERATURE CITED

1. J. A. Milko, R. E. Adams, and V. O. Harms, Thorium [Russian translation], G. A. Meerson (editor), Atomizdat, Moscow (1962), p. 166.
2. V. T. Elwell and D. F. Wood, Analysis of New Metals [Russian translation], Khimiya, Moscow (1970), p. 28.
3. I. Point, Radioisotopes in Scientific Research, Internat'l. Conf. Paris, Vol. 2, UNESCO (1957), p. 180.
4. P. Ya. Yakovlev, A. A. Fedorov, and N. V. Buyanov, in: Analysis of Materials in Metallurgical Production [in Russian], Metallurgizdat, Moscow (1961), p. 9.

LINEAR RESONANCE ACCELERATOR WITH A STEADY ELECTRON FLUX

B. A. Snedkov and B. A. Turenko

UDC 621.384.64

Electrostatic accelerators of charged particles, guaranteeing relative energy homogeneity, equal to 10^{-4}-10^{-5} [1] are utilized in electron-optical engineering equipment, in electron microscopes, and in some nuclear physics instruments. The possible application of radio frequency accelerators in similar devices was reported in [2-4]; however, we did not find to be practical the utilization of an accelerator with small energy spread in the clusters; this is explained by inhomogeneities in the electron clusters, increasing significantly the loss of particles during collimation.

In the present paper, the characteristics of a linear, resonance high frequency accelerator for monoenergetic electrons, based on the following operational principles, are presented. A cyclically varying field with frequency ω acts on a gun-injected steady, homogeneous beam of low energy electrons with $v_i \sim \sqrt{U_i}$ (U; is on the order of 20 keV). As a result, an electron helix with a constant pitch, which enters an accelerating system—helical wave guide, or a group of ring-shaped, traveling-wave resonators, arranged coaxially, is formed. The use of ring-shaped, traveling-wave resonators reduces the output of the superhigh frequency generator feeding the accelerator. Ring-shaped resonators in the middle of wide walls have a slit for the passage of the electron flux, while the distance between the walls, as is the case with the accelerator resonators, is determined by the coupling between the flux and the field. An H_{10} wave is excited in the resonators and is produced with the aid of a matching device by a system of traveling waves, during which the amplitude of the electric field is displaced in the space bounded by the walls of the resonator at the same angular velocity ω to ensure the synchronization of the electron gyration and the

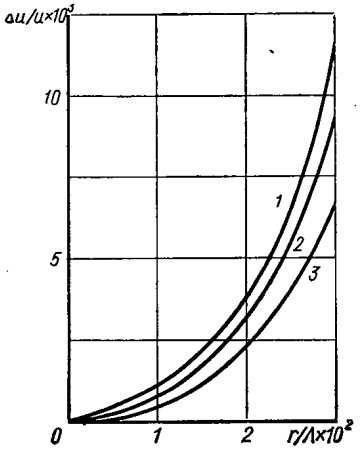

Fig. 1

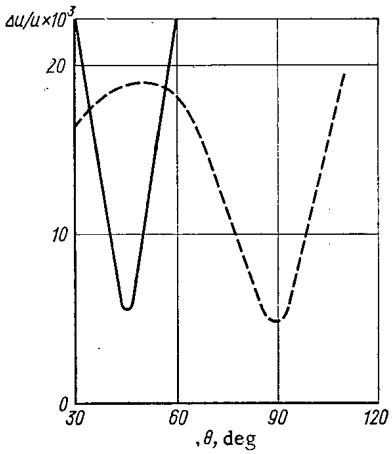

Fig. 2

Fig. 1. Dependence of the electron energy spread on 1) $u_i = 0.02$; 2) $u_i = 0.06$; 3) $u_i = 0.1$.

Fig. 2. Dependence of the electron energy spread on the initial phase (———) and on the transit angle in the resonator (-----).

Translated from Atomnaya Énergiya, Vol. 34, No. 1, pp. 55-56, January, 1973. Original article submitted September 30, 1971; revision submitted January 6, 1972.

motion of the wave crests. The spatial helix of accelerated electrons is converted into a rectilinear electron flux by means of an electrostatic or magnetic focusing system.

The stability of the resonator field amplitudes, the tuning frequency, the pulse duration, and the beam current influence the energy spectrum width in linear, monoenergetic accelerators [5]. The modulating resonator, manifesting the principal source of spread in the electron energies, is absent in the accelerator under consideration.

The equation relating the energy of the electrons to the phase of the resonator's accelerating field, neglecting the space charge, has the form [6]

$$\cos\varphi=\cos\varphi_i-\frac{\sqrt{u^2+2u}-\sqrt{u_i^2+2u_i}}{E}kU_0, \tag{1}$$

where U_0 is the energy of the electron current; $u = U/U_0$ is the relative energy; $u_i = U_i/U_0$ is the relative initial energy; φ_i is the initial phase; k is the wave number. This equation permits one to determine the energy of the electrons at the exit of the ring-shaped resonator for a prescribed entrance phase and injection energy. For example, when the amplitude of the field E = 120 kV/cm, the increase in the energy of the electrons during the transmission of a single ring-shaped resonator comrpises 60 keV.

Let us rewrite Eq. (1) in terms of u:

$$u=-1+\sqrt{(1-u_i)^2+\frac{\varepsilon^2}{k^2}(\cos\varphi_i-\cos\varphi)^2+\frac{2\varepsilon\sqrt{u_i^2+2u_i}}{k}(\cos\varphi_i-\cos\varphi)}, \tag{2}$$

where $\varepsilon = E/U_0$.

In order to calculate the relative spread in the energy of the electrons due to the finite radius, let us take and compare the energy of the central and outer diametrically opposed electrons in the flux. Let us introduce the symbols: θ is the angle of transit in the resonator; φ_c is the phase of a central electron; φ_{rt} is the phase of a right end electron; φ_l is the phase of a left end electron; r is the flux radius. Let us write the phase shift between the central and boundary electrons relative to the distribution of the field in the resonator, taking account of the wavelength in the wave guide:

$$\Delta\varphi=\pm 2\pi\frac{r}{\Lambda}. \tag{3}$$

Then the final phases of the accelerated central and boundary electrons assume the form:

$$\left.\begin{aligned}\varphi_{c.b}&=\varphi_c+\theta;\\ \varphi_{rt.b}&=\varphi_c+2\pi\frac{r}{\Lambda}+\theta;\\ \varphi_{l.b}&=\varphi_c-2\pi\frac{r}{\Lambda}+\theta.\end{aligned}\right\} \tag{4}$$

According to Eq. (2), taking account of Eqs. (3), (4), one can calculate the root-mean-square dependence of the relative energy spread of the electrons:

$$\frac{\Delta u}{u_c}=\sqrt{\left(\frac{u_c-u_l}{u_c}\right)^2+\left(\frac{u_c-u_{rt}}{u_c}\right)^2},$$

where u_l and u_{rt} are the terminal values for the energies of the diametrically opposed flux electrons. The relationship $\Delta u/u_c = f(r/\Lambda)$ with $\varphi_c-45°$, $\theta = 90°$; $\lambda = 3.2$ cm and the injection energy u_i in the capacity of a parameter is plotted in Fig. 1. As is seen from Fig. 1, the nonlinearity begins to appear when the beam radius exceeds 1% of the accelerating field wavelength. In Fig. 2, the solid curve displays the dependence of the relative energy spread in the electrons as a function of the initial phase $\Delta u/u_c = f(\varphi_c)$ when $\theta = 90°$, while the broken curve displays the dependence of the energy spread on the transit angle in the resonator $\Delta u/u_c = f(\theta)$ when $\varphi_c = 45°$. One assumes that $u_i = 0.04$, $\lambda = 3.2$ cm, and $r/\Lambda = 0.02$ for the calculation of both relationships.

One can reduce the energy spread for a given beam radius by increasing the injection energy or by decreasing the frequency of the power supply for the accelerating system.

LITERATURE CITED

1. A. K. Walter et al., Electrostatic Generators of Charged Particles [Russian translation], Gosatomizdat, Moscow (1963).
2. R. G. Mimanova (editor), Millimeter and Submillimeter Waves [Russian translation], IL, Moscow (1959).
3. G. I. Zhileiko, Zh. Tekh. Fiz., 34, No. 12 (1964).
4. B. A. Snedkov, At. Énerg., 19, No. 3, 287 (1965).
5. G. I. Zhileiko and B. A. Snedkov, At. Énerg., 24, No. 3, 256 (1968).
6. B. A. Snedkov, Radiotekhnika, Proceedings of the Moscow Institute of Radio Engineering, Electronics, and Automation, Vol. 1, No. 40, Moscow (1969).

COMMISSIONING OF LINEAR ACCELERATOR SECTION IN HIGH-FREQUENCY QUADRUPOLE FOCUSING

S. A. Il'evskii, I. M. Kapchinskii,
G. F. Kuznetsov, A. P. Mal'tsev,
K. G. Mirzoev, V. V. Nizhegorodtsev,
V. B. Stepanov, V. A. Teplyakov,
M. A. Kholodenko, and I. M. Shalashov

UDC 621.384.64

One of the options open for improving linear ion accelerators is to use focusing by a high-frequency (hf) quadrupole field. The theory of linear accelerators with hf quadrupole focusing has been put forth in a number of contributions to the literature; the reader will find a list of publications and reference list of formulas in [1]. A model of such an accelerator is now under study at IFVÉ (Institute of High-Energy Physics).

Figure 1 shows a schematic diagram of the arrangement devised for conducting experiments on proton acceleration. The proton injector impelling protons into the linear accelerator section is a standby preinjector of the I-100 linear accelerator; this preinjector provides current up to 100 mA, of energy 500 to 600 keV, at the input to the section. The current at the input to the section was measured with an inductive sensor, while the current at the output was measured with a Faraday cup which, if required, can be used to close up the foil admitting protons of energy greater than 2.5 MeV. The hf power supplies for the accelerator section are provided from a separately excited generator, which is identical in its design to the generators used in the I-100 accelerator. A vacuum of the order of 10^{-6} torr in the preinjector and in the accelerator section is kept inact through the use of microdischarge titanium pumps of model NÉM-1T.

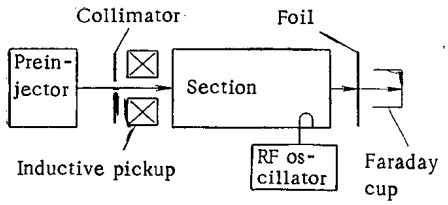

Fig. 1. Block diagram of facility.

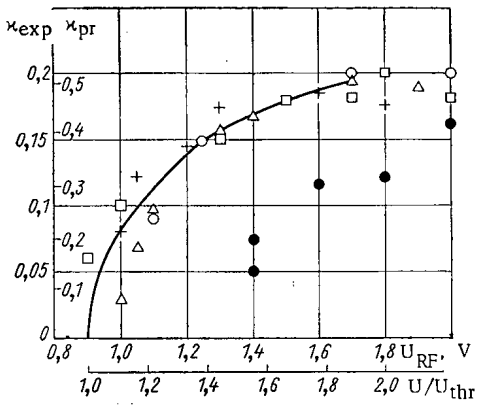

Fig. 2. Capture coefficient as a function of hf power supplied: •) 410 kV; Δ) 454 kV; ○) 475 kV; □) 497 kV; +) 505 kV.

The backbone of the accelerator section is the H-resonator [2], which is loaded with accelerating electrodes featuring a double gap [3]. The accelerator design features a vacuum container shield and the resonator cavity proper, which is made of three distinct parts each extending 700 mm in length. In its electronic engineering design, the resonator is a broad shielded turn in the form of a tube slit along the generatrix. Drift tubes (the accelerating electrodes) are fastened to the edges of the slit. The clearance between drift tubes accommodates an intermediate electrode kept at zero potential. The focusing component is devised by means of horns on the end faces of the electrodes. The accelerating electrodes are mounted in place with the aid of a special stand, and are soldered in position with alloy selected for slow contraction. The electrode mounting tolerances are of the order of 30 μ. Resonator sections are mounted in the container on insulators. A

Translated from Atomnaya Énergiya, Vol. 34, No. 1, pp. 56-58, January, 1973. Original article submitted June 20, 1972.

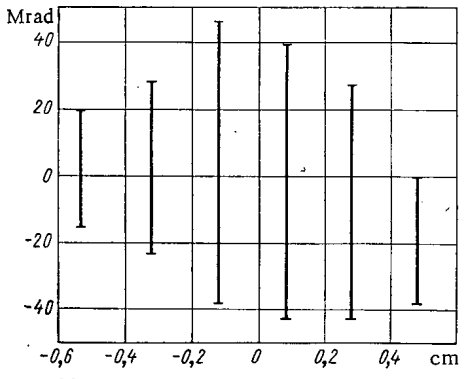

Fig. 3

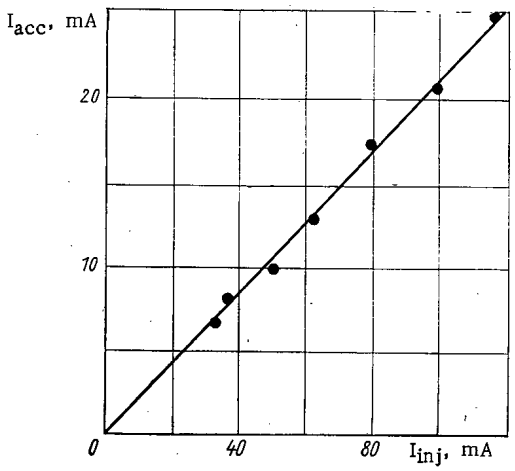

Fig. 4

Fig. 3. Accelerator acceptance (deflection of particles from accelerator axis plotted as abscissa, angle of inclination to accelerator axis plotted as ordinate.)

Fig. 4. Accelerated current as a function of injection current.

constant voltage of 2 to 3 kV is supplied between the container and the resonator in order to remove the electron resonant load. With that design, it becomes possible to introduce hf power into the resonator cavity without any preconditioning. The voltage in the resonator, almost twice the rated voltage, can be raised immediately after a 10^{-6} torr is achieved in the container.

A small portion of the current from the preinjector, which disappears as the hf power is introduced, is passed through the accelerator section to the Faraday coil uncovered by foil, when the hf voltage is absent. Resonance acceleration becomes possible starting with a certain threshold level U_{thr} of the hf field, and a current of accelerated protons appears on the other side of the foil. As theory would lead us to expect, the current maximum is observed at the rated injection power. The experimentally determined injection power at which the current of accelerated particles is maximized agrees with the calculated power. By using the dependence of the accelerated current on the hf voltage in the resonator at the rated injection power, we can find the threshold field U_{thr} and we can obtain the dependence of the empirically determined capture coefficient $\varkappa_{exp}$ on the synchronous phase (Fig. 2). The capture coefficient is defined here as the ratio of the current of accelerated particles to the current injected. The injection current is not divided by masses. The experimental data points lie on a curve which in its shape repeats quite closely the theoretical dependence of the calculated capture coefficient $\varkappa_{pr}$ on the hf voltage in the resonator. This result seems to constitute evidence to the effect that the capture coefficient is determined solely by longitudinal motion, and that there are no restrictions on the part of transverse motion.

Basic Parameters of Accelerator Section

Injection energy	0.51 MeV
Output power	3.26 MeV
Frequency of accelerating field	132.5 MHz
Resonator cavity length	2.4 m
Outer diameter	0.41 m
Number of electrons	65
Accelerating channel aperture	16 mm
Mode of focusing	FFDD
Normalized acceptance	10^{-3} radian · cm
Synchronous phase	30°
Voltage across resonator	153 kV
Duration of hf pulse	35 μsec
Duration of preinjector current pulse	40 μsec

This assumption is confirmed by measurements of the accelerator acceptance, which was carried out by two-slot method. The measured beam acceptance (Fig. 3) is $(1 \pm 0.1) \cdot 10^{-3}$ rad·cm, which is in close agreement with the calculated value, and gives ground for hoping for proton current on the order of 100 mA at the accelerator exit. The current at the accelerator discharge end increases in proportion to the current at the accelerator entrance (Fig. 4). The maximum current attained at the accelerator exit, 25 mA, is limited by the fact that it was not raised above 100 mA at the accelerator accelerator.

Experience in fabricating the section, and the first experiments staged, allow us to draw the following conclusions:

1) the design of a small compact linear proton accelerator has been successfully worked out, with fabrication technologically much simpler than in a conventional Alvarez type accelerator with the same physical parameters otherwise;

2) the accelerator section boasts a high reserve margin of electric breakdown strength in the accelerating gaps;

3) no fundamental difficulties hindering an increase in the current of accelerated particles have come to light as of this writing.

In conclusion, the authors welcome this opportunity to thank A. A. Naumov for support in this work, and all of those who took part in developing the accelerator section and allied systems and in putting them into operation, and in particular V. S. Sevost'yanov, V. V. Klokov, S. I. Zinov'ev, V. G. Atroshchenko, N. S. Sakharov, I. A. Zhuravlev, V. A. Butenko, L. M. Popinenkov, G. M. Kolomenskii, and others.

LITERATURE CITED

1. A. P. Mal'tsev, V. B. Stepanov, and V. A. Teplyakov, Preprint IFVÉ, InZh 69-2 [in Russian], Serpukhov (1969).
2. V. A. Teplyakov and V. B. Stepanov, Radiotekhnika i Élektronika, 13, No. 11, 1965 (1968).
3. A. P. Mal'tsev, S. M. Ermakov, and V. A. Teplyakov, At. Énerg., 23, No. 3, 195 (1967).

CONFERENCE ON DEACTIVATION OF RADIOACTIVE WASTES

V. V. Kulichenko and N. A. Rakov

The third science and engineering conference of COMECON member-nations on reprocessing and disposal of radioactive wastes and deactivation of contaminated surfaces was held October 2-7, 1972, at Kolobrzeg (Poland). The conference attracted over a hundred specialists from Bulgaria, Hungary, the German Democratic Republic, Poland, Rumania, the USSR, and Czechoslovakia. The program of the conference encompassed the following basic divisions:

1) methods of cleanup and concentration of liquid radioactive low-level and medium-level wastes;
2) solidification and immobilization of medium-level and high-level wastes;
3) disposal of wastes in underground strata and in salt pits;
4) cleanup of gaseous discharges and wastes;
5) deactivation of contaminated surfaces of equipment and rooms;
6) monitoring contamination of surface water sources and of the Baltic Sea;
7) engineering cost estimates for methods and flowsheets used in decontamination and deactivation of wastes.

The proceedings of the conference will be published very shortly, so that the present review need reflect only what we view as the most salient scientific and engineering results.

In a review report, E. Minczewski (Poland) stressed the importance of the topics discussed and the need for combining the efforts of specialists from different COMECON member-nations to find solutions to the problem. The author focused attention on ways of decontaminating radioactive wastes, now in practical use in virtually all of the countries represented: wastes are concentrated and buried, but not subjected to definitive safe burial, which must be the ultimate aim of all work along those lines.

Reports devoted to improvements in wastes processing flowsheets and in processing equipment for cleanup and concentration of liquid radioactive wastes formed at research centers and at nuclear-fuelled electric power generating stations occupied a prominent place on the conference agenda. In particular, the use of inorganic natural and artificial sorbents for selective removal of the most dangerous long-lived fission-fragment isotopes and transuranium elements before these get a chance to accompany the wastes to the burial grounds was discussed. The use of sorbents is regarded as a useful method for compacting recovery slurries when ion exchange filters are employed. Reports were presented by representatives of Bulgaria, Hungary, Poland, the USSR, and Czechoslovakia.

Close attention was given to methods for producing granulated sorbents suitable for use under dynamic conditions. A method for preparing bentonite with urea–formaldehyde resin binder has been worked out in Poland, with cupric ferrocyanide and calcium phosphate precipitating on the material so that the Cs^{137} and Sr^{90} capacity of the resin is increased. In addition, a mixed sorbent with a zirconium phosphate and ammonium phosphomolybdate base is proposed. Methods for preparing granulated sorbents for different isotopes by heat processing, freezing, and precipitation on granular materials, are suggested in Soviet papers. Investigators in Czechoslovakia continued work on Sr^{90} sorption on mixed barium sulfate and calcium sulfate crystals.

Translated from Atomnaya Énergiya, Vol. 34, No. 1, pp. 59-60, January, 1973.

Considerably less attention was given to the use of organic ion exchange resins. One of the reports (East Germany) dealt with curtailment of the amount of reagents used in the regeneration of ion exchange filters when weakly or strongly dissociable resins are employed.

Soviet and Czechoslovak reports discussed applications of equipment in continuous ion exchange. East German and USSR papers also discussed reprocessing of boron-containing wastes. Several papers were devoted to the development of reagent-free methods for cleanup, immobilization, and concentration of wastes: reverse osmosis, freezing, electrodialysis, separate evaporation of the regenerating solutions (USSR), and the use of precoated filters (East Germany). The report demonstrated the developmental outlook of technology and equipment useful in curtailing the volume of wastes and in cutting wastes reprocessing costs.

As is clear from the conference materials, the development of techniques for solidifying and fixing radioactive wastes is being pursued in several directions in the COMECON member-nations. East German specialists presented two papers on immobilization of liquid active concentrates with attention given to storage in salt pits. The use of this method, despite a few negative factors (volume increased 1.8 to 2 times, high rate of leaching out of radiosotopes), is explained by the fact that the fixated wastes must perform the role of shoring up the roofing in the salt workings. The specific features of the method predetermine the direction of research: retaining the strength of blocks in the brine when water infiltrates into the salt pit, the mechanism by which radioisotopes become leached out into the brine, the effect of boric acid and of borates on the properties of the fixated cements, and so forth.

Reports on bitumen-immobilization of wastes awakened the greatest amount of interest. USSR reports gave results of work now completed on determining the conditions governing immobilization in bitumen of radioactive wastes containing sodium nitrate, and storage conditions of such wastes. Specialists from Poland presented findings of pilot plant tests on bitumen-immobilization of slurries of ferric hydroxide, calcium phosphate, and cupric ferrocyanide, as well as studies of the structural properties of bitumen compounds and optimization of the composition of the mixture of bitumen-fixed wastes, making it possible to maximize the stability of the immobilized material during storage.

A facility for bitumen-immobilization of wastes has been developed in Hungary, and is based on the principle of the tubular heat exchanger. In order to facilitate mixing of the bitumens with the wastes, and also in order to minimize the danger of combustion in the equipment, the process is carried out at a constant rate of nitrogen feed. The simplicity of the bituminization technology has encouraged work on expanding the range of wastes that can be immobilized in bitumens. Reports by Soviet specialists demonstrated suitable bitumenizing conditions for wastes of different composition (solutions of nitrates of the heavy metals, borates, sulfates, pearlite pulps, and so on). The possibility of fixing wastes having a specific activity as high as 10 Ci/liter has been demonstrated on the basis of studies of the mechanism underlying radiation-chemical processes and on the basis of direct observations. A laboratory facility with a capacity of one liter per hour has been built in Czechoslovakia for fixation of wastes with specific activities ranging to 50 Ci/liter, in bitumens.

Reports from the USSR and from Poland on vitrification of high-level wastes stimulated a certain amount of interest. The use of natural ferruginous clay as flux and as a filter for scrubbing the gas stream is worth noting.

A report delivered by Hungarian specialists discussed solidification of organic solvents (dioxane, toluene, benzene, etc.), including tritiated solvents, by polymerizing them with the aid of stearic acid. A special session was devoted to underground disposal of liquid, gaseous, and solid radioactive wastes in porous and fractured water-bearing strata, and also in existing abandoned salt mines or artificially excavated cavities in salt formations.

Representatives of the German Democratic Republic discussed a broad range of topics involving disposal of radioactive wastes in deep-lying aquifer complexes and salt pits. An estimate was advanced of geological conditions prevailing on the territories of the German Democratic Republic, from the vantage point of the feasibility of disposal by burial, and suitable methematical models of the migration of gaseous fission fragments were discussed, and an attempt was also made to analyze possible unfavorable, or even dangerous, conditions in the storage and retention of wastes of whatever level of activity, from the general theoretical standpoints and considerations.

USSR reports dealt with basic trends in research and in the practice of underground burial of radioactive wastes and other highly toxic wastes in the Soviet Union and in foreign countries. Problems of techniques in the design of underground burial facilities, heating of host rock where high-level wastes are buried, interactions between wastes and the material comprising the encompassing storage strata, and development of methods for preparing wastes for burial, were discussed, and the sorption characteristics of soils of different mineralogical composition were cited, with the different modes of burial of wastes taken into account.

There was considerable interest in reports devoted to decontamination. An East German paper cited results on decontamination of the primary loop of the Rheinsberg power station, at which four blowdowns were carried out in the 1968-1971 period. Soviet papers presented results of development projects on engineering equipment for decontamination of contaminated surfaces of equipment and rooms with the aid of superheated steam and hydraulic monitor jets. A Polish paper dealt with the use of decontaminating abrasive pastes, and a review paper from Czechoslovakia surveyed decontamination techniques in use in different countries on the basis of information reported in the literature.

Cleanup of air discharge to remove radioactive gases and aerosols was discussed in 11 papers (Hungary, East Germany, Poland, the USSR). The focus was on methods for testing the efficiency of filtering materials.

Informational reports on research on radioactive pollution of the Baltic Sea was discussed at the Conference (Poland and USSR), as well as pollution of Poland's rivers, and on maintenance of water quality in Hungary. A USSR report on development of methods for determinations of radionuclides in water samples and bottom sediments was heard.

Close attention is being given by COMECON member-nations to engineering cost considerations in siting wastes disposal grounds, and in working out technological flowsheets for wastes disposal processes.

The reports presented at the conference demonstrated that intensive research and experimental work is underway in practically all of the countries on effecting improvements in existing arrangements for cleanup of wastes, cutting operating costs, and optimum siting and optimum operation of wastes treatment facilities, as well as work on solving problems in deactivation of radioactive wastes from nuclear power stations now under construction or still in the design stage. The high scientific and technical level of the work being done is noteworthy. Coordination of this work by COMECON member-nations supports hope for successful solution of the pressing problems associated with the rapid growth of the nuclear power industry in the countries of the socialist commonwealth.

COLLABORATION LOGBOOK

The third session of the Council of the International Economic Association for Nuclear Instrumentation, Interatominstrument, was held in Warsaw on September 5-7, 1972. Chairing was the director of the amalgamated Izotop plants (Bulgaria), Council member I. Traikov.

The council discussed and approved the financial plans of the Association for 1973, and took decisions on questions concerning cadres, specifically appointing a vice-director of the Association for commercial and economic matters, G. Korff (GDR), and a vice-director in charge of scientific and technical matters, V. Sinitsyn of the USSR. An auditing commission was also set up.

It was reported that Council members are interested in setting up Interatominstrument organizations for technical servicing and maintenance of nucleonic instruments and devices in service in countries whose economic organizations are members of the Association.

The Council heard reports presented by the director of the Association, Z. Twardon, on progress in the work of the Association, and by an advisor of the Section on peaceful uses of atomic energy attached to the COMECON Secretariat, L. Korotkov, on the work of the XXII session of the Permanent Commission on the peaceful uses of atomic energy (PKIAÉ SÉV).

The next session of the Council was scheduled for November, 1972; a tentative agenda was drawn up for that occasion.

The session took place in a businesslike atmosphere and in a spirit of complete mutual understanding.

* * *

The first session of the coordinating scientific and technical council (KNTS) on radiation safety was held at Potsdam (GDR), in September, 1972. A resolution on the feasibility of setting up the Council was approved by PKIAÉ in line with the need to find a comprehensive solution to radiation safety problems, and find ways of coordinating development work on those and related problems in the COMECON member-nations. Members of the Council and experts from Bulgaria, Hungary, the German Democratic Republic, Rumania, the USSR, Czechoslovakia, and staffmembers of the COMECON Secretariat took part in the deliberations of this session. The program of collaboration between COMECON member-nations in the field of radiation safety was discussed, and a plan of work for the Council, covering the 1972-1975 period, was agreed upon. Future plans call for:

1) the development of regulatory documents unique to the COMECON member-nations (public health rules governing design and operation of nuclear power generating stations, requirements imposed on shielding and protection of the environment in the event of radiation accidents at nuclear power stations, etc.);

2) recommendations on the design of radiation shielding, techniques for removal and deactivation of radioactive gases and aerosols, recommendations on optimization of dosimetric monitoring systems, techniques and devices for making determinations of the radiation situation at nuclear power stations and at research reactor facilities, and the like;

3) unified procedure for calculating the dissemination of radioactive products in the environs of nuclear power stations under conditions of a nuclear accident, estimates of the probability of radiation damage, determinations of the limiting permissible levels of discharge of radioactive products at nuclear power stations and research reactor facilities, etc.;

Translated from Atomnaya Énergiya, Vol. 34, No. 1, pp. 60-61, January, 1973.

4) recommendations of unitization and standardization. In addition, the program and work plan drawn up by the Council envisages preparation of reports on the most urgent topics, mutual exchange of information, holding of conferences, symposia, and workshops of specialists.

* * *

A conference of specialists of COMECON member-nations (Bulgaria, Hungary, Poland, Rumania, the USSR, and Czechoslovakia) on collaboration in the field of production of radiation protection equipment was held in Moscow in September, 1972. The conference was attended by colleagues of the COMECON Secretariat and by representatives of the International Economic Association for Nuclear Instrumentation, Interatominstrument. Topics reported on and discussed included:

1) listings of process equipment and operational-technological devices and fixtures used in glove boxes and hot cells for handling radioactive substances and materials, and also suggestions on how to best organize future work along the guidelines of specialization and cooperation in the manufacture of those commodities;

2) analysis of national standards bearing on radiation protection equipment, identity in basic indices and normative standards, and a draft catalog of items and parts manufactured along these lines in various member-nations;

3) listings of items of radiation protection equipment for nuclear medicine, and proposals on how to go about organizing future work in developing those endeavors further;

4) a draft of "General technical requirements for standard technological equipment";

5) progress in carrying out the "Program of collaboration of COMECON member-nations in the field of radiation protection work," and improvements in the program;

6) a 1973-1974 work plan.

Solutions were agreed upon with respect to all of the topics discussed at the session.

* * *

A conference of specialists of COMECON member-nations and the second session of the coordinating scientific and technical council (KNTS) on reprocessing of spent fuel was held in Leningrad on September 25-30, 1972. Delegations from Bulgaria, Hungary, the German Democratic Republic, Poland, Rumania, the USSR, and Czechoslovakia, were in attendance.

The status of work on such topics as "Fluoride methods of fuel reprocessing," and "Development of techniques for process monitoring and process control," envisaged in the "Program of collaboration of COMECON member-nations in the field of scientific and engineering research on the topic 'Research on fuel reprocessing at nuclear power stations,' "was discussed at the conference of specialists. Stress was laid on the importance of further concretization of collaboration on these central fields. The feasibility of arriving at a fluoride process flowsheet for the reprocessing of spent fuels was emphasized, as were plans for process monitoring of solvent-extraction and fluoride spent fuel reprocessing systems. Attention was turned to the urgency of research and development work on techniques for determining and monitoring the degree of burnup and the composition of fuel arriving at the reprocessing step.

The second session of the KNTS discussed preparation of a conference of specialists of the COMECON member-nations on safe transportation of spent fuel elements from nuclear power stations, approved an agenda for the conference, and prepared measures to expedite the conference.

Suggestions on establishing and compiling technical specifications for the fabrication of equipment for cutting off fuel-element shanks, breaking up spent fuel elements for processing, decladding of fuel elements, dissolving fuel, and clarification of solutions were discussed. The technical specifications are to be discussed at the forthcoming third congress of the KNTS.

In discussing the draft of the program of collaboration on engineering cost research topics in the field of reprocessing spent nuclear fuel from nuclear power stations, the principal problems in the research were determined, and the necessity of refining the work prgram still further was acknowledged.

The KNTS also discussed the "Information on the work of the KNTS," a work plan drawn up for 1973-1974 KNTS activities, and suggestions on refining the program of collaboration in this area of work.

THE IAEA SYMPOSIUM ON BURIAL OF RADIOACTIVE WASTES

B. S. Kolychev

A meeting of IAEA experts on the burial of solidified wastes according to their properties and level of activity was held in Moscow on September 4-8, 1972.

The reliable and safe burial of radioactive wastes is one of the outstanding problems of today. For this reason, intensive research is being carried on to find a process for converting liquid wastes of high and medium levels of activity to the solid state. The burial of such wastes in solid form with their radioisotopes securely fixed in them makes it completely impossible in practice for the radioactivity to spread into the environment.

The September, 1972, meeting was a continuation of the meetings held in Dubna from 1965 to 1968 on the solidification of liquid wastes.

The choice of the correct conditions for the burial of solidified materials according to their properties and levels of activity is a logical continuation of the questions considered at the previous meetings and is one of the decisive factors in preserving a clean environment. Scientists may work hard to design a technique for solidification, but their efforts will be worthless if the conditions for the safe burial of the solidified substances are not defined.

The meeting attracted great interest and was attended by 25 experts from 17 countries. Also present were representatives of four international organizations: Euratom, the Commission of European Associations, the World Health Organization, and the Council for Mutual Economic Assistance.

The following questions were considered.

1. The latest advances in the solidification of wastes by enclosing them in bitumen, cement, or other binding materials. It was noted that special attention must be paid to experimental studies on the leaching-out and migration of radioisotopes under various burial conditions.
2. Experience in the burial of radioactive wastes of low and medium levels of activity. Emphasis was placed on the need for special measures to prevent contamination of the environment.
3. The variation of the reliability of radioactive-waste burial as a function of the design of the burial site, the properties of the wastes, and their levels of activity, with a view to working out the fundamental principles for safe burial of the wastes and monitoring of their condition.

In addition, the participants heard reports on techniques for the final removal of concentrates of highly radioactive wastes and the burial of wastes with high alpha activity and measures for preventing contamination of the environment; they also considered questions relating to the removal of highly active wastes in relation to the further development of nuclear power. Reports were given on the thermal stability and cooling of the resulting radioactive substances.

A total of 23 reports were heard.

Great interest was aroused by reports devoted to the present practices followed in the burial of solid wastes and to experimental studies on the burial of solidified preparations. In particular, the report presented by Great Britain compared five possible methods for the burial of wastes: burial in the earth, burial in the sea, storage in salt mines, storage in air-cooled tunnels, and storage in water-cooled basins.

Translated from Atomnaya Énergiya, Vol. 34, No. 1, pp. 62-63, January, 1973.

The general view accepted in England is that solidified highly active wastes must be stored under conditions such that they can always be monitored, and consequently the last two methods are considered preferable. In addition, they are less expensive than the other methods.

One Japanese report presented calculation methods which make it possible to obtain, in a first approximation, a comparative assessment of the site chosen for the burial of radioactive wastes in the ground, as well as of the safety of sites selected for the construction of nuclear installations. A special Japanese report was devoted to the use of electronic computers for selecting the optimum site for the burial of radioactive wastes. It compared various man-made structures (underground reinforced-concrete pits, underground impenetrable walls, or dams). The authors found this calculation method very promising.

A report by Polish specialists gave a general description of a system for handling radioactive wastes and also described the operation of a radioactive-waste bitumination plant with a capacity of 25 liters/h. The resulting bitumen preparations are loaded into 180 liter sheet-iron barrels. These barrels are placed in earth ditches and covered with soil.

A brief report by the United States was devoted mainly to glimpses of the burial of wastes with low-level activity and reaffirmed the possibility of burying such wastes directly in the earth, counting on the high sorptive properties of the soils. The report made no reference to wastes with high levels of activity.

The report presented by Czechoslovakia was devoted to a continuation of work of a continuous process for cementing in a vacuum. In addition to an experimental installation, test work is being done on a pilot plant with a capacity of 400 m^3 of concentrates and slurries per year. A fairly low cement-to-water ratio (≤ 0.35) has been achieved. Work is also being done to develop a cold-bitumination process at a small experimental installation. The main problems involved in this are those of finding the optimum composition of the bitumen preparations and the conditions for enclosing the wastes in bitumen and cooling them. Consideration is being given to a combined cementing and bitumination process.

The investigations of Bulgarian specialists showed that bitumen blocks may be stored either at the surface or underground.

The representatives from the Netherlands noted in their country there are no substantial amounts of highly active wastes as yet. Problems with highly active wastes will arise when it becomes necessary to reprocess burned fuel elements. Prior to that time, studies are being conducted on the possibility of burying solidified highly active wastes in salt formations. Netherlands scientists have considered four cases of the possible entry of water into the storage site and the possible consequences that might result. Salt formations are considered the most suitable for the burial of solidified highly active wastes.

An interesting report presented by France dealt with two methods for the final burial of radioactive wastes: in safe geological formations (salt mines, deep rock strata) and in burial pits constructed at the solidification site, kept well cooled for the necessary period by means of circulating water. The second method is considered preferable, since it does not require transportation of highly active wastes, permits monitoring and also makes it possible to process the wastes a second time if necessary. Work on solidification was begun in 1957; in 1967 it was extended to an experimental installation with simulators, and in 1969 work was begun on the solidification of wastes with full-level activity. Two processes are being tested: a semicontinuous process (vitrification in crucibles) and a continuous process consisting of two stages (calcination in a rotary furnace and vitrification in a crucible with periodic decantation). The latter process has a capacity of about 10 liters/h. It is expected that an industrial plant will go into operation in 1974. Since the experimental plant went into operation, it has produced 8 tons of glass containing more than 2 million Ci. The glass is stored in burial sites consisting of 32 underground concrete chambers situated 10 m below the surface. Each chamber contains the usual type of concrete-covered steel tubes which can hold 20 cans or 3 crucibles (approximately 1.5 tons of glass). Cooling is supplied by circulating air. The report discussed the outlook for the storage of highly active wastes.

Considerable discussion was devoted to a report by Soviet representatives concerning methods for selecting the conditions for burying radioactive wastes, taking into account their properties and levels of activity (which was the principal purpose of the meeting).

The participants agreed that at the present state of knowledge it is possible to develop methods for selecting the conditions for the burial of solidified wastes with low and medium levels of activity according to their properties; they asked the IAEA Secretariat to prepare a recommendation for such a method which took account of the proposals made at the meeting. The meeting was conducted on a high scientific plane and in an atmosphere of friendship.

THE FIFTH EUROPEAN CONFERENCE ON CONTROLLED THERMONUCLEAR FUSION AND PLASMA PHYSICS

V. A. Chuyanov

The Fifth European Conference of Plasma Physics and Controlled Thermonuclear Fusion, organized by the Plasma Physics Division of the European Physics Society, was held in Grenoble, France, from August 21-25, 1972.*

According to the official list, 378 people from 19 countries of the world, including the USA, Japan, and other non-European countries, participated in the conference, at which were presented 177 contributed and 20 review papers.

Review and invited papers were presented at the morning plenary sessions, and original contributed papers were presented at four simultaneous sessions in the evenings. The number of review papers was greater than at the preceding conference in Rome. Those on the status and prospects of thermonuclear research in the USSR, in the USA, and in Europe, presented by L. A. Artsimovich (read by B. B. Kadomtsev), R. Gould, and D. Palumbo, afforded the conference participants a fairly complete picture of the current status of thermonuclear research in the whole world.

The successful Tokamak experiments conducted in the I. V. Kurchatov Institute of Atomic Energy led many laboratories in Europe and in the USA to reexamine their plans and to switch to construction and study of Tokamaks. Therefore the Tokamak experiments were the focal point of the conference. Although the "Tokamak boom" has not yet led to a sharp increase in the flow of scientific experimental information (most of the devices are presently under construction or undergoing initial alignment), interesting new results were communicated at the conference.

The review of Soviet Tokamak results was presented by V. S. Strelkov. Marked progress in the parameters of the plasma obtained is observed (see Fig. 1). In the biggest Soviet Tokamak, T-4, the electron temperature has now reached several kiloelectron volts, the deuterium ion temperature is above 600 eV, the energy confinement time is on the order to 10^{-2} sec, and the particle confinement time is on the order of 0.1 sec. Future research is directed towards studying supplementary heating methods, instabilities, and the dependence of transport processes on plasma parameters. The experiments conducted on T-3a and T-6 have shown that, using programmed plasma current and a conducting liner near the plasma surface, an MHD-stable plasma can be obtained for values of the safety margin q down to 1, which is significantly less than the value q = 3 assumed earlier to be necessary. Experiments with electron–cyclotron heating, which are only beginning, show that rf energy is absorbed in the plasma. This permits one to expect further growth of plasma temperature. The supplementary heating provided the opportunity to "decouple" the plasma parameters and study the dependence of plasma confinement on temperature with a fixed plasma current. It has been shown in experiments with TM-3 that the energy confinement time grows with increasing electron temperature, at least at low densities.

V. Stodiek (USA) summarized the results of research on the Princeton ST Tokamak. The results of studying the plasma energy balance, instabilities, and other topics in general agree with Soviet experimental

* The proceedings of the conference (except for review papers and invited papers, which will be published later) were published by the organizers before the beginning of the conference and distributed to the participants.

Translated from Atomnaya Énergiya, Vol. 34, No. 1, pp. 63-66, January, 1973.

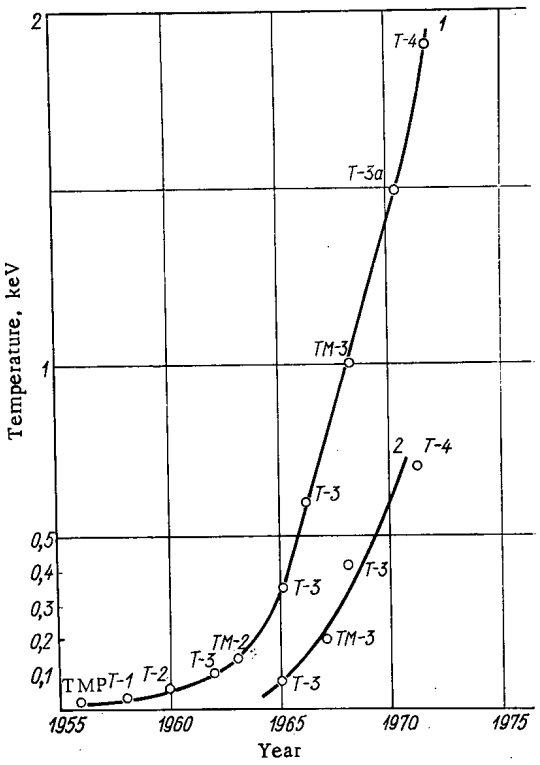

Fig. 1. Growth of electron temperature (curve 1) and of ion temperature (curve 2) in Soviet Tokamaks during the past 15 years.

data; however, the great use of laser diagnostics permitted the American physicists to obtain a detailed picture of the evolution of the radial plasma density and temperature profiles. At the early stages of the discharge a small skin-effect of the temperature is observed, which is then replaced by thermal contraction of the plasma column: the electron temperature profile becomes narrower and narrower in time. The energy losses at the center of the column are limited by anomalous electron thermal conductivity, as in the T-3 and T-4 experiments. The plasma ohmic heating is described well by the Spitzer equation, taking into account the comparatively large number of impurities (oxygen comprised 12-14% of the total number of atoms). The absence of anomalous resistivity permitted the American physicists to calculate the current distribution across the plasma column, knowing the temperature profiles, and the density and impurity concentration. The calculation shows that at the center of the plasma there is a safety margin $q < 1$. This and other results permit the author to draw the conclusion that the limitation of electron temperature and the changes in its profile at the end of the discharge and caused by an MHD instability at the center of the plasma. It is noted in the report that the plasma in Tokamaks is well confined only in a narrow density range around 10^{13} cm^{-3}. At high densities an MHD instability, which the author identifies as a resistive mode helical instability, is observed. The higher modes of this instability do not have catastrophic consequences for the plasma column as a whole. Development of the $m = 2$ mode leads to the plasma column striking the walls, a significant plasma-energy loss, a negative discharge voltage, and other phenomena, well-known as a "disruptive instability."

Of the theoretical papers on Tokamaks, the paper by G. Laval et al. (Fontenay-aux-Roses, France) should be mentioned. In this paper the stability of a toroidal plasma column with elliptical cross section and uniform current was studied relative to the helical instability. It was shown that, with an increase of the ellipticity simultaneously with a decrease of the critical q, a broadening occurs, and then even an overlapping of the instability regions of various modes, so that the transition to a "ring Tokamak" could impair MHD stability. This unpleasant effect, according to the author, should be weaker, but nevertheless conserved, for more realistic current distributions.

In comparison with previous conferences, there was a significant growth in the proportion of papers dealing with numerical simulation of plasma processes, especially in Tokamaks: numerical calculations of the equilibrium plasma column, including some with noncircular cross section, calculations of spatial and time evolution of plasma parameters, and of plasma heating by fast neutral atom beam injection. The goal of almost all of these papers was to define and optimize the parameters of the devices being constructed at the present time.

The other traditional direction of thermonuclear research is the study of magnetic mirror devices. The report of F. Coentsgen on the 2XII experiments in the Livermore laboratory (plasma density $6 \cdot 10^{13}$ cm^{-3}; ion temperature several keV) elicited great interest. It was established that the nature of the plasma decay depends on the perpendicular ion energy distribution. If this distribution has two maxima, oscillations are observed at the ion cyclotron frequency and its harmonics, accompanied by unstable decay. If there is only one maximum (which can be achieved by selecting the interval between plasma injection and pulsing on the magnetic field), then there are no signs of instabilities, and the decay constant is only two or three times different from the value calculated for classical Coulomb scattering of the ions. However, as the density decreases this disagreement grows. The particle energy lifetime also does not agree with the Coulomb scattering value. These discrepancies between theory and experiment are removed by taking

into account a new effect: the "collective scattering" of the ions by the noise arising from a convective form of the Post–Rosenbluth cone instability. The theory of the effect, developed by D. Baldwin and G. Collin, was compared with the experimental data obtained on the 2X and 2XII installations. It appeared that this effect can explain the variation of decay rate with plasma density, magnetic field, and ion temperature. At present, experiments are continuing to check the theory. Its validity will evidently signify stronger limitations (though not very much stronger) on the plasma length in a mirror reactor.

In the paper of V. A. Kanaev and E. E. Yushmanov (USSR) on the experiments with the PR-6 mirror device it was shown that the decay of the collisional plasma with a density of 10^{12} cm^{-3} and an ion temperature of 100 eV, beginning with "classical" decay, becomes accelerated and accompanied by instabilities as the decay proceeds. The report elicited great interest, since it demonstrated the phenomenon of feedback between the plasma parameters, leading the plasma away from a state of equilibrium. In the opinion of the authors this phenomenon has a universal nature and can appear as a barrier on the road to attainment of stable confinement in mirror systems.

Stellerator experiments were discussed in the review paper by D. Lees (Culham Laboratories, Great Britain) and in contributed papers by participants from the USSR and Japan. The observed confinement times for all devices were approximately an order of magnitude less than would be expected for purely collisional "classical" diffusion. However, for the Uragan stellerator (USSR) and Proto–Cleo stellerator (UK) the variation of confinement time with plasma density and temperature was close to neoclassical. The refinement of theory done by T. Stringer allowed even quantitative agreement to be obtained between theory and experiment. Therefore testing the collisional nature of the diffusion by an independent means is of great interest. To this end an attempt was made on the Proto–Cleo stellerator to observe the longitudinal current which, according to theory, must arise under the influence of collisional diffusion. Experiments with a sensitivity 50 times better than the expected current gave negative results. It is possible that the current is unable to establish itself in the given experiment due to the insufficient confinement time. Nevertheless, the total absence of such a current causes doubts about the collisional nature of the observed plasma loss. Again in this regard the question arises as to about the influence of oscillations on plasma confinement in stellerators. According to the British experiments the role of oscillations is insignificant; but direct experiments on the L-1 stellerator in the Physical Institute of the Academy of Sciences of the USSR show that suppression of the oscillations leads to a doubling of the lifetime; and in the experiments in Novosibirsk presented by V. I Volosov, a large azimuthal inhomogeneity of the radius plasma flow is observed under the influence of oscillations. Therefore the conclusions about the small role of oscillations, based on localized measurements, may be in error.

Significant attention is devoted to pinch devices, both in Europe and in the USA. Three review papers and over ten contributed papers dealt with this topic. D. Robinson discussed experiments with a high-beta toroidal pinch at Culham, where an attempt is being made to obtain a stable plasma column with a reverse field on the outside. The experiments demonstrated the possibility of creating a stable plasma in such a configuration, but due to the rapid diffusion of the magnetic field with the low-temperature plasma the plasma lifetime was short. F. Jahoda (Los Alamos, USA) reported on the status of Scyllac. The construction of a complete torus is only being planned, but it has been shown on the toroidal sector that the combination of corrugated and $l = 1$ helical fields permits compensation of the toroidal drift. On the linear pinch Scyllac-4 a powerful feedback stabilization system has been introduced to stabilize the m = 1 MHD instability. The first experiments have confirmed the validity of the principles on which the system operates.

Discussions of laser fusion evoked great interest. G. Bobin (Limeil, France) discussed the current status of this research. In his opinion, the rapid progress of laser technology permits one to hope that by 1975 neodymium glass lasers with 10 kJ energies and nanosecond and subnanosecond pulses will be created, as will CO_2 lasers with nanosecond pulses of 200 GW. The development of chemical lasers using iodine and ultraviolet lasers using xenon, promising very high efficiencies (greater than 50%), is of interest. Lasers with a photon flux of about 10^{14} W/cm^2 already produce plasmas with electron temperatures about 1 keV, ion temperatures about 500 eV, and neutron yield from 10^2 to 10^5 per pulse during irradiation of solid targets. Two important questions stand at present: whether the absorption of the light is linear or nonlinear; and the nature of the mechanism of plasma heating by the absorbed energy. The theoreticians propose two models of heating: thermal wave, and free flare, controlled by the laser beam. Since the given models lead to different dependences of the neutron yield on energy, the experimental study of this dependence can clarify this question. (The neutron yield is proportional to the square of the energy according

to the thermal wave theory, and proportional to the fifth power of the energy according to the flare theory.)

The results obtained in various laboratories show that if the neutrons are thermonuclear they are produced by the free flare mechanism at low light powers, but that the dominant mechanism at high powers is the thermal wave. However, the thermonuclear nature of these neutrons is not yet established, and the correlation of neutron yield with increase in reflection of laser light, the appearance of very hot ions, and the generation of hard x-rays indicates the presence of instabilities, which are associated with the nonlinear absorption of laser light by the plasma. There are many theoretical papers on this question, but the experimental work is only beginning.

In coming years nonlinear effects will become dominant in work with more powerful lasers, and study of these effects will comprise the most important part of the research program.

The following schemes being discussed at present for application of lasers to controlled fusion were also surveyed by G. Bobin.

1. Plasma with density about 10^{18} cm^{-3} is heated using a CO_2 laser during its one-dimensional spreading in a magnetic field of 1-10 MG. An energy of about 10^8 J/cm^2 is necessary to obtain thermonuclear conditions in this case.
2. Solid pellets are subjected to fast laser heating. In this case the laser pulse energy must be 10^8-10^{12} J (most likely 10^9 J). This energy may be substantially diminished by strong compression of target:

$$w = 10^9 (n_s/n)^2 \text{ J},$$

where n_s is the initial density of the solid target; n is the compressed material density. Detailed calculations performed by Nuckolls at Lawrence Livermore Laboratory show that, during symmetric irradiation of the target by a laser pulse with a specially shaped front, a growth of density to 1000 times the initial target density may be achieved. Thus the minimum laser energy for ignition is lowered to 10^3-10^6 J (depending upon the amount of compression).

M. Rosenbluth gave an unscheduled report on the theoretical problems of laser heating. He dealt with the problems which may arise during attempts at ultrahigh compression of matter by very powerful laser beams: in particular he discussed possibilities of anomalously large reflection of laser light and of generation of fast electrons. The electrons could heat the center of the target too soon and thus interfere with the compression.

The studies of the dense plasma focus have been continuing in a number of laboratories in Europe and in the USA. In a review paper by S. Mesonnier (Frascati, Italy), new ideas about the processes in the plasma focus and in the generation of neutrons were developed. According to the author after the first compression anomalous resistivity arises in the expanding plasma. This resistivity, exceeding classical by a factor of 100 to 1000, enables dissipation of the extra magnetic field energy, which leads to turbulent heating and generation of the main neutron pulse. At this time the plasma focus has relatively large dimensions.

The conference demonstrated the progress in all areas of thermonuclear research and the prospects for attainment of its final goals. As is evident in R. Gould's report on the status of thermonuclear research in the USA, the USAEC is planning significant increase in its appropriations for thermonuclear research in the USA.

The next European Conference on Controlled Fusion and Plasma Physics is planned to be held in Moscow in 1973.

THE INTERNATIONAL CONFERENCE OF THE STUDY OF NUCLEAR STRUCTURE BY MEANS OF NEUTRONS

V. I. Lushchikov

The Conference, held in Budapest from July 31 to August 5, 1972, was organized by the Central Physics Institute and the Eötvös Physical Society with the cooperation of the Hungarian Academy of Sciences and the Hungarian Atomic Energy Commission, as well as of the International Association for Pure and Applied Physics. The Conference was attended by more than 200 scientists from 25 countries. The largest delegations were those of the USSR, and Federal Republic of Germany, France, and the United States of America. The plenary meetings heard 20 survey reports on the following branches of the subject: 1) the statistical model of the nucleus; 2) deviations from the statistical model, intermediate structure; 3) the optical model of the nucleus; 40 radiative capture of neutrons; 5) properties of fissionable nuclei; 6) ultracold neutrons; 7) high-intensity neutron sources. The first four branches, divided into three parallel sections, were dealt with in about 100 brief communications. The Soviet delegation presented 20 reports, five of which were surveys. All the brief communications had been published before the start of the Conference. The survey reports will be published towards the end of 1972.

H. Weidenmueller (Federal Republic of Germany) presented information on new directions in the development of the statistical model; these involved consideration of the two-particle nature of the nuclear forces (TBRE ensembles). Experimental verification of these new ideas is based on a study of the satistical properties of the distribution of the distances between remote compound-system levels. According to the first calculations, carried out for finite-dimensional matrices, these properties should be different for the TBRE and for the Gaussian ensembles (GOE) used earlier. The results obtained by A. Jane et al. (France) with Pu^{239}, Ho^{165}, Tm^{169}, Nd^{142}, Nd^{146}, and Nd^{148} nuclei provide evidence in favor of the TBRE model. However, as became clear in the course of the Conference, the latest calculations have led to the conclusion that in the limiting case, for infinite-dimensional matrices, the properties of the distance distributions for the GOE and TBRE types of ensemble should coincide, i.e., analysis of the distances between the levels does not provide a criterion for choosing one model in preference to the other. G. Harrison developed a method for the statistical analysis of neutron cross sections for the case in which the average widths are not small in relation to the distances between the resonances. The method is based on comparison of experimental cross sections and statistically generated cross sections with average resonance parameters.

An important place was occupied by reports on the investigation and analysis of nonstatistical effects. A report by K. Mahaut (Belgium) described the present-day theoretical view of such effects and gave a survey of available experimental results. It was noted that many experimental results on nonstatistical effects are not yet supported by convincing proofs. For this reason, the report considered the statistical criteria for the analysis of structure in reaction cross sections.

Correlation analysis of the energy intervals between neutron resonances (S. I. Sukhoruchkin, USSR; K. Ideno, Japan) supports earlier data on the existence of a quasiperiodic structure. Attempts to establish a connection between this structure and the level parameters (Yu. P. Popov et al., USSR) failed to yield positive results. A report by V. G. Solov'ev (USSR) predicted a wide class of nonstatistical effects in reactions with resonance neutrons, on the basis of the author's own semimicroscopic approach to the description of complicated compound states of nuclei. In particular, the effect of strengthening the reduced probabilities of α-decay of compound states to the one-phonon state 2^+ in comparison with α-decay in the ground state was experimentally observed (Yu. P. Popov).

Translated from Atomnaya Énergiya, Vol. 34, No. 1, pp. 66-67, January, 1973.

The greatest advances have been made in recent years on investigations of radiative capture of neutrons; this was facilitated by semiconductor detector techniques and large neutron sources (the high-current reactor of the Brookhaven laboratory, the linear accelerators at Oak Ridge and Jelais, and the pulse reactor at Dubna). This research makes it possible not only to study the mechanism of nuclear reactions [in comparison with the (d, p) and (γ, n) reactions] but also to investigate the structure of low levels of the nucleus, as well as to determine the characteristics of nuclear levels over a wide range of excitation energies. A survey report by R. Krien (United States) described experimental methods for the investigation of (n, γ) reactions. S. Mugabgab (United States) discussed the appearance in experiments of such processes as direct radiative capture of neutrons, an effect of the valence neutron, and also a semidirect process, or capture after an input state.

Fission physics and related questions were represented at the Conference by only a few reports. A brief survey by K. Pauli (Switzerland) gave some interesting experimental data which seemed to prove for the first time the existence of a second potential well in Pu^{240}. The paper discussed E2 transitions belonging to isomeric states of Pu^{240}. The energy of the transitions obeyed the I(I + 1) rule, which corresponds to a rotational band of levels for a nonspherical nucleus. The quantity $h^2/2J$ was found to be 3.33 keV, considerably less than the value (7.16 keV) found for the rotational band of the ground state in the first well. From this it follows directly that the deformation in the isometric state is considerably greater than in the ground state. Pauli used Strutinskii's envelope correction method to calculate some problems in nucleus dynamics. The moments of inertia calculated by Pauli for the ground and isomeric states of Pu^{240} were in very good agreement with the experimental data. P. Matusek et al. (Federal Republic of Germany) successfully measured the spectra of capture γ-radiation in (n, γ) reactions involving U^{235}, Pu^{239}, and Pu^{241} nuclei. These data are valuable not only for their scientific signifance but also for applications – for example, for the design of reactor shields and the nondestructive investigation of fuel-element burnup. A novel method for the analysis of nuclear materials in fuel elements is proposed in a report by S. Shalev (Israel). It is based on measurements of the structure of the energy spectrum of delayed neutrons by means of an He^3 spectrometer; this structure was discovered by the author. The method is highly sensitive to change in the amounts of various fissionable isotopes contained in the specimen.

A report on the first successful experiments for obtaining and storing ultracold neutrons was delivered by F. L. Shapiro (USSR). The maximum storage time was 100 sec, but this is far less than the theoretically expected time. The reasons for the deviation from theory are not yet clear. Interest in research on ultracold neutrons is mainly due to the possibility of using them for highly sensitive experiments to discover the electrical dipole moment of the neutron.

E Moller (Federal Republic of Germany) reported on the main characteristics of the reactor of the Laué–Langevin Institute (France and the Federal Republic of Germany), which went into operation in 1971. It has a power of about 60 MW and a flux density of up to $1.5 \cdot 10^{15}$ neutrons/cm^2·sec; the fuel used is U^{235}; heavy water is used as the moderator for the reflector and as the coolant. The reactor is designed for physical experiments on beam; the most important field of investigation is the physics of condensed media. Nuclear physics constitutes about 20% of the research. The reactor includes various devices for improving the experimental conditions (a cold moderator of liquid deuterium, neutron guides with complete internal reflection, etc.). A large number of spectrometers – a fission-product spectrometer, various types of γ-spectrometers, and in internal-conversion electron spectrometer – have been set up for nuclear investigations. A report by S. Kirjak (Federal Republic of Germany) describes a time-of-flight fast-neutron spectrometer based on the isochronous cyclotron at Karlsruhe. The installation began to operate in 1965 and holds the record for resolution. The average neutron yield is $2 \cdot 10^3$ sec^{-1}, the pulse duration is 1 nsec, the frequency of pulsing is 20 kHz, and the flight base is 67 m. The main field of investigation is the study of interaction between fast neutrons and light nuclei (chiefly the measurement of total effective cross sections). Considerable attention was aroused by a report (S. Moore, United States) describing the WNR neutron source project, based on the Los Alamos high-current accelerator (LAMPF). The accelerator went into operation in June, 1972, and the first physics experiments are planned for the beginning of 1973. The neutron installation is constructed in two stages. The first presupposes cutting off part of an LAMPF pulse to generate pulses lasting up to 5-10 μsec. It is designed primarily for time-of-flight investigations of the effective cross sections of structural materials, as well as for integral measurements on critical assemblies; the aim is to check and improve the design method used for fast reactors; it is also expected that condensed media will be investigated. The second stage is designed to utilize an accumulator ring for protons in order to compress the pulse to a few nanoseconds. This is accompanied by a 6,000-fold increase in the intensity of the beam. The number of neutrons per pulse is $2 \cdot 10^{15}$.

A report on the IBR-2 reactor, now under construction at the Joint Institute for Nuclear Research, was delivered by Yu. S. Yazvitskii. The thermal power of the reactor is 4 MW, and the power per pulse may reach 7,700 MW. The neutron yield is $2 \cdot 10^{17}$ sec^{-1}. The pulse duration in reactor operation is 100 μsec, and the frequency is 5-50 sec^{-1}. The installation can operate in a booster regime with an LIU-30 injector, with pulse duration of 3 μsec and average power values of 300 kW.

The Conference was devoted to the fundamental problems of nuclear structure and did not deal with questions of an applied nature. Nevertheless, many reports pointed out the importance of current research for the development of atomic and thermonuclear reactor construction.

THE FOURTH ALL-UNION SYMPOSIUM ON THE USE OF STABLE ISOTOPES IN GEOCHEMISTRY

S. F. Karpenko

The Fourth All-Union Symposium on the Use of Stable Isotopes in Geochemistry, organized by the V. I. Vernadskii Institute of Geochemistry and Analytical Chemistry of the Academy of Sciences of the USSR, was held in Moscow from September 26 to 29, 1972. Reports delivered at the Symposium presented the latest achievements of Soviet scientists working on the application of stable isotopes of various elements to geochemical and cosmochemical research.

Special interest was aroused by the reports devoted to the results of investigations of lunar soil brought back to earth by the Soviet Luna 16 and Luna 20 automatic interplanetary stations. Study of the isotope composition of inert gases, He, Ne, Ar, Xe (G. S. Anufriev et al.; A. P. Vinogradov and I. K. Zadorozhnyi) has made it possible to establish a number of characteristics of their distribution in various structural and mineralogical fractions of the lunar soil. In particular, it has been found that the concentrations and isotope compositions of the gases were independent of the depth from which the sample was taken. The concentration of the gases in a regolith sample was greater by several orders of magnitude than the concentration in ordinary chondrites, whereas the concentration in crystalline specimens of lunar rock was lower by 1 to 3 orders of magnitude. The bulk of the gases in the regolith consisted of gases from the solar wind, while in the crystalline fragments cosmogenic and radiogenic components predominated. It was also established that the separation of gases from the regolith when it is heated exhibits a number of peaks, which are apparently caused by the different activation energies of migration of the atoms of an inert gas in the lattices of different regolith minerals.

A study of the isotope composition of Sr, K, and Rb in regolith specimens from the Sea of Fertility (A. P. Vinogradov and Yu. M. Artemov) showed that, within the limits of experimental error, no changes are observed in the K^{41}/K^{40}, Sr^{84}/Sr^{88}, and Rb^{85}/Rb^{87} ratios in the materials investigated. This is a very important fact, which must be taken into account in constructing various models of the origin of the regolith.

E. M. Galimov, A. B. Ronov, A. A. Migdisov, A. I. Ermishkina, V. A. Grinenko, and N. V. Barskaya presented very interesting data on the changes that have occurred over the course of geological history in the isotope composition of the carbon in carbonates and organic substances dispersed in sediments, as well as of the reduced forms of sulfur. The data were based on a study of many samples and gave convincing evidence of the regularity of the periodic oscillations in the isotope composition of the materials studied. The increased concentration of the heavy isotope C^{13} in carbonates during the Phanerozoic eon is confined to the intermediate stages of the Hercynian and Alpine tectonic cycles, and the periods during which the carbon in the carbonates became lighter correspond to the initial and final stages of these cycles. These changes agree precisely with the time-dependent variations in the intensity of the formation of carbonate rocks: an increased accumulation of carbonates and a low degree of terrigenous removal result in an increase in the C^{13} content of the carbonates. The isotope composition of carbon in an organic substance does not remain constant; in particular, such substances are found to have become considerably heavier in post-Devonian times.

These data may be regarded as evidence of some time-dependent variation in the isotope composition of the carbon dioxide in the atmosphere.

The variations in the isotope composition of the sulfur in sedimentary sulfides also correspond, in general, to the periodicity of the tectonic processes. The isotope compositions of sulfate sulfur and sulfide sulfur

Translated from Atomnaya Énergiya, Vol. 34, No. 1, pp. 67-69, January, 1973.

in the sediments are found to have changed in opposite directions: during the periods when the concentration of heavy isotope S^{34} in the sulfates was the highest, the pyrites deposited were usually the "lightest."

A number of reports were devoted to the use of isotope research in clarifying the genesis of similar geological entities. For example, A. V. Sidorenko et al. reported the results of isotope-oxygen research on the amphibolites of the Kola Peninsula. According to these data, the orthoamphibolites of the Keiv complex are characterized by oxygen whose isotope composition (δO^{18} = + 2.1 to + 8.6‰) is different from that of the paraamphibolites of the Polmos–Poros series (δO^{18} = + 11.0 to + 15.5‰). According to the data of V. A. Snezhko and A. L. Rabinovich, The paraamphibolites and orthoamphibolites of the River Tiberda differ in the isotope composition of the sulfur they contain: the former are characterized by δS^{34} values ranging from + 7.8 to +10.0‰, while the values for the latter range from + 3.5 to 3.7‰. Research on siderites of different genesis (E. I. Dontsova et al.) showed that they are all characterized by particular isotope compositions of their oxygen, each different from the rest.

A study of the isotope composition of the sulfur contained in the sulfates, sulfides, and organic material found in sediments in the volcanic rocks of the Caucasian geosyncline (A. B. Ronov et al.) showed that as depth downward from the platform to the deeper parts of the geosyncline increases, there is a systematic increase in the amount of δS^{34} in the various forms of sulfur, and this increase is correlated with a progressive increase in the thickness of the sedimentary deposits.

These data indicate that the reduction of sulfates in such a situation took place under closed-system conditions.

A report by E. K. Gerling et al. dealt with the study of the isotope composition of helium and argon in the rocks, gaseous inclusions, and free gases of Sopchi (Monche tundra). It was shown that these rocks, characterized by anomalously high percentages of radiogenic argon (so high that the K–Ar method yields age values of up to 10^{10} years) are also distinguished by a high percentage of helium. It should be noted that the inert gases occur largely in the form of microinclusions and can be extracted by crushing the rocks in a vacuum. This appears to be a remarkable geological phenomenon the nature of which has not yet been established.

A report on the isotope composition of helium in specimens of mud and bedrock taken from the ocean bottom (A. Ya. Krylov et al.) aroused great interest. The authors made extremely precise and complicated measurements of the He^3/He^4 ratio in these specimens and some other geological objects and clearly showed that cosmic material plays an important role in red deep-water muds, while the bedrock of the ocean floor is affected by mantle material to a very notable degree. These observations in themselves are not new, but considerable interest was aroused by the precise and probably incontrovertible data cited to support them.

An analysis of the isotope composition of rocks from the rift zones of the oceans (V. A. Grinenko et al.) led to the conclusion that variations in the isotope composition of sulfur in basic rocks are related to magma differentiation processes and postmagmatic changes in the rocks, and not to the heterogeneous nature of the mantle material.

An old but still unanswered question in geology concerns the nature of hydrothermal waters. Data obtained in a study of the isotope composition of argon found in gas–liquid inclusions in minerals of the Sori copper–molybdenum deposits (Khakassia) indicate that underground water of meteoric origin played an active role in the formation of this deposit (V. I. Sotnikov et al.).

Similar conclusions were drawn by I. K. Zadorozhnyi et al. from a study of the distribution and isotope composition of inert gases in volcanic exhalations.

A series of reports was devoted to the use of isotope geochemical data for determining the origin of petroleum. In general, these investigations indicate that the isotope compositions of carbon (T. A. Botneva) and hydrogen (R. G. Pankina et al.) in petroleum are determined by the initial organic material of the oil-and-gas-bearing mother rock. The differences in the isotope composition of the carbon contained in oils are due to redistribution of the low-molecular and high-molecular components when the oils filtered through low-permeability rocks (F. A. Alekseev et al.).

The Symposium included a methodological seminar, at which the participants heard interesting communications concerning the development of new methods for determining the isotope composition of various chemical elements and the application of these methods to geochemical research.

In recent years isotope investigations have come to involve a growing number of geochemical problems and are being used to facilitate their solution. As Academician A. P. Vinogradov noted, the time has now come to formulate and solve a number of major problems in geochemistry and geology.

The Symposium was an important event not only in the scientific life of geochemists in the Soviet Union but also in science in the world at large. This is demonstrated, in particular, by the great interest taken in the Symposium by foreign researchers. Participants in the Symposium included noted scientists from Czechoslovakia, the German Democratic Republic, Hungary, Poland, the United States of America, and France.

J. Hamilton and J. Manthuruthil (editors) RADIOACTIVITY IN NUCLEAR SPECTROSCOPY. MODERN TECHNIQUES AND APPLICATIONS*

Reviewed by N. A. Vlasov

This publication is the first volume of a compendium of reports to a conference on "Radioactivity in nuclear spectroscopy." The conference was held in August, 1969, at Vanderbilt University in Nashville (USA). The first volume contains reports from the first three sections of the conference: 1) production and analysis of spectra; 2) multiparameter systems and the study of complex decay schemes; 3) study of short-lived states on beams.

Experience amassed in five or six years of work with semiconductor spectrometers, which have brought about a revolution in techniques of nuclear spectroscopy, is reviewed. The high resolution of semicondutor spectrometers (10^{-4} to 10^{-5}) combined with large aperture (high transmission) has made it possible to investigate a multiplicity of spectra and to determine the energy of spectral lines to such high accuracy that the compilation of transition schemes becomes reliable even on the basis of a single energy balance. Even faint lines are within range of detection, thanks to the high resolution of the spectrometers. Recent achievements in electronics now make it possible to carry out updated multichannel observations of coincidences and to detect cascades of transitions. The abundant flow of results of spectral measurements has naturally placed in the foreground the problem of making use of that flood of data, and while that problem was one of the first discussed at the conference, a solution is not yet in sight. As in the case of optical spectroscopy, nuclear spectroscopy also appears to have need of extensive catalogs of spectral lines and nuclear levels. Such catalogs or tabular data will also be utilized in applied analytical problems, and in theoretical analysis for uncovering and explaining spectral regularities. Experimental physicists quite frequently justify their labor by comparisons with theoretical predictions, even though they understand perfectly well that, at the present level of computation expertise and technology, it is theoretically impossible to calculate the spectrum of levels of any nuclide, even the lightest nuclide, with satisfactory accuracy, and that the only road open for constructing schemes of levels and transitions is the experimental road. The value of spectrometric results for a catalog of spectra must become one of the principal criteria for the quality of research efforts.

The reports submitted to the conference discussed methods for working with modern spectrometric equipment: the properties of several variants of Ge-(Li)-spectrometers, ways of analyzing spectra with the aid of computers, methods of storing and analyzing data obtained with the aid of many-parameter systems, methods for combining an accelerator, a spectrometer, and a computer into a matched and compatible ensemble. One of the reports presented examples of analysis of complex decay schemes on the basis of measurements of $\gamma-\gamma$-coincidences with a 16-channel memory unit; another gave an example of a scheme of levels and of γ-transitions of a nucleus read out on the display screen of a computer readout oscillograph.

Methods for generating and analyzing nuclear-spectrometric information are developing at a fairly vigorous pace, but the proceedings of this conference held three years ago are not obsolete reading just the same. The proceedings of the conference can be used to great advantage by spectrometrists.

* Vol. 1, Gordon and Breach, Science Publishers, New York–London–Paris, 1972.

Translated from Atomnaya Énergiya, Vol. 34, No. 1, p. 70, January, 1973.

D. De Soete, R. Gijbels,

and J. Hoste

NEUTRON ACTIVATION ANALYSIS*

Reviewed by K. A. Baskova

In the twelve chapters of this book the neutron activation of material is discussed in detail. Activation analysis is widely used in scientific-research institutes and in industry; by its use amounts of impurities too small for measured by ordinary chemical analysis can be determined quantitatively. The high sensitivity and selectivity of the method permits the determination of extremely small traces of impurities in pure substances. Owing to recent advances in experimental techniques the activation method can be used for plant control of production processes. The neutron activation method is most sensitive at neutron fluxes of about 10^{15} $cm^{-2} \cdot sec^{-1}$.

In this monographic the reactions induced by neutrons are described in detail. A separate chapter is devoted to neutron sources. A large section is allocated to methods for detecting the reaction products, and the detection methods for α- and β-particles and γ-quanta are analyzed. The laws governing the build-up and decay of radioactivity are described.

In order to determine the amount of an impurity the detection apparatus must be well calibrated per absolute "count." Much space is allocated to this question. Methods of preparing experimental and standard samples in various states (solid, powder, liquid, gaseous, and aerosol) are set out in detail.

Various forms of rabbit and canning material for the irradiation of samples are suggested, and recommendations made as to the choice of can for irradiations with neutrons from various sources, in order that the optimum irradiation conditions be chosen. Methods are given for radiochemical separations of a substance or group of substances. If chemical analysis is not possible, the most accurate means of quantitative analysis is suggested.

In the final chapters evaluations of the accuracy of the quantitative analyses are given.

Many reference tables are included, giving the reaction cross-sections for thermal and resonance neutrons, fission neutrons, and 14 MeV neutrons. In addition, there are tables of the energies of γ-rays formed via thermal neutron capture by various nuclei from oxygen to neptunium, and a table to γ-lines in order of increasing energy from 50 to 4000 keV, with information regarding the isotopic emitter, the relative line intensity, and the half-life. In the last table methods for the analysis of various elements are given, with references to the original literature.

All sections and reference tables are provided with detailed bibliographies.

The book will be of interest to a wide circle of readers.

* Chemical Analysis, Vol. 34, P. Elving and J. Kolthoff (editors), Wiley–Interscience, New York–Sydney–Toronto (1972).

Translated from Atomnaya Énergiya, Vol. 34, No. 1, p. 71, January, 1973.

Yu. I. Gal'perin, L. S. Gorn,

and B. I. Khazanov

MEASUREMENT OF RADIATIONS IN THE COSMOS*

Reviewed by V. V. Matveev

At the present time the measurement of the characteristic constants of the ionizing radiations in near-terrestial and cosmic space is one of the more important fields of cosmic study.

This book is perhaps the first monograph published either in this country or elsewhere in which consideration is given to the basic set of problems associated with the measurements of ionizing radiations in cosmic space. The characteristics of radiation sources in near-terrestrial and cosmic space, and the streams of particles and quanta created by them, are discussed and the principle methods for the detection of radiations of a given type are described. Methods are given for the construction of measuring and recording units, with a description of the subassemblies characteristic of cosmic electronics. The descriptions of the physical processes in cosmic space, the techniques of ionizing radiation detection, and the treatment of the information obtained are up-to-date. Thus the book gives a representative picture of modern cosmic nuclear instrument manufacture.

Particularly noteworthy is a discussion of the principal methods of solving the problems associated with the radiation measurements and with the results achieved, and also a description of circuits tested and proved in practice.

Streams of radiation in the cosmos differ in complexity and in multiplicity of components. The range of measurements of stream density and of particle and quantum energies can be very wide, while the large volume of information is difficult to transmit to earth by the telemetric channels of the link. Therefore, for the successful measurement of ionizing radiations in cosmic space it is necessary to ensure a high discrimination in the measuring apparatus, so that the characteristics of one type of radiation can be determined on a background of other extremely significant radiation components. Wide-range measuring and recording equipment is also required, with concentration of the information and initial processing before its input into the telemetric channels.

Such problems are now also pertinent to the whole field of nuclear instrument manufacture. Their detailed consideration in the book makes it extremely timely, useful, and interesting both for specialists working on the development of instruments for measuring ionizing radiations and for those in other fields in which they are applicable.

The necessary reference material on the interaction of radiations with detector and shielding materials is given in the form of graphs and will be of great practical help.

In conclusion, the excellent layout and high printing quality of the publication should be mentioned.

* Atomizdat, Moscow (1972).

Translated from Atomnaya Énergiya, Vol. 34, No. 1, p. 71, January, 1973.

breaking the language barrier

WITH COVER-TO-COVER ENGLISH TRANSLATIONS OF SOVIET JOURNALS

in mathematics and information science

Title	# of Issues	Subscription Price
Algebra and Logic *Algebra i logika*	6	$120.00
Automation and Remote Control *Avtomatika i telemekhanika*	24	$195.00
Cybernetics *Kibernetika*	6	$125.00
Differential Equations *Differentsial'nye uravneniya*	12	$150.00
Functional Analysis and Its Applications *Funktsional'nyi analiz i ego prilozheniya*	4	$110.00
Journal of Soviet Mathematics	6	$135.00
Mathematical Notes *Matematicheskie zametki*	12 (2 vols./yr. 6 issues ea.)	$185.00
Mathematical Transactions of the Academy of Sciences of the Lithuanian SSR *Litovskii Matematicheskii Sbornik*	4	$150.00
Problems of Information Transmission *Problemy peredachi informatsii*	4	$100.00
Siberian Mathematical Journal of the Academy of Sciences of the USSR Novosibirski *Sibirskii matematicheskii zhurnal*	6	$195.00
Theoretical and Mathematical Physics *Teoreticheskaya i matematicheskáya fizika*	12 (4 vols./yr. 3 issues ea.)	$145.00
Ukrainian Mathematical Journal *Ukrainskii matematicheskii zhurnal*	6	$155.00

Back volumes are available.
For further information, please contact the Publishers.

SEND FOR YOUR
FREE EXAMINATION COPIES

PLENUM PUBLISHING CORPORATION
Plenum Press • Consultants Bureau
• IFI/Plenum Data Corporation
227 WEST 17th STREET
NEW YORK, N. Y. 10011

In United Kingdom
Plenur Publishing Co. Ltd., Davis House (4th Floor)
8 Scrubs Lane, Harlesden, NW10 6SE, England

Declassified and Approved For Release 2013/09/15 : CIA-RDP10-02196R000400010001-9

breaking the language barrier

WITH COVER-TO-COVER ENGLISH TRANSLATIONS OF SOVIET JOURNALS

in physics

Title	# of Issues	Subscription Price
Astrophysics *Astrofizika*	4	$100.00
Fluid Dynamics *Izvestiya Akademii Nauk SSSR mekhanika zhidkosti i gaza*	6	$160.00
High-Energy Chemistry *Khimiya vysokikh énergii*	6	$155.00
High Temperature *Teplofizika vysokikh temperatur*	6	$125.00
Journal of Applied Mechanics and Technical Physics *Zhurnal prikladnoi mekhaniki i tekhnicheskoi fiziki*	6	$150.00
Journal of Engineering Physics *Inzhenerno-fizicheskii zhurnal*	12 (2 vols./yr. 6 issues ea.)	$150.00
Magnetohydrodynamics *Magnitnaya gidrodinamika*	4	$100.00
Mathematical Notes *Matematicheskie zametki*	12 (2 vols./yr. 6 issues ea.)	$185.00
Polymer Mechanics *Mekhanika polimerov*	6	$120.00
Radiophysics and Quantum Electronics (Formerly Soviet Radiophysics) *Izvestiya VUZ. radiofizika*	12	$160.00
Solar System Research *Astronomicheskii vestnik*	4	$ 95.00
Soviet Applied Mechanics *Prikladnaya mekhanika*	12	$160.00
Soviet Atomic Energy *Atomnaya énergiya*	12 (2 vols./yr. 6 issues ea.)	$160.00
Soviet Physics Journal *Izvestiya VUZ. fizika*	12	$160.00
Soviet Radiochemistry *Radiokhimiya*	6	$155.00
Theoretical and Mathematical Physics *Teoreticheskaya i matematicheskaya fizika*	12 (4 vols./yr. 3 issues ea.)	$145.00

Back volumes are available. For further information, please contact the Publishers.

SEND FOR YOUR FREE EXAMINATION COPIES

PLENUM PUBLISHING CORPORATION
227 WEST 17th STREET
NEW YORK, N. Y. 10011
Plenum Press • Consultants Bureau
• IFI/Plenum Data Corporation

In United Kingdom
Plenum Publishing Co. Ltd., Davis House (4th Floor)
8 Scrubs Lane, Harlesden, NW10 6SE, England